The Abdus Salam
International Centre for Theoretical Physics

United Nations
Educational, Scientific and
Cultural Organization

IAEA
International Atomic Energy Agency

The International Union of Geodesy and Geophysics

2339-15

Workshop on Atmospheric Deposition: Processesand Environmental Impacts

21 - 25 May 2012

Dust deposition:
Biogeochemical Impacts and Uncertainties

G. Bergametti

Universities Paris-Diderot and Paris Est Creteil
Creteil
France

Dust deposition: Biogeochemical Impacts and Uncertainties

G. Bergametti

and colleagues

(B. Chatenet, A. de Roubaix, G. Foret, B. Marticorena, J.L. Rajot…)

lisa | Laboratoire Inter-Universitaire des Systèmes Atmosphériques

UMR CNRS 7583, Universities Paris-Diderot and Paris Est Créteil

Institut Paul Simon Laplace (IPSL)

CMC, 61 avenue du Général de Gaulle,

94010 Créteil cedex

France

Workshop on Atmospheric Deposition: Processes and Environmental Impacts, Trieste (Italy), 21-25 May 2012

Deposition as a process controlling the biogeochemical effects of dust

Table 1. Deposition of Dust Into Various Ocean Basins[a]

	Duce et al. [1991]	*Prospero* [1996]	*Ginoux et al.* [2001]	*Zender et al.* [2003a]	*Tegen et al.* [2004]	*Luo et al.* [2003]	Composite Dust Deposition [*Jickells et al.*, 2005]
North Pacific	480	96	92	31	56 (0.29)	35 (0.13)	72
South Pacific	39	8	28	8	11 (0.47)	20 (0.22)	29
North Atlantic	220	220	184	178	259 (0.21)	230 (0.14)	202
South Atlantic	24	5	20	29	35 (0.20)	30 (0.17)	17
Indian Ocean	144	29	154	48	61 (0.12)	113 (0.10)	118
Global emissions	-	-	1814	1490	1800	1650	1790

[a]Units are Mt/yr. The numbers in brackets are variability estimates (stdv/mean).

From Mahowald et al., GBC, 2005

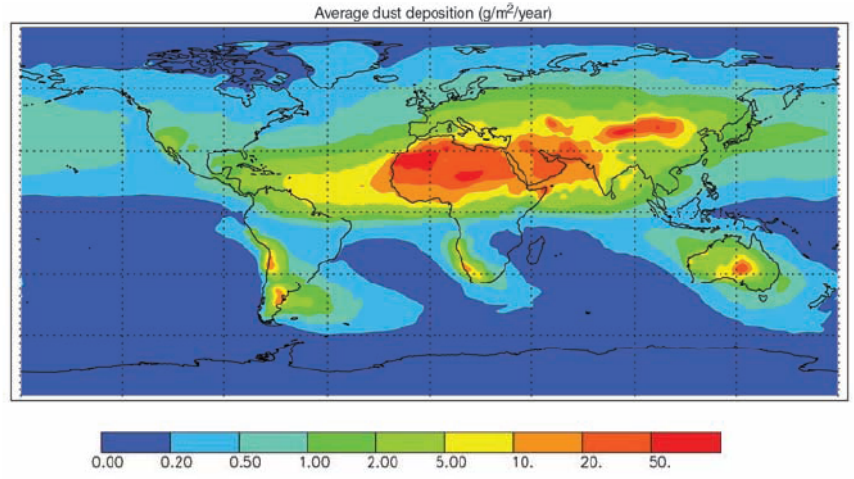

Between 300 and 500 Mt/yr of dust are deposited onto the oceans

This represents between 19 and 26% of the annual dust emissions

Dust fluxes to the world oceans based on a composite of three published modeling studies that match satellite optical depth, in situ concentration, and deposition observations (from Jickells et al., Science, 2005)

lisa | Laboratoire Inter-Universitaire des Systèmes Atmosphériques

Table 4. Budget of phosphorus in the photic layer of the western Mediterranean Sea (µg/m^2/d). Estimates are a: From ^{14}C measurements (Minas et al., 1988) and using C/P Redfield ratio (106); b: From the C particulate flux out of the photic zone as measured by sediment traps at 200 m depth (J.C Micquel and S. Fowler, personal communication) and using P/C Redfield ratio; * lower than the annual mean but not precisely known.

	annual	summer
Phosphorus required to support :		
primary production	3000-5300[a]	*
new production	680-1500[a]	70[b]
Atmospheric input of dissolved phosphorus	36-70	40-85

Bergametti et al., J. Atmos. Chem., 1992

Deposition as a process controlling the biogeochemical effects of dust

- **Productivity of the Amazon rain forest depends in part upon critical elements (e.g. K and P) contained in 10-15 Mtons of soil dust imported annually from Sahara/Sahel** *(Swap et al., 1992)*

- **Alkaline dust deposition limits nutrient losses from soils due to acid rains** *(Roda et al.,1993)*

- **Aeolian dust additions significantly contribute to quaternary soils** *(Yaalon and Ganor, 1973; Herrmann et al., 1996)* **and Saharan dust is the most important parent material for clay-rich soils on Caribbean islands** *(Muhs et al., 1990)*

Dust deposition as a proxy of climate and environmental changes

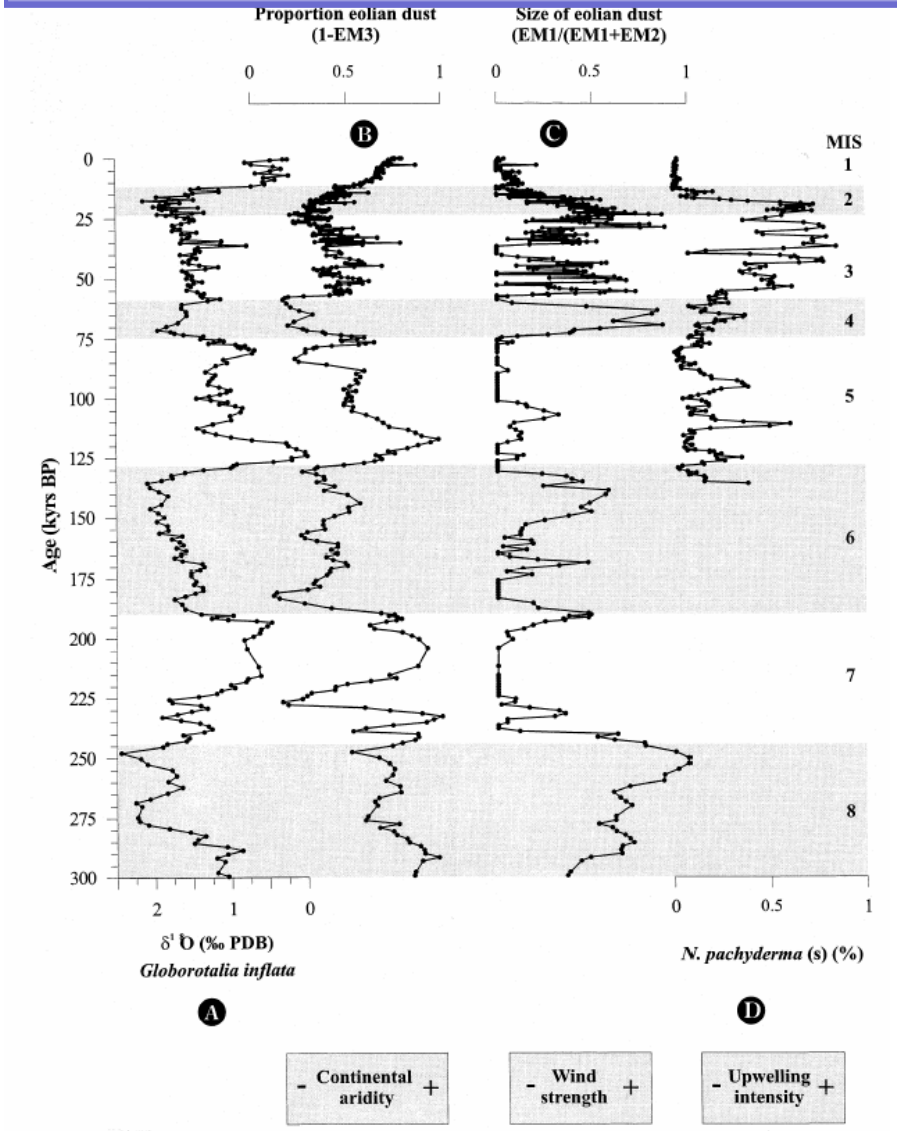

Fig. 5. Reconstructions of Late Quaternary aridity and trade-wind strength in southwestern Africa. (A) $\delta^{18}O$ record of *Globorotalia inflata*. (B) The proportion of the eolian end members is used as a proxy for continental aridity. (C) The ratio of coarse over fine eolian dust is used as a proxy for SE trade-wind intensity. (D) Relative abundance of the planktonic foraminifer *Neogloboquadrina pachyderma* (s) in core GeoB 1711 reflects Benguela upwelling intensity (Little et al., 1997b).

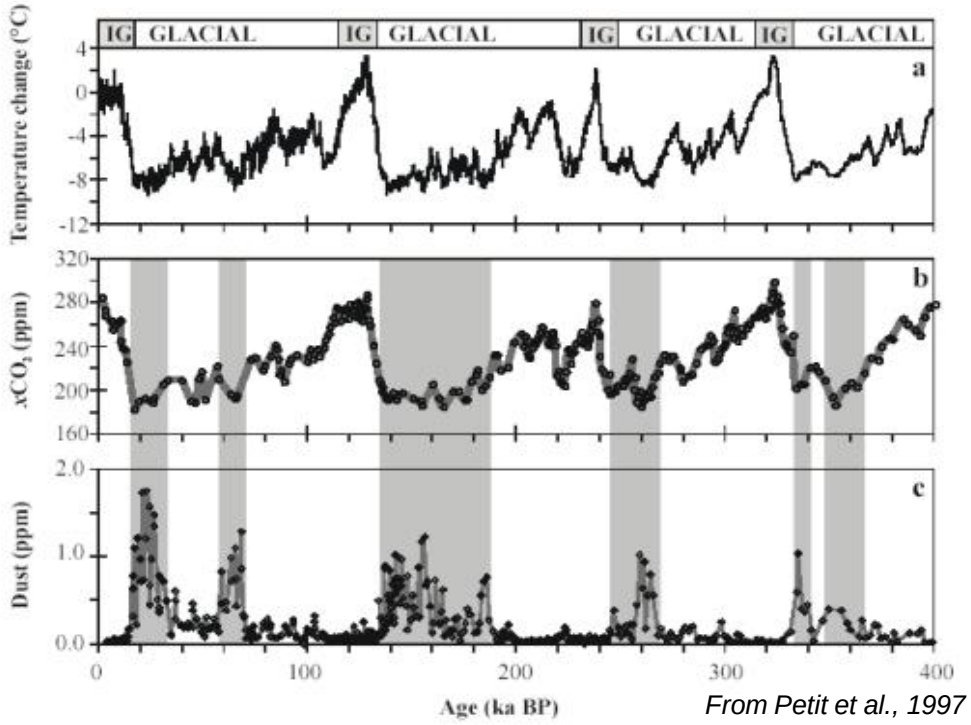

From Petit et al., 1997

Dust content in snow deposits, ice cores, loess deposits and sediments is a tracer of paleo-atmospheric circulations, paleoenvironments and past climate parameters (such as wind strength)

lisa | Laboratoire Inter-Universitaire des Systèmes Atmosphériques

What are our real capabilities to correctly assess dust deposition?

Dust global models

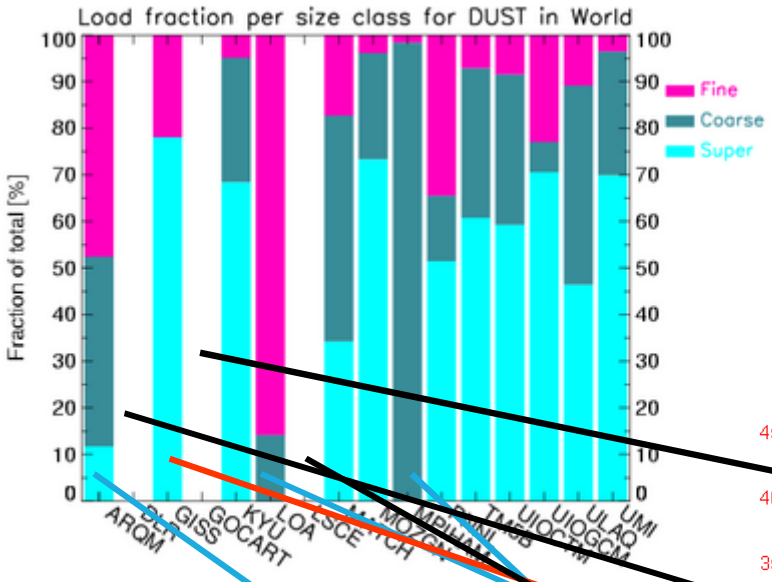

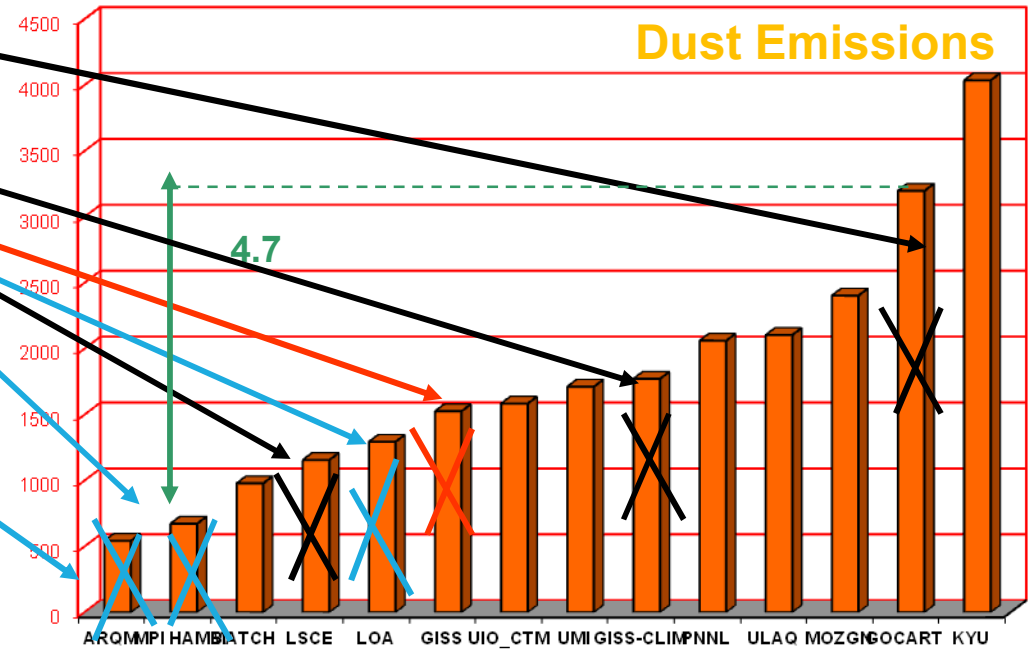

Large uncertainties/differences remain on dust emissions

Various initial size distributions and size range?

No (or limited) supermicron mode

No coarse mode

No **information** on size classes

Adapted from AEROCOM (Aerosol Model Comparison; http://dataipsl.ipsl.jussieu.fr/cgi-bin/AEROCOM/; Textor et al., Atmos. Chem. Phys., 2006; 2007)

lisa | Laboratoire Inter-Universitaire des Systèmes Atmosphériques

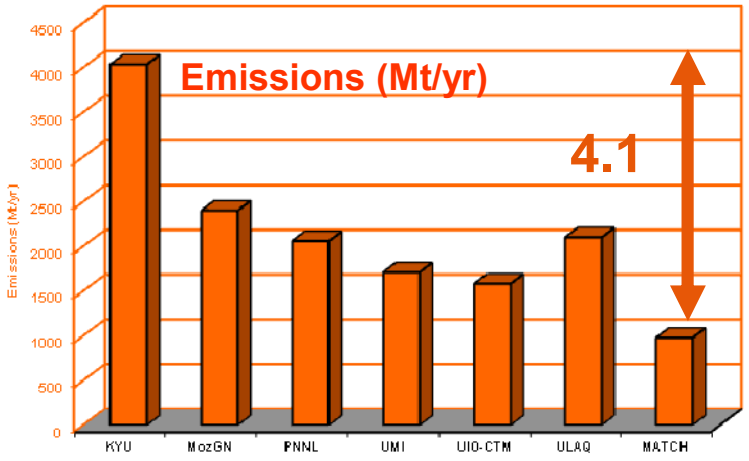

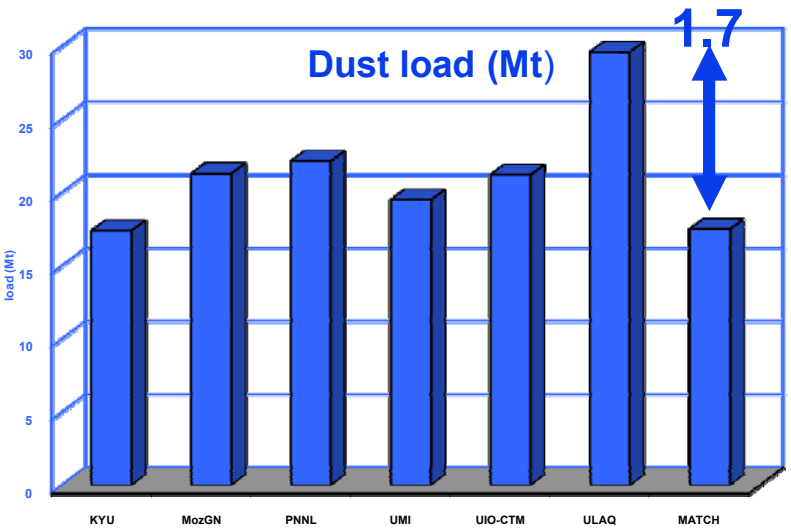

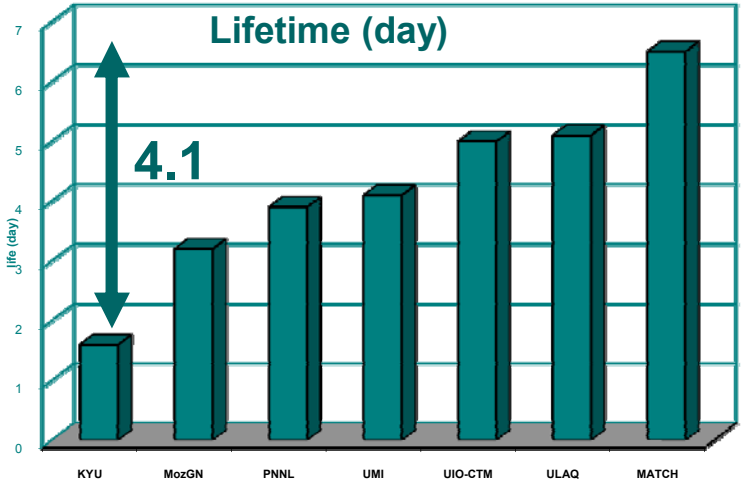

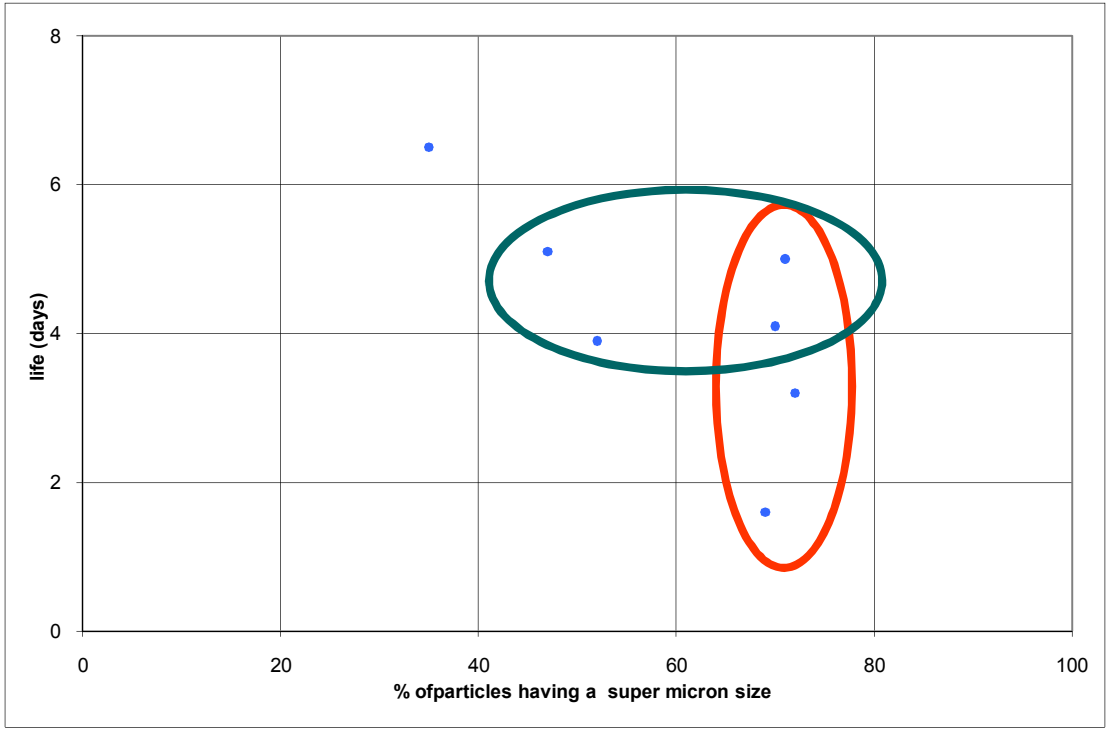

data from AEROCOM (Aerosol Model Comparison; http://dataipsl.ipsl.jussieu.fr/cgi-bin/AEROCOM/; Textor et al., Atmos. Chem. Phys., 2006; 2007)

lisa | Laboratoire Inter-Universitaire des Systèmes Atmosphériques

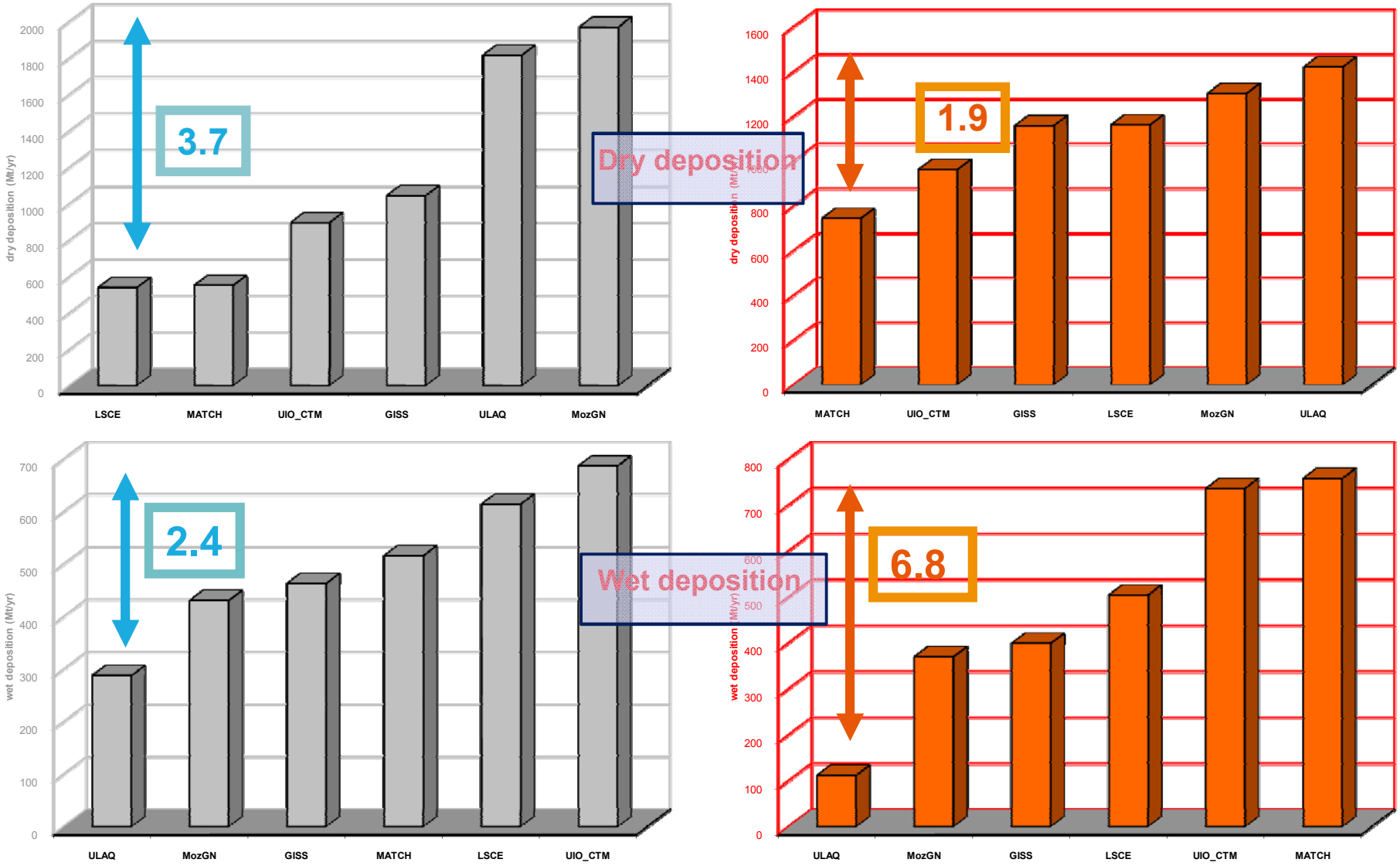

AEROCOM EXPERIENCE A

No constraint on dust sources

AEROCOM EXPERIENCE B

Mass fluxes, injection height and emitted particle size prescribed

Data from AEROCOM (Aerosol Model Comparison; http://dataipsl.ipsl.jussieu.fr/cgi-bin/AEROCOM/; Textor et al., Atmos. Chem. Phys., 2006; 2007)

lisa | Laboratoire Inter-Universitaire des Systèmes Atmosphériques

Size-resolved dust emission fluxes

(Sow et al., ACP, 2009)

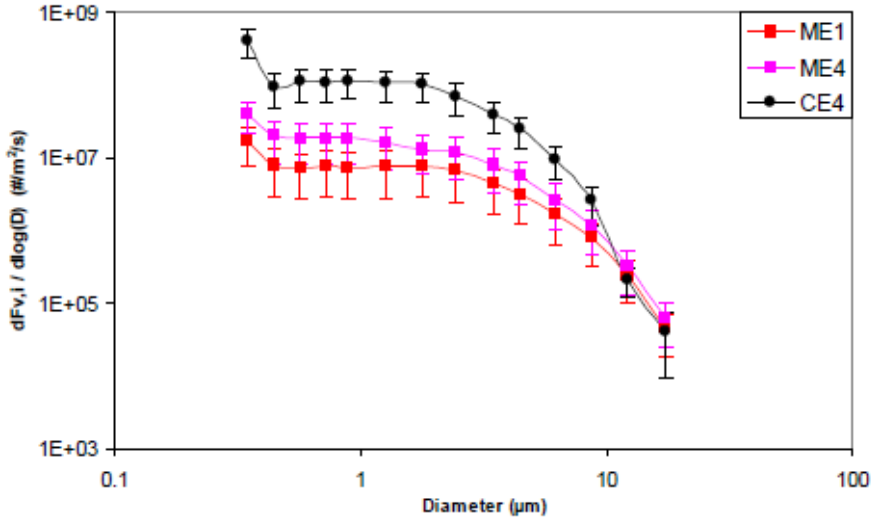

Fig. 9. Average size-resolved fluxes measured during the convective (CE4) and Monsoon (ME1 and ME4) events. The length of the error bars corresponds to the standard deviation.

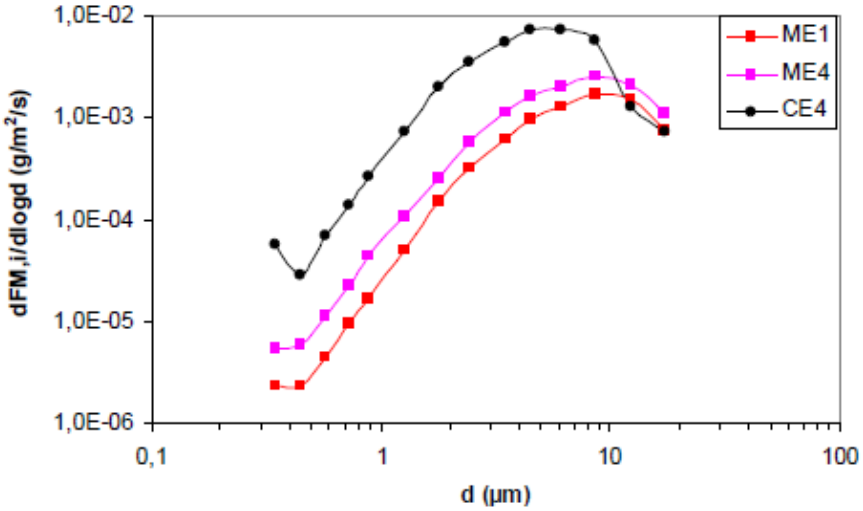

Fig. 11. Average emission fluxes for the 3 events of this study. These mass fluxes have been computed from the number fluxes of fig.9. Note the shift of the mass distribution towards smaller sizes in the case of the energetic event (CE4).

Size-distribution of the dust emission fluxes

(Sow et al., ACP, 2009)

(log normal modes; gmd, = geometric mean diameter in µm)

	mode1			mode2			mode3		
	σ	gmd	%	σ	gmd	%	σ	gmd	%
ME1				1,7	4,9	42%	1,5	10,4	58
ME4				1,8	5,1	43%	1,5	10,4	57%
CE4	1,50	1,70	11%	1,7	5,1	77%	1,5	10,0	12%
Wind tunnel	1.7	1.5		1.6	6.7		1.5	14.2	

(Alfaro et al., JGR, 1998)

The median of the two coarser modes are finer than in the wind tunnel experiment!!!

Simulation of the size-distribution of emitted dust with a brittle fragmentation theory (Kok, 2011)

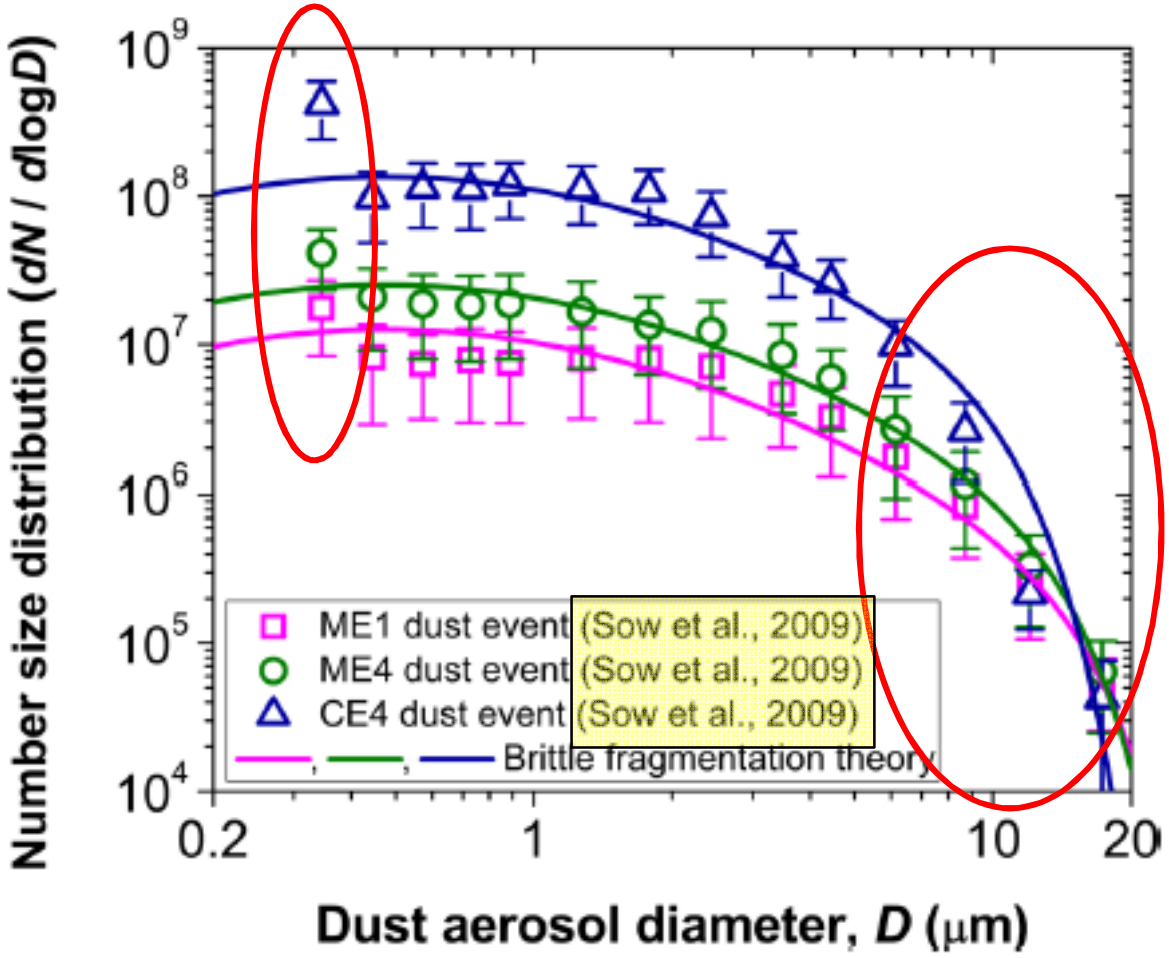

λ= 15.5
λ= 13.5
λ=10.3

With Ds, σ_s, C_N and C_v constant

(Kok et al., 2011)

We can conclude that:

- It remains large uncertainties in dust emission fluxes mainly because they cannot be quantitatively constrained.

-The size distribution of the dust particles at the emission is not well known; whatever, dust covers a large range of particle diameters

-The most important data set we have to check the quality of the dust model simulations concerns the Aerosol Optical Depth, a proxy of the dust atmospheric load.

⇨*deposition terms are used as tuning parameters to fit the prescribed emissions and size distribution to the measured dust optical depth: there is no sufficient dust deposition measurements, especially in the vicinity of deserts to constrain the mass budget in dust models,*

Some recent results on:

1-how to improve the way by which the mass size distribution of dust is treated into dust models

2-Some experiments allowing to check how work the dust dry deposition parametrization

3-the implementation of stations able to perform continuous long term measurements of dust deposition

1- The treatment of the size distribution in dust models

According to what we know, the dust size distribution covers a large domain of diameters, ranging from a 0.1 µm to more than 60 µm.

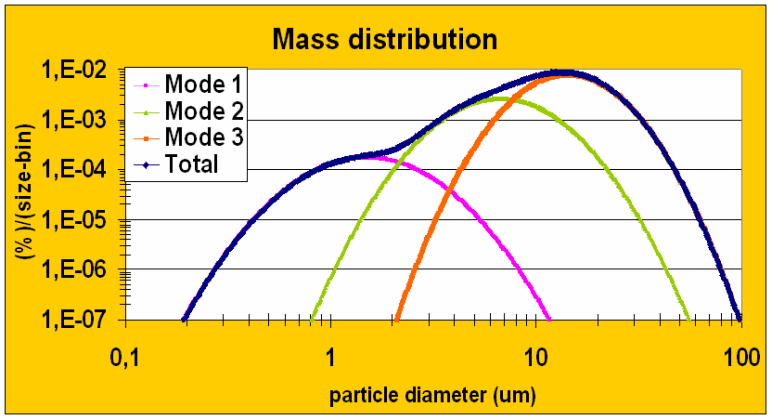

A very complete sensitivity study performed by *Gong et al.*, (*J.G.R.*, 2003) concludes that a minimum number of twelve bins should be necessary to correctly describe the evolution of the dust size distribution (while global models use frequently no more than four bins).

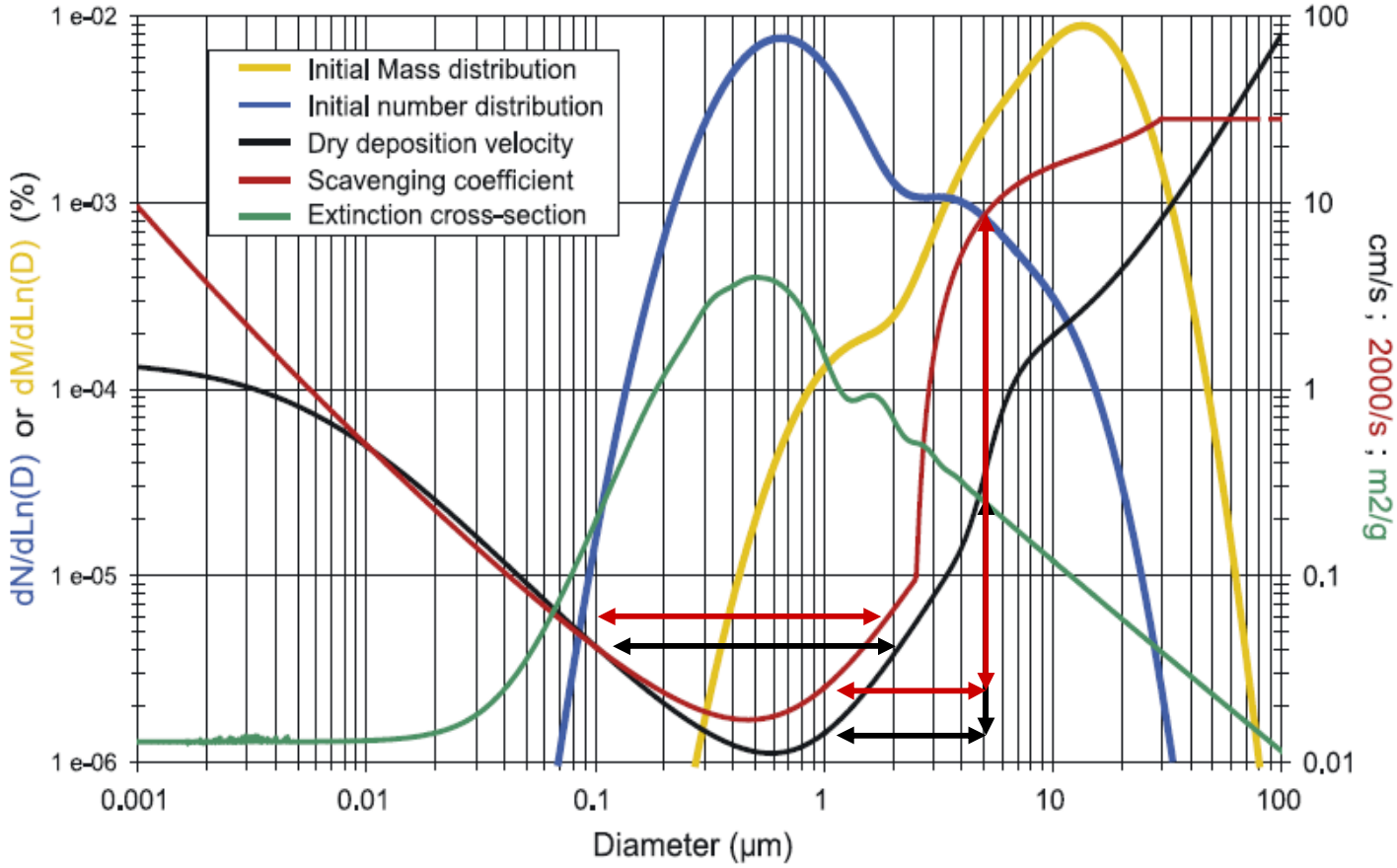

Figure 1. Variations with particle diameter of (left axis) the initial dust number (blue curve) and mass (yellow curve) reference particle size distributions, and (right axis) of the dry deposition velocity (black, in cm s^{-1}), the below-cloud scavenging coefficient (red, in 2000 s^{-1}), and the specific extinction cross section of dust at 550 nm (green, in m^2 g^{-1}).

Foret et al., J. Geophys. Res., 2006

Isolog bins scheme

Isogradient bins scheme

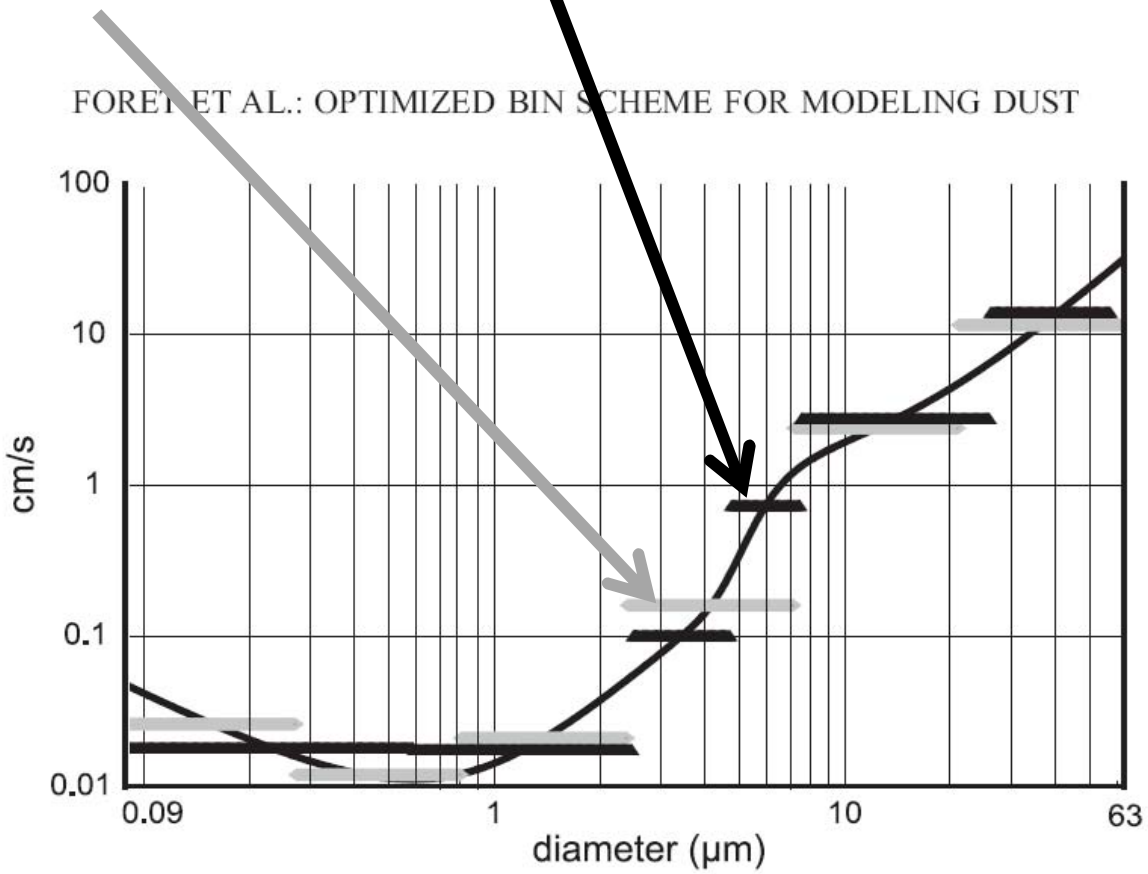

Figure 4. Comparison of the dry deposition velocity as a function of particle size for the 1000-bin reference case (black curve) and for 6-bin case with the isolog scheme (grey bars) and the isogradient scheme (black bars).

Foret et al., J. Geophys. Res., 2006

Table 1. Statistical Parameters of the Selected Mass and Number Size Distributions of Dust Particles Over Source Areas (After *Alfaro and Gomes* [2001])

	Mass (Number) Median Diameter, μm	Geometric Standard Deviation	Percentage of Total Mass (Number)
Mode 1	1.5 (0.64)	1.7	2 (89)
Mode 2	6.7 (3.46)	1.6	27 (9)
Mode 3	14.2 (8.67)	1.5	71 (2)

One-box model simulations

Reference: a simulation with 1000 bins over the size range 0.09-63 µm

- ***Isolog bins (geometric mean diameter)***
- ***Isolog bins (weighted geometric diameter)***
- ***Isogradient bins***

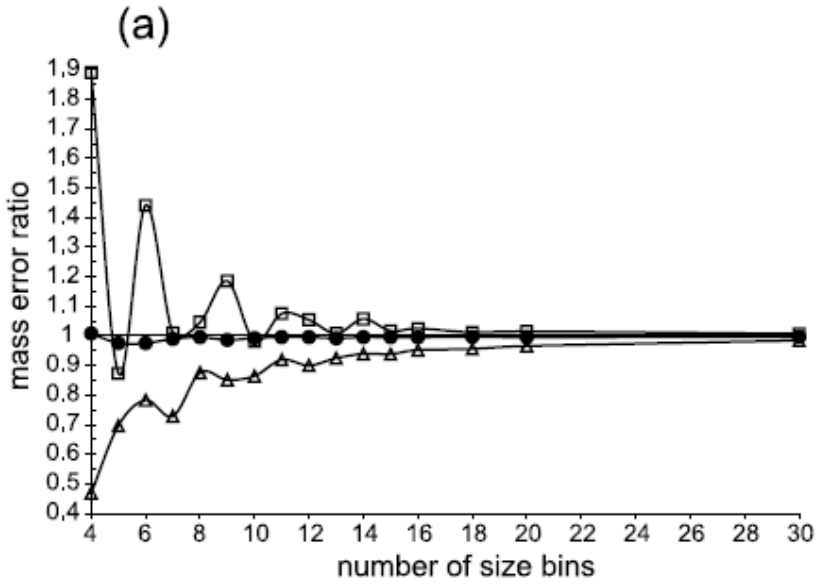

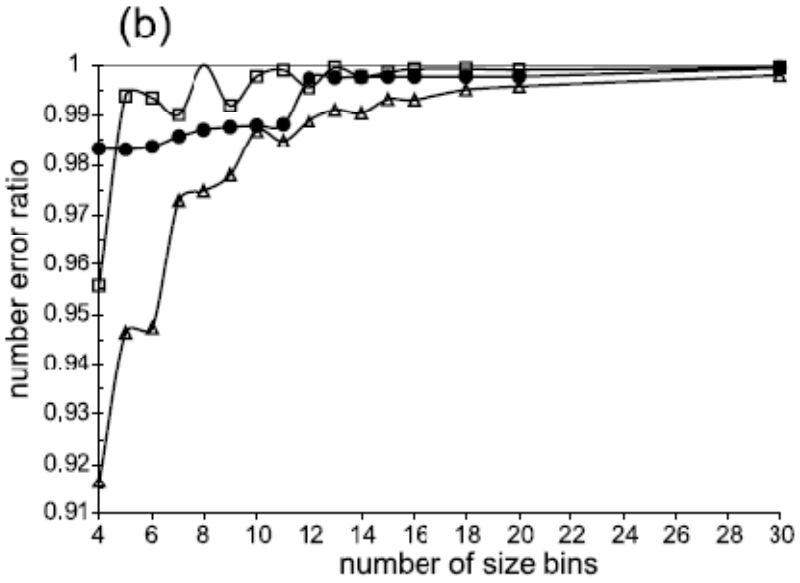

$$\text{Error ratio} = \frac{\text{M (or N) simulated for a given bin scheme}}{\text{M (or N) simulated in the reference case}}$$

lisa | Laboratoire Inter-Universitaire des Systèmes Atmosphériques

Foret et al., J. Geophys. Res., 2006

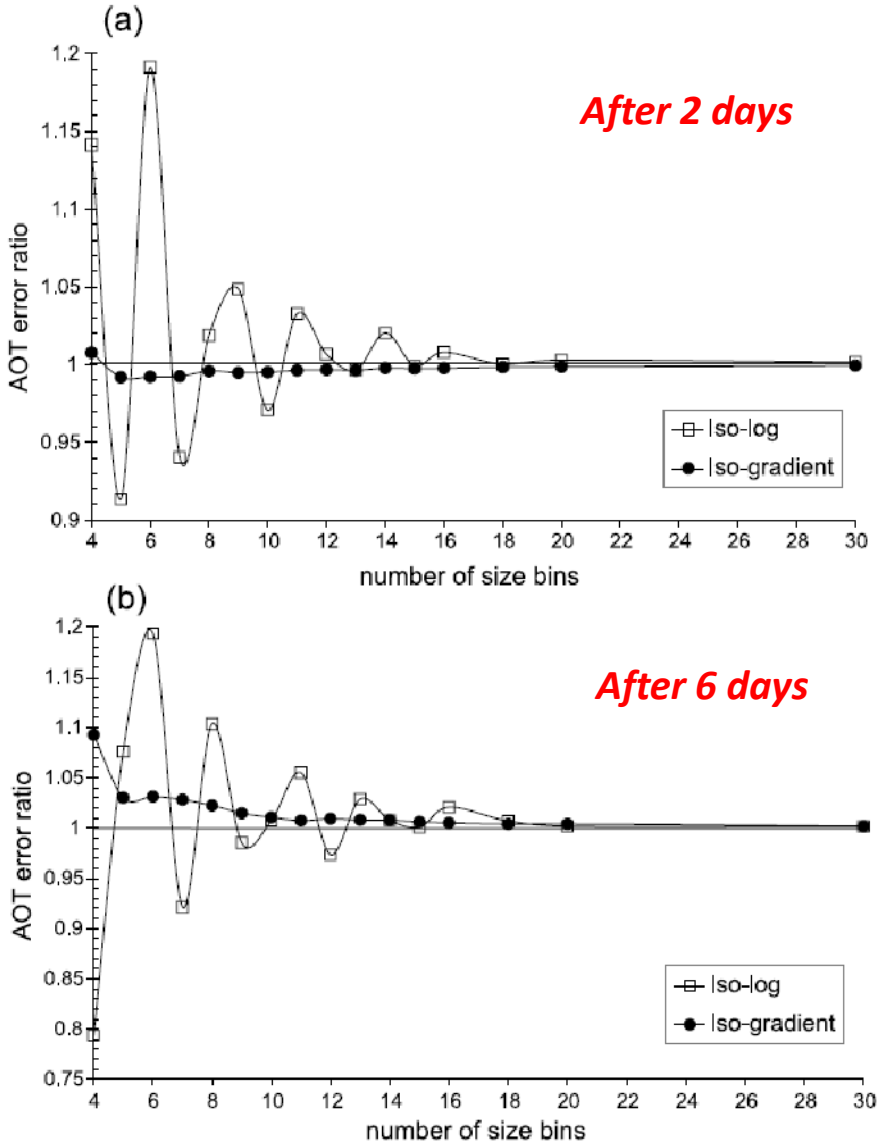

Figure 9. Error ratios in *AOT* using the isolog size bin scheme (open squares) and the isogradient scheme (filled circles) as a number of size bins used, and using the weighted geometric mean of the dust specific extinction cross section within each size bin: (a) after 2 days of simulated dry deposition, (b) after 6 days of simulated dry deposition.

Foret et al., J. Geophys. Res., 2006

ISOLOG

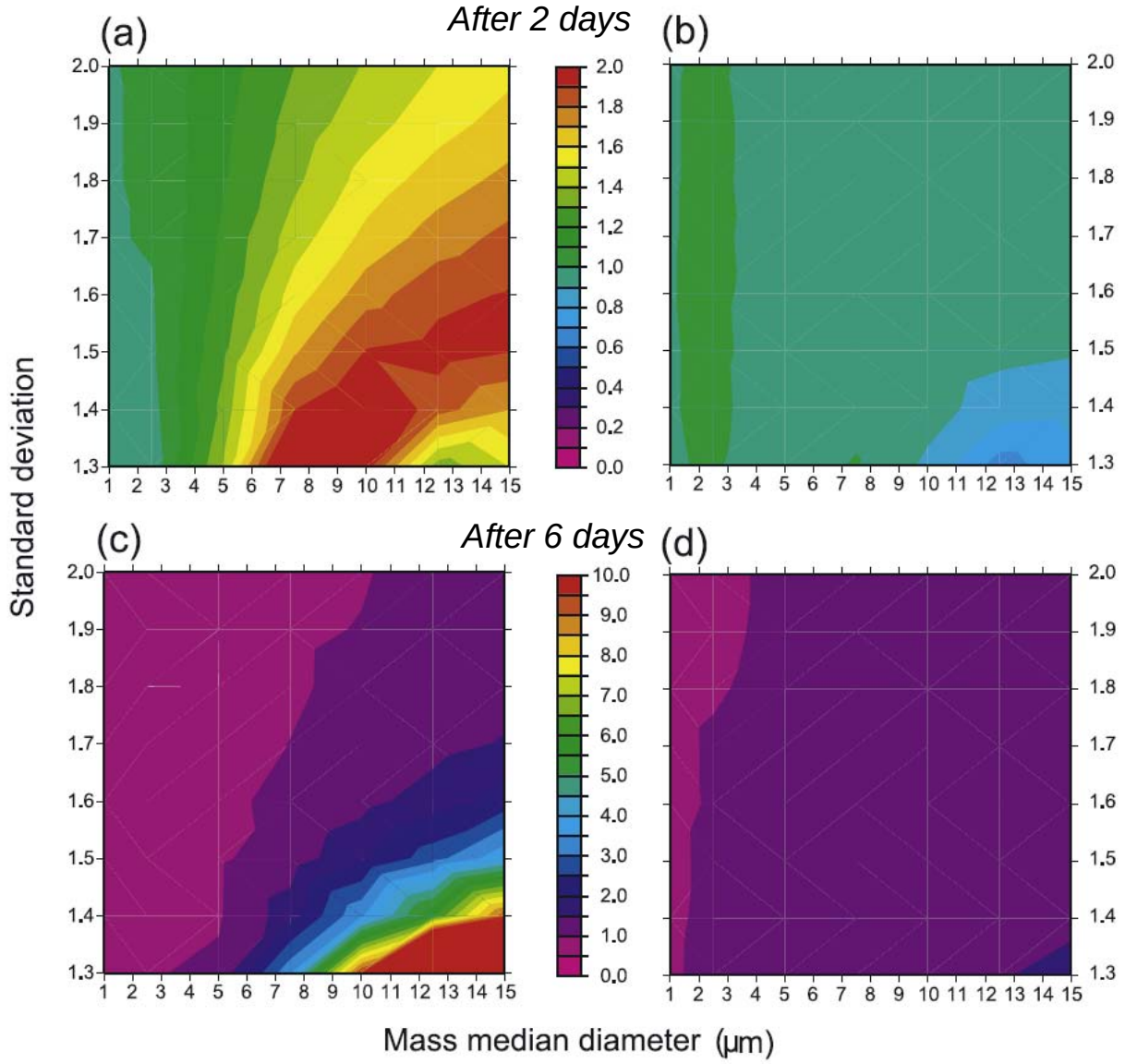

ISOGRADIENT

Figure 5. Error ratios from sensitivity tests of particle size bin schemes to varying mass and number monomodal lognormal particles size distributions: (a) mass error ratio for the isolog case (2-day simulation); (b) mass error ratio for the isogradient case (2-day simulation); (c) number error ratio for the isolog case (6-day simulation); (d) number error ratio for the isogradient case (6-day simulation).

-The large domain of diameters covered by the dust size distribution is difficult to manage into dust models (limited number of bins)

- The use of an algorithm managing the size dependent parameters of the dust cycle using an iso-gradient instead of an isolog method, allows a better numerical precision for a given number of size bins.

2- Checking the modeled dust dry deposition velocity

❑ ***Problem:***

There is a very limited number of field experiments during which dust dry deposition velocities have been determined. Almost none in source regions. Thus we assume that classical dry deposition scheme works well…

❑ ***Difficulty:***

no satisfying masurement technics, especially no rapid method for dust, thus we generally must use the gradient method which is not very precise and sensitive

lisa | Laboratoire Inter-Universitaire des Systèmes Atmosphériques

The dust deposition event of June 18, 2006 in Banizoumbou

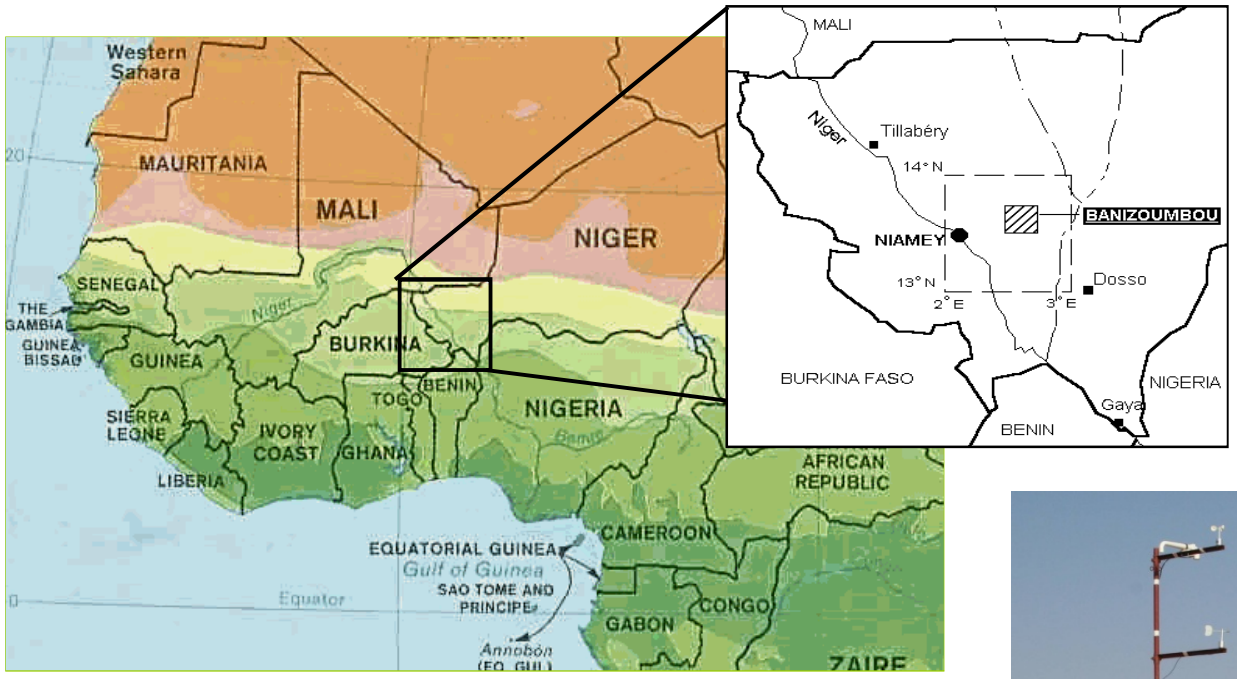

AMMA

lisa | Laboratoire Inter-Universitaire des Systèmes Atmosphériques

Aerosol property	Instruments
Number size distribution (0.3-20 µm diameter)	**GRIMM Optical Particle Counter (OPC) (2 levels: 2 and 6m above ground level)**
Aerosol scattering coefficient	Spectral nephelometer
Aerosol absorption coefficient	Spectral aethalometer
Aerosol backscatter ratio and depolarisation	Spectral Lidar
Mass concentration	**TEOM (2 levels: 2 and 6m above ground level)**
Soil particles horizontal flux	**BNSE / Saltiphone**
P, T, RH, wind speed / dir	**Basic meteorological sensors**
Solar / terrestrial radiation	Pyranometer / pyrgeometer / Shadowband radiometer

Convective Mesoscale Systems

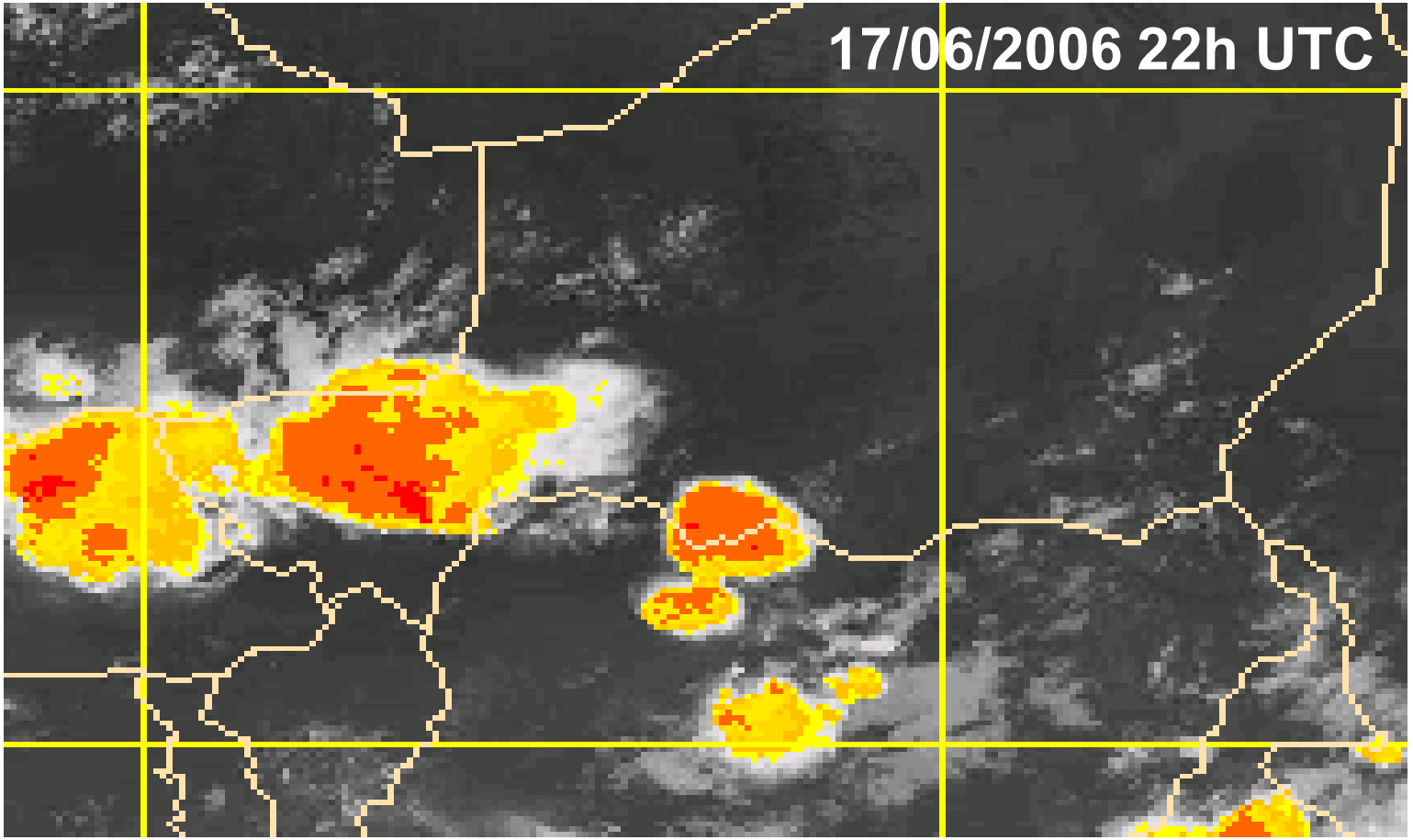

Meteosat brightness temperature.
The coldest values (colored) reveal the convective systems.

lisa | Laboratoire Inter-Universitaire des Systèmes Atmosphériques

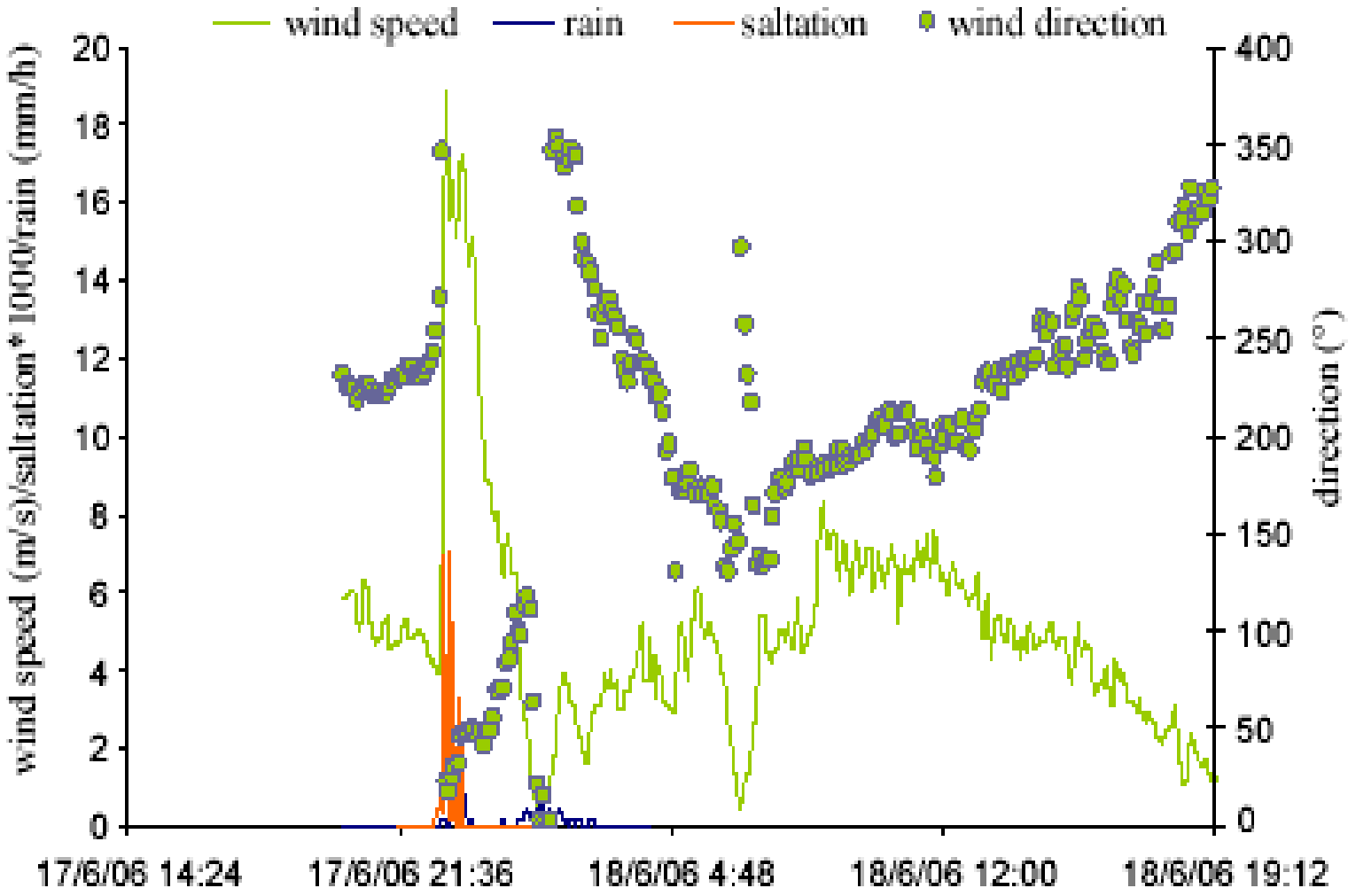

Wind speed and direction at Banizoumbou during the passage of the convective cell and the following day (06/18/2006).
Rain and saltation events are also plotted.

lisa | Laboratoire Inter-Universitaire des Systèmes Atmosphériques

Forward (backward) trajectories starting (ending) at Banizoumbou (central point) computed using Hysplit

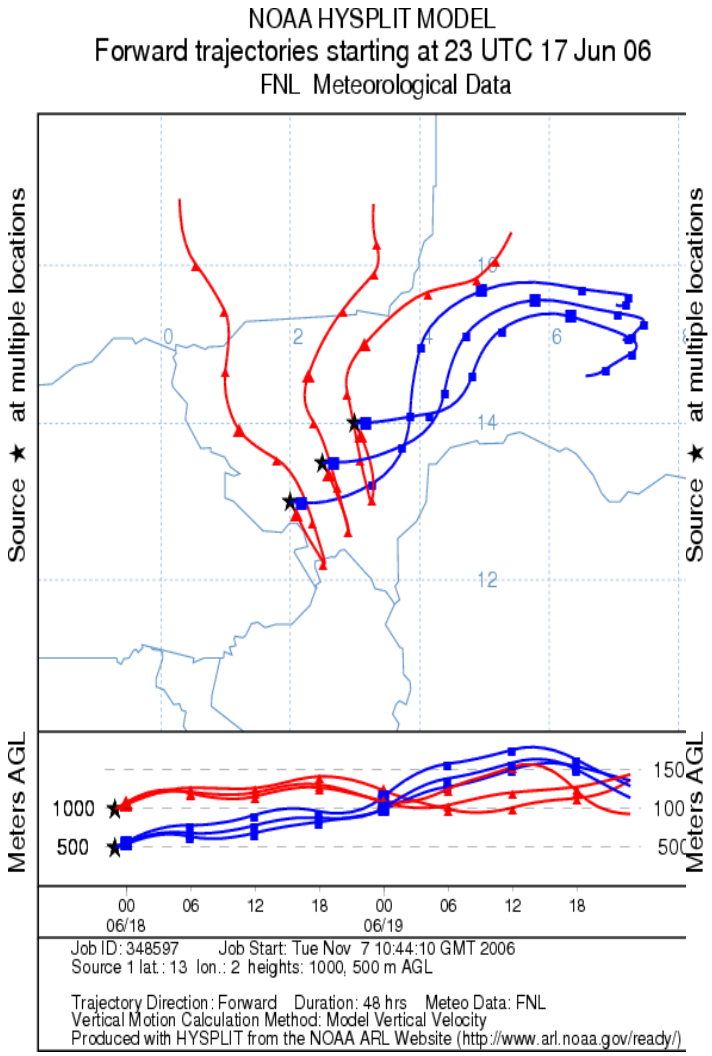

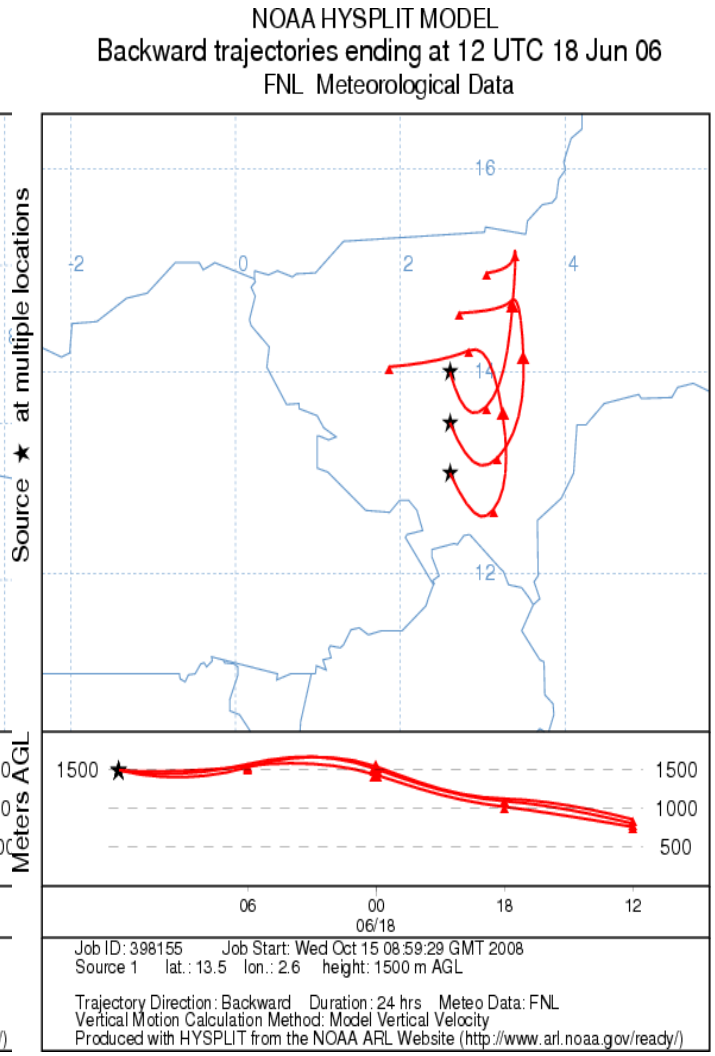

lisa | Laboratoire Inter-Universitaire des Systèmes Atmosphériques

The dust deposition event of June 18, 2006

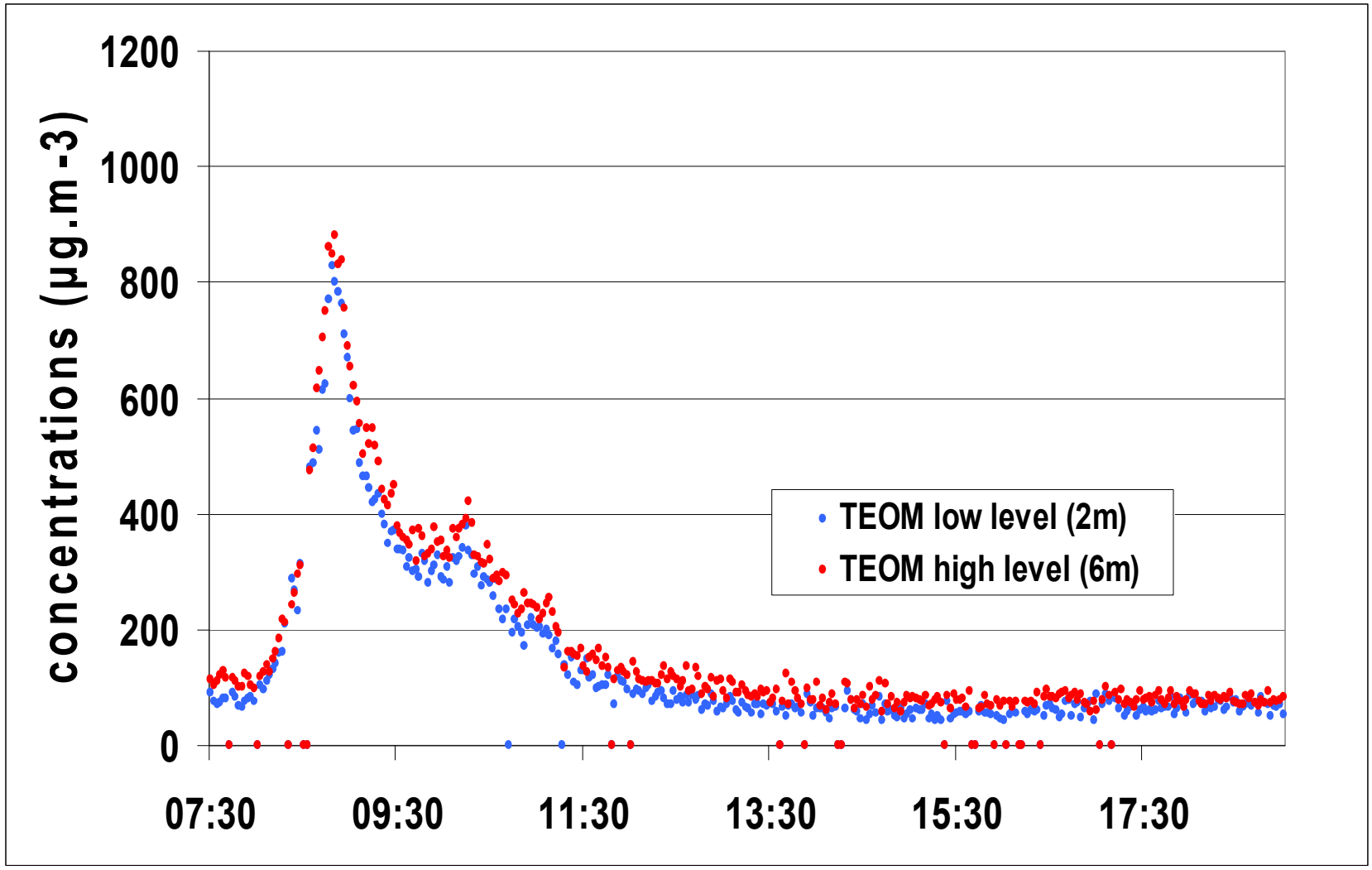

Time evolution of the mass concentrations (µg m^{-3}) measured with TEOMs

lisa | Laboratoire Inter-Universitaire des Systèmes Atmosphériques

The dust deposition event of June 18, 2006

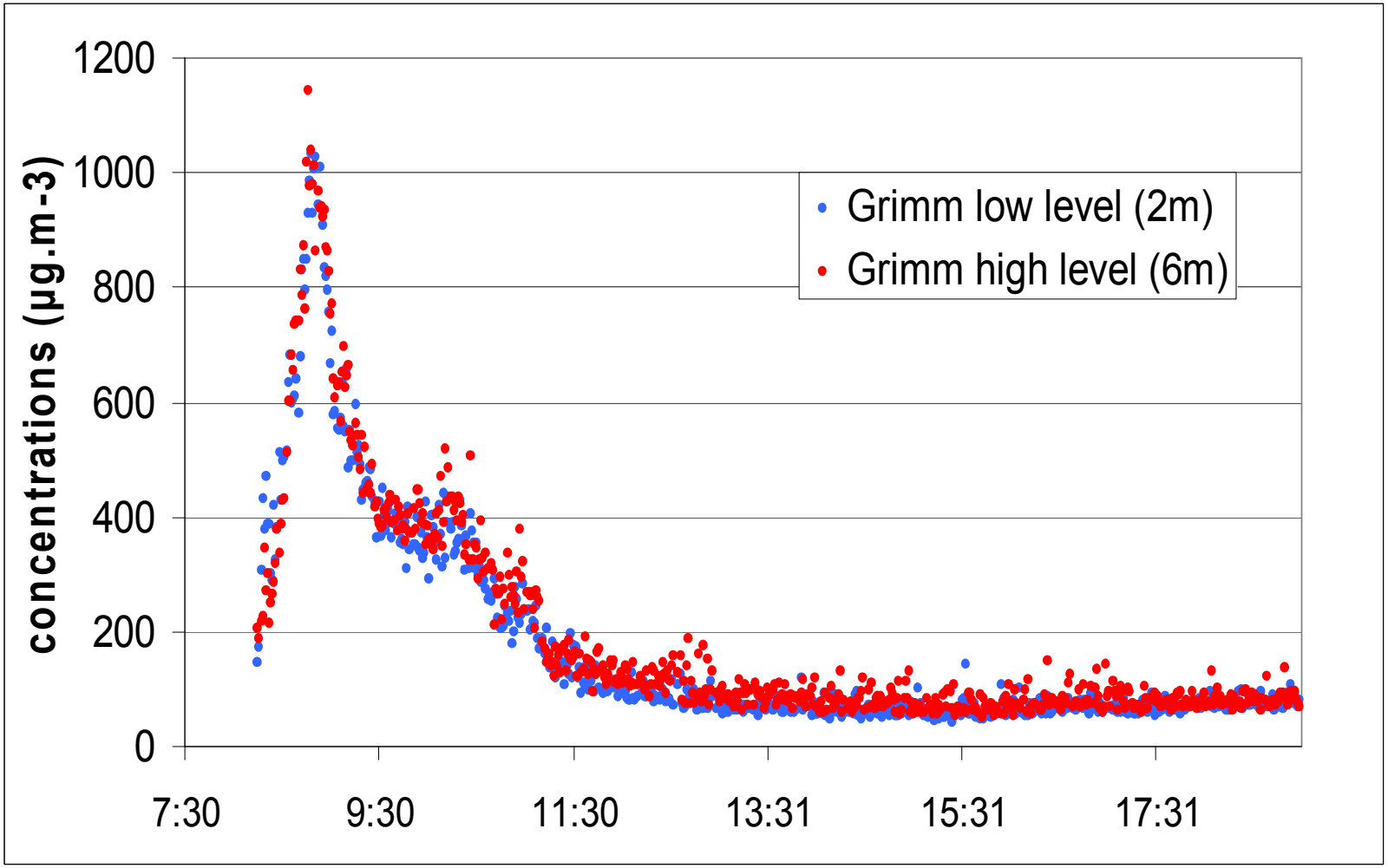

Time evolution of mass concentrations (µg m^{-3}) derived from GRIMMs, assuming spherical particles with a density of 2.5 $g.cm^{-3}$.

lisa | Laboratoire Inter-Universitaire des Systèmes Atmosphériques

Laboratoire Inter-Universitaire des Systèmes Atmosphériques

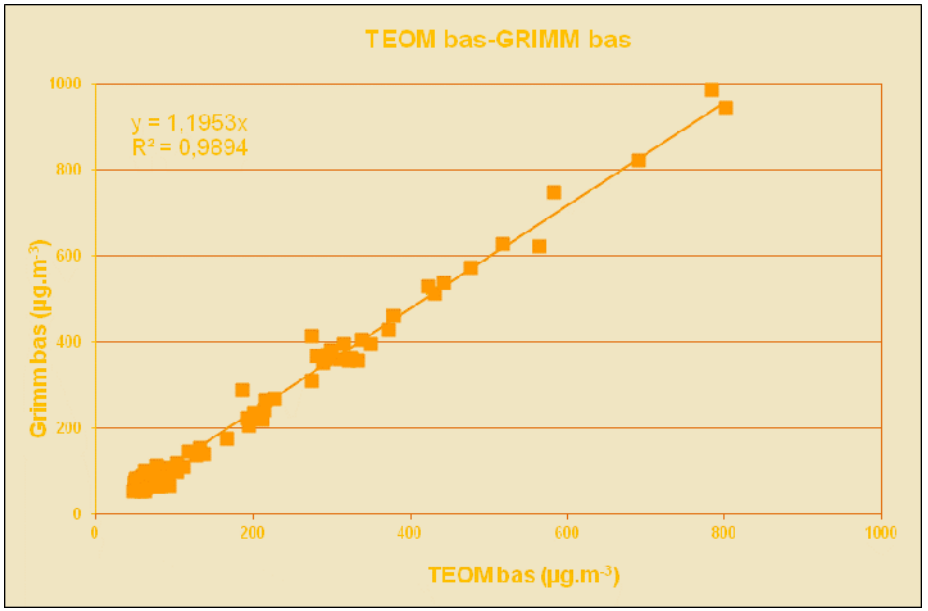

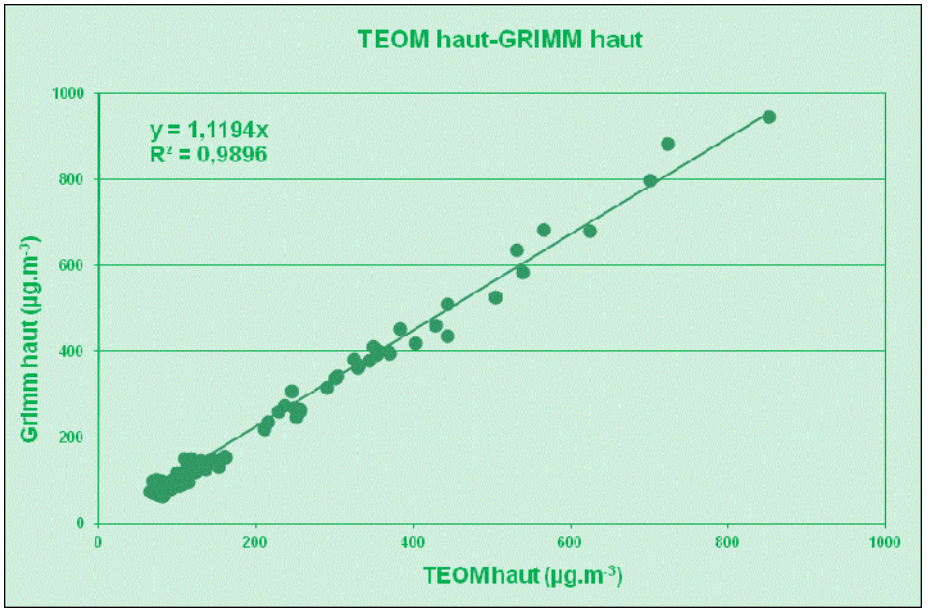

comparisons of mass concentrations measured by TEOM and computed from GRIMM number measurements

The dust deposition event of June 18, 2006

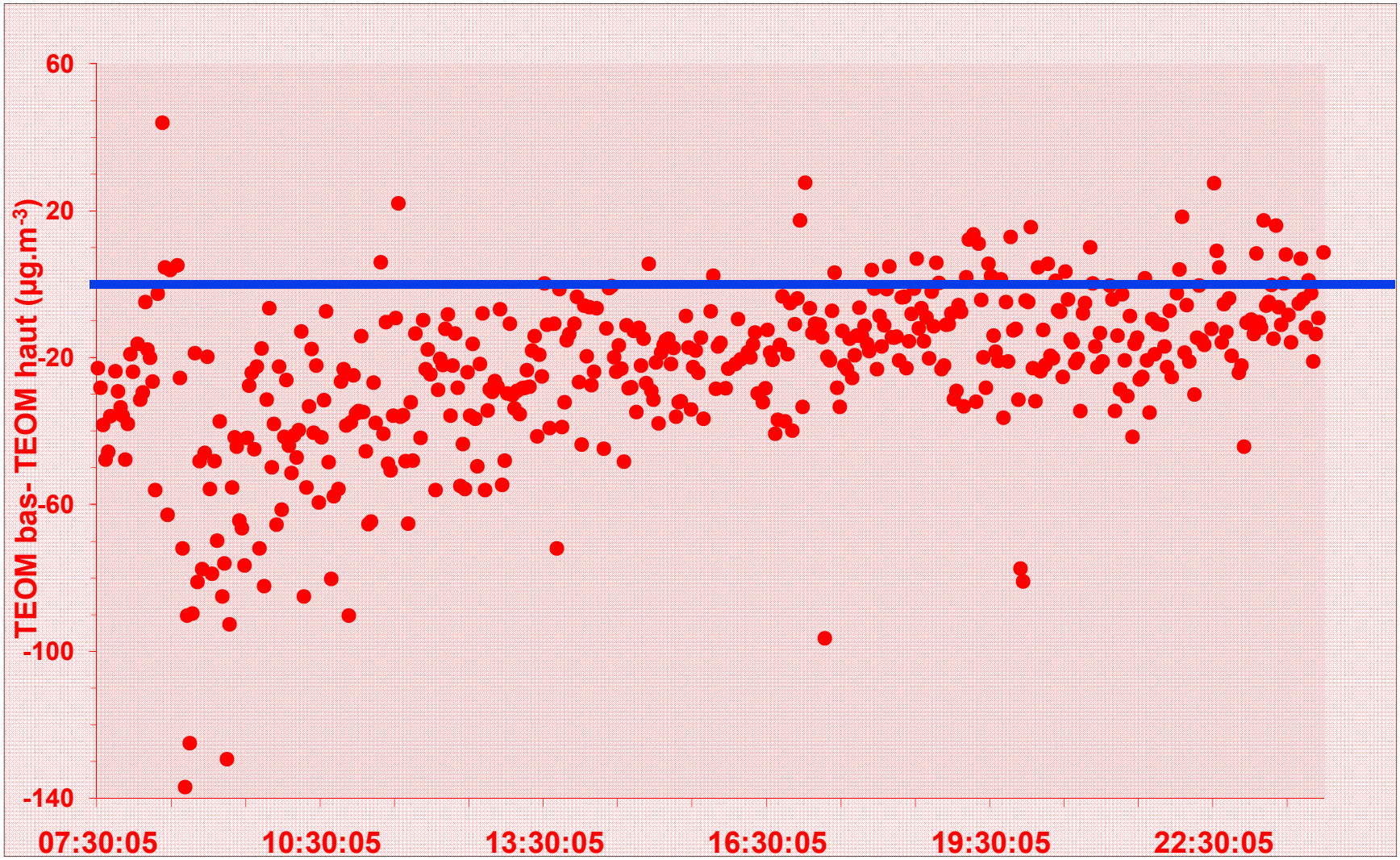

Differences in measured mass concentrations ($TEOM_{low} - TEOM_{high}$) in $\mu g.m^{-3}$ on June 18, 2006

lisa | Laboratoire Inter-Universitaire des Systèmes Atmosphériques

The dust deposition event of June 18, 2006

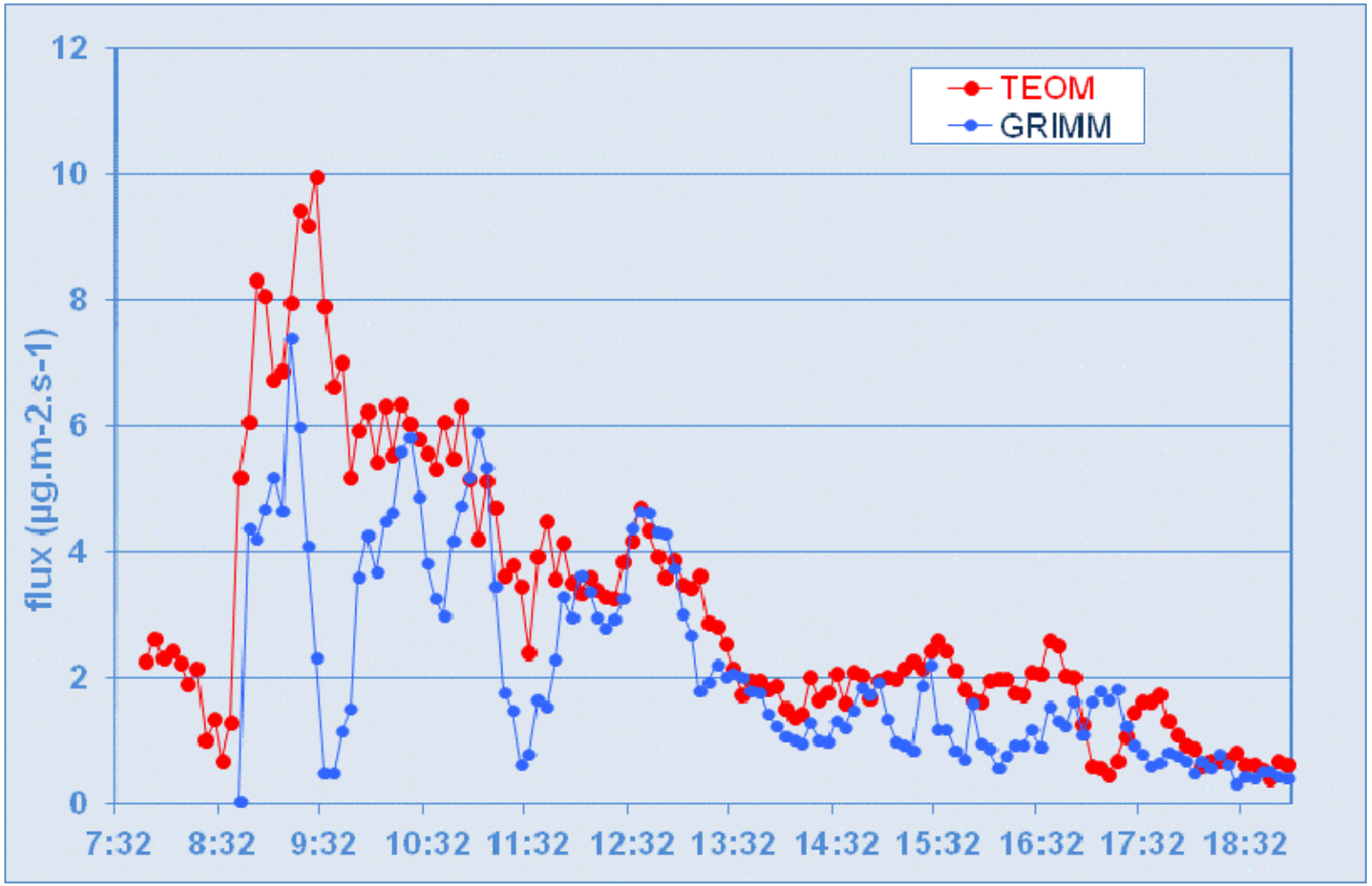

Time evolution of deposition fluxes (20-mn sliding averages).

lisa | Laboratoire Inter-Universitaire des Systèmes Atmosphériques

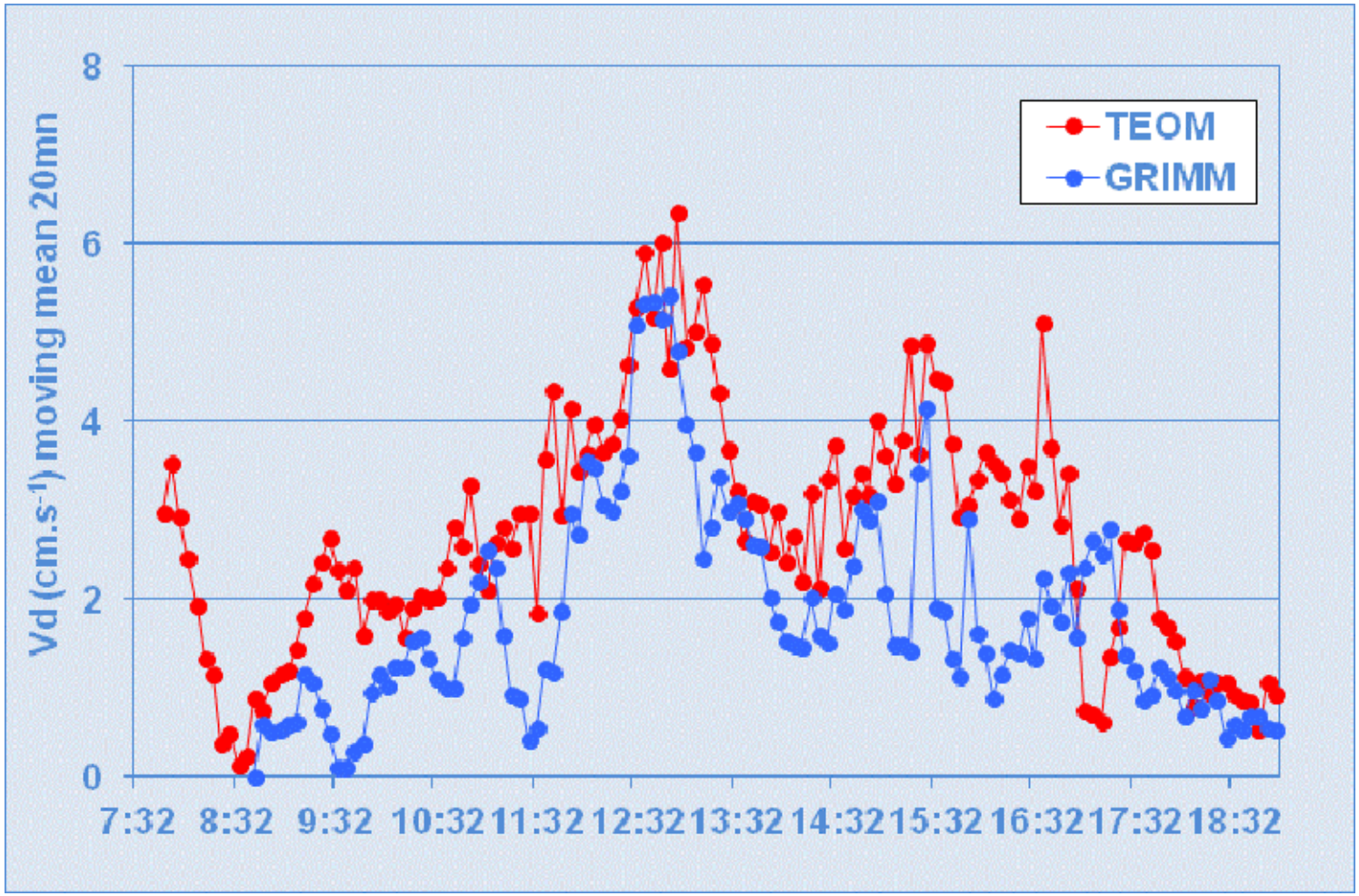

Time evolution of deposition velocities (20-mn sliding averages).

lisa | Laboratoire Inter-Universitaire des Systèmes Atmosphériques

DRY DEPOSITION MODELING

Dry deposition velocities are calculated using the pseudo resistance approach (Wesely,1989; Zhang et al., 2003)

U^* is derived from measured meteorological parameters ($z_0 = 6\times10^{-4}$ m)

□ $\boldsymbol{V_d}$ is modeled for each GRIMM channel using its corresponding median diameter. $\boldsymbol{V_{db}}$ is the bulk dry deposition velocity and represent a mean dry deposition velocity:

$$V_{db} = \sum_{i=1}^{15} V_{di} \times C_i$$

V_{di}, dry deposition velocity for each channel, (cm s^{-1})

C_i, relative mass concentration measured in each channel (%)

lisa | Laboratoire Inter-Universitaire des Systèmes Atmosphériques

The dust deposition event of June 18, 2006

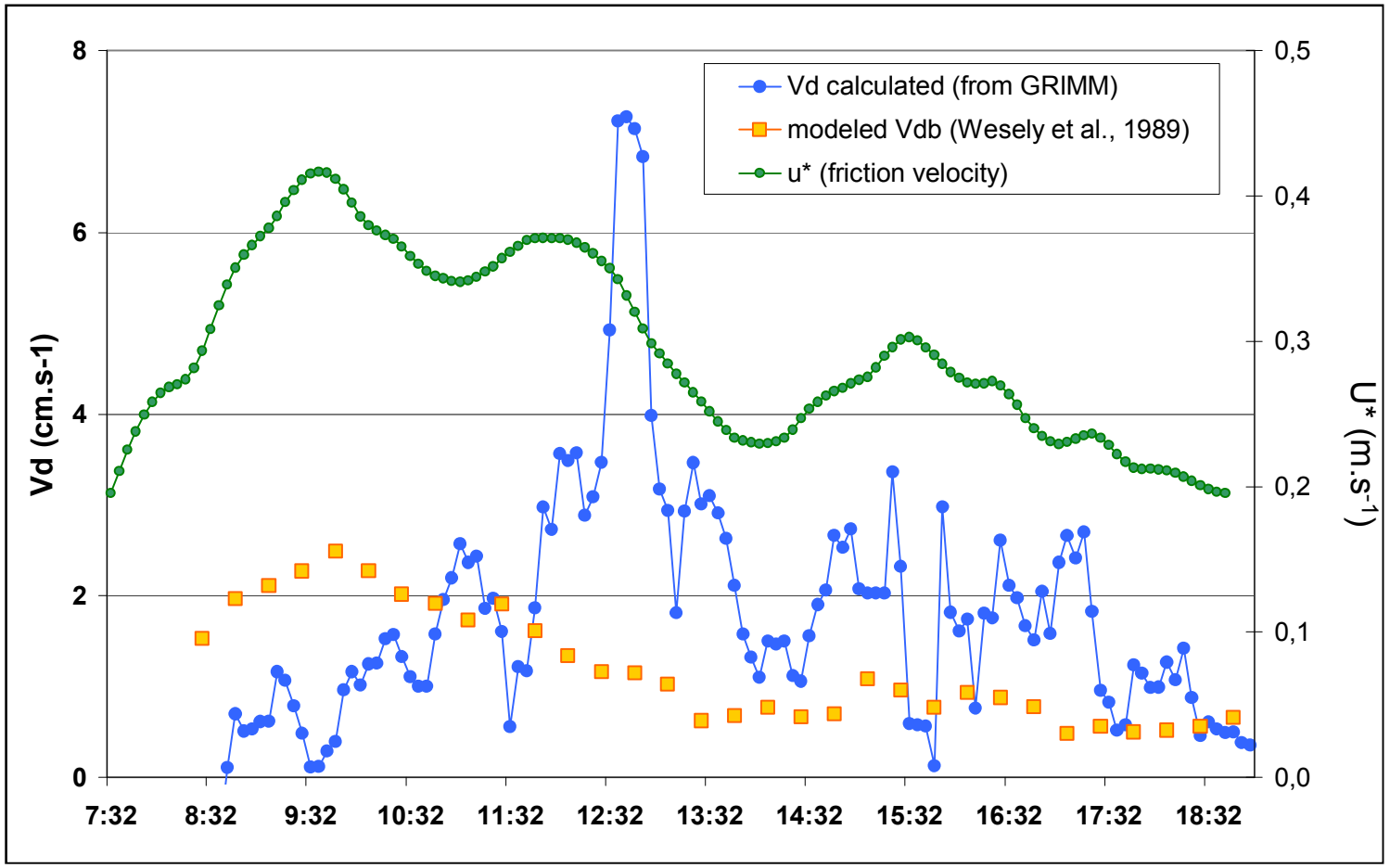

Temporal evolution of the modeled (bulk) and observed (with GRIMM) averaged dry deposition velocity (20-mn sliding averages).

lisa | Laboratoire Inter-Universitaire des Systèmes Atmosphériques

The dust deposition event of June 18, 2006

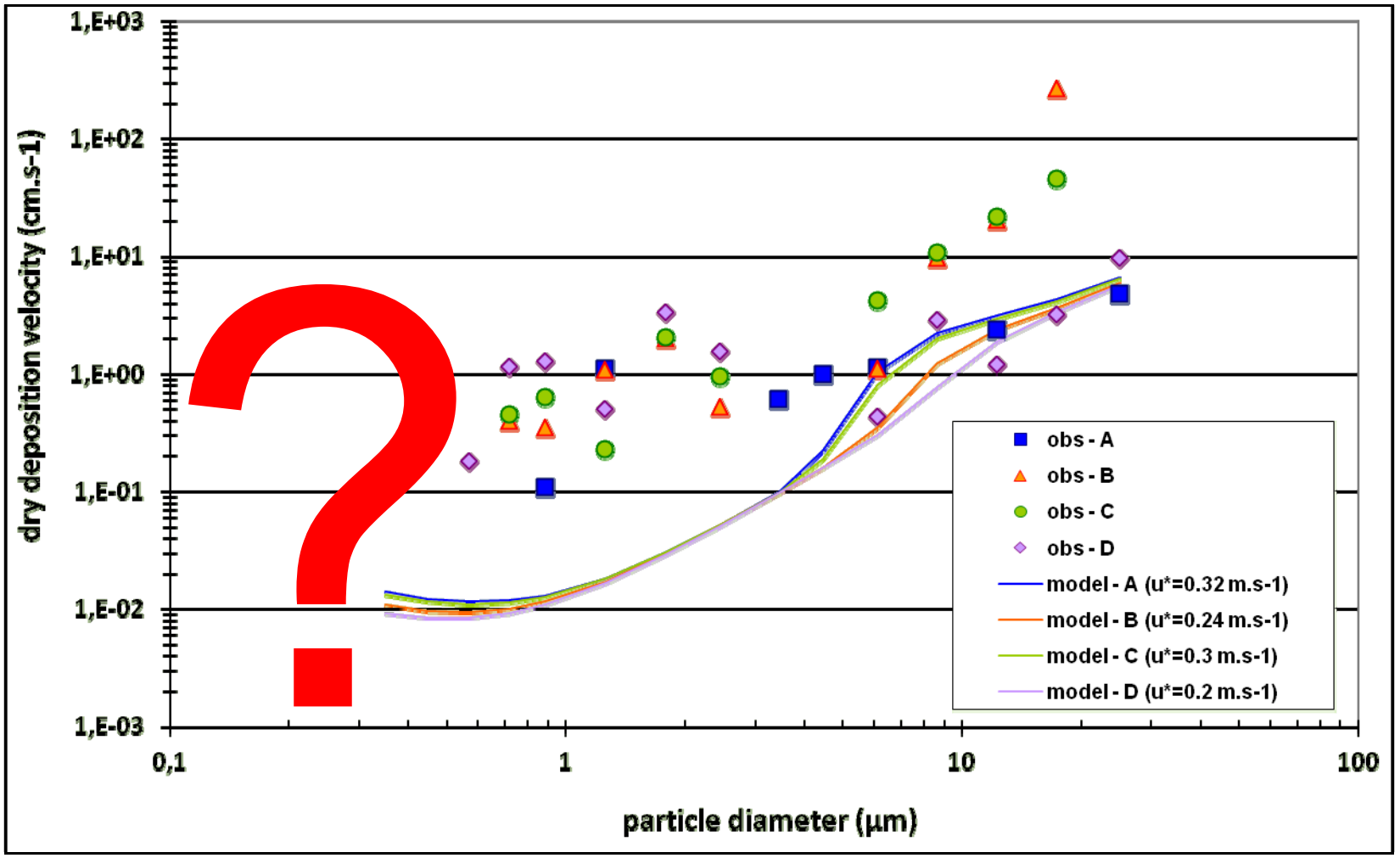

Model and observed dry deposition velocity as a function of particle size during the 4 time slots A-D

lisa | Laboratoire Inter-Universitaire des Systèmes Atmosphériques

- Dust concentration and deposition continuous measurements

❑ ***Problem:***

No sufficient data on dust deposition to constrain dust model simulations, very few joint deposition measurements and dust mass concentration over long periods

❑ ***Difficulty:*** *access to source regions, capability of measurements, costs, …*

The AMMA Sahelian Dust transect

To investigate the variability of the mineral dust content over the North of Africa, a "**Sahelian Dust Transect**" (SDT) composed of three stations has been deployed in the framework of the international program African Monsoon Multidisciplinary Analysis (AMMA) (Marticorena et al., 2010).

The three stations, namely Banizoumbou (Niger), Cinzana (Mali) and M'Bour (Senegal) are located at between 13°N and 14°N along the east-west main pathway of the Saharan and Sahelian dust toward the Atlantic Ocean.

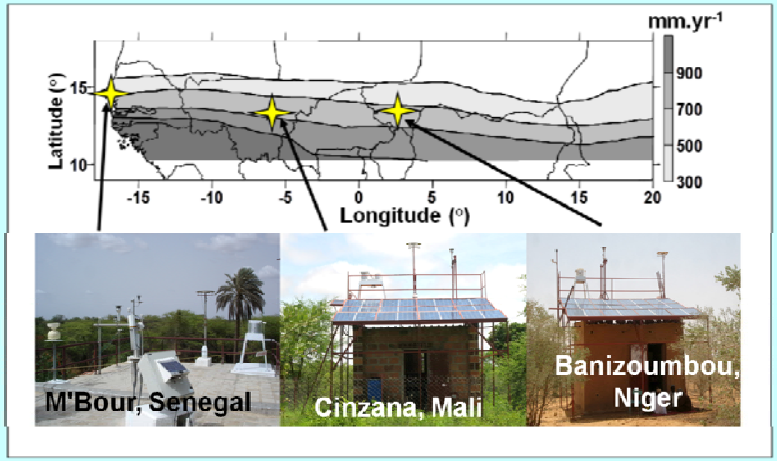

Figure 1: Location of the stations and mean (1990-2007 annual precipitation rates (from Lebel and Ali, 2009)

The objective of the SDT is to provide for the period 2005–2008, a set of aerosol measurements to better **constrain the mineral dust budget** at the regional scale, namely :

- Column-integrated aerosol optical depth
- Surface mass concentration
- Aerosol vertical profile
- **Total and wet deposition fluxes.**

Total deposition sampler

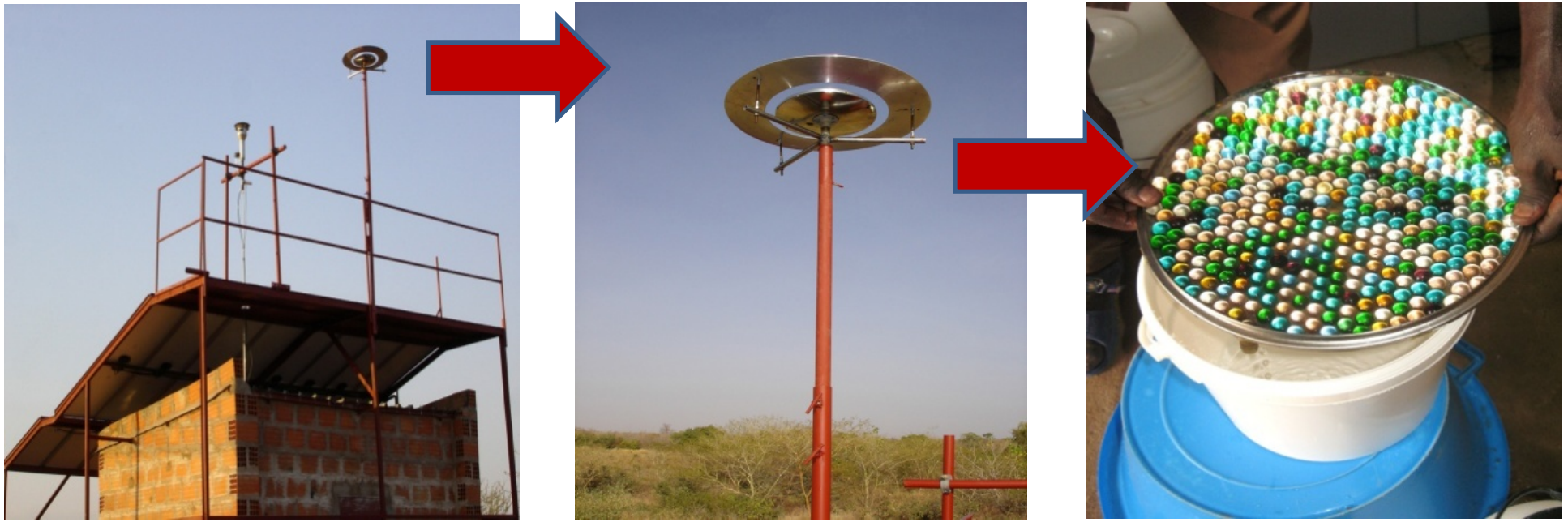

The sampler is an inverted « frisbee » trap equipped with a flow deflector ring (Wiggs et al. 2002) and filled with marbles. Wind tunnel experiments shows that this device has the highest efficiency (Sow et al., 2006) .

Deposition samples are collected weekly since January 2006 (i.e., ~900 samples in 6 years).

Sample collection

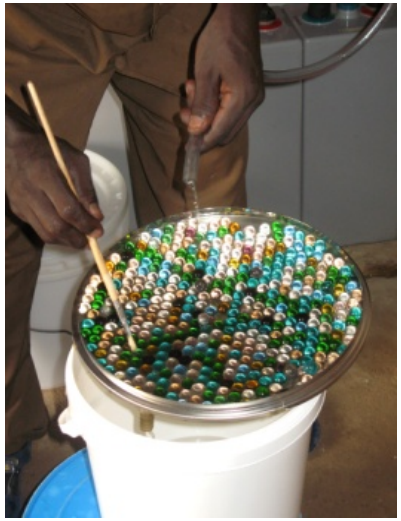

Samples are collected with water, three to four decantation cycles of ~6 hours are performed before the removal of the excess water. The sample is then dried at 50°C. The collected mass is weighted three times..

Wet deposition sampler

Wet deposition is collected using an automatic tip bucket system. A precipitation sensor, allows the wet deposition collector to get open when precipitation starts and to close when precipitation stops.

Wet deposition samples are collected for each rain event (i.e., ~700 samples in 6 years).

Dust concentrations and local emissions

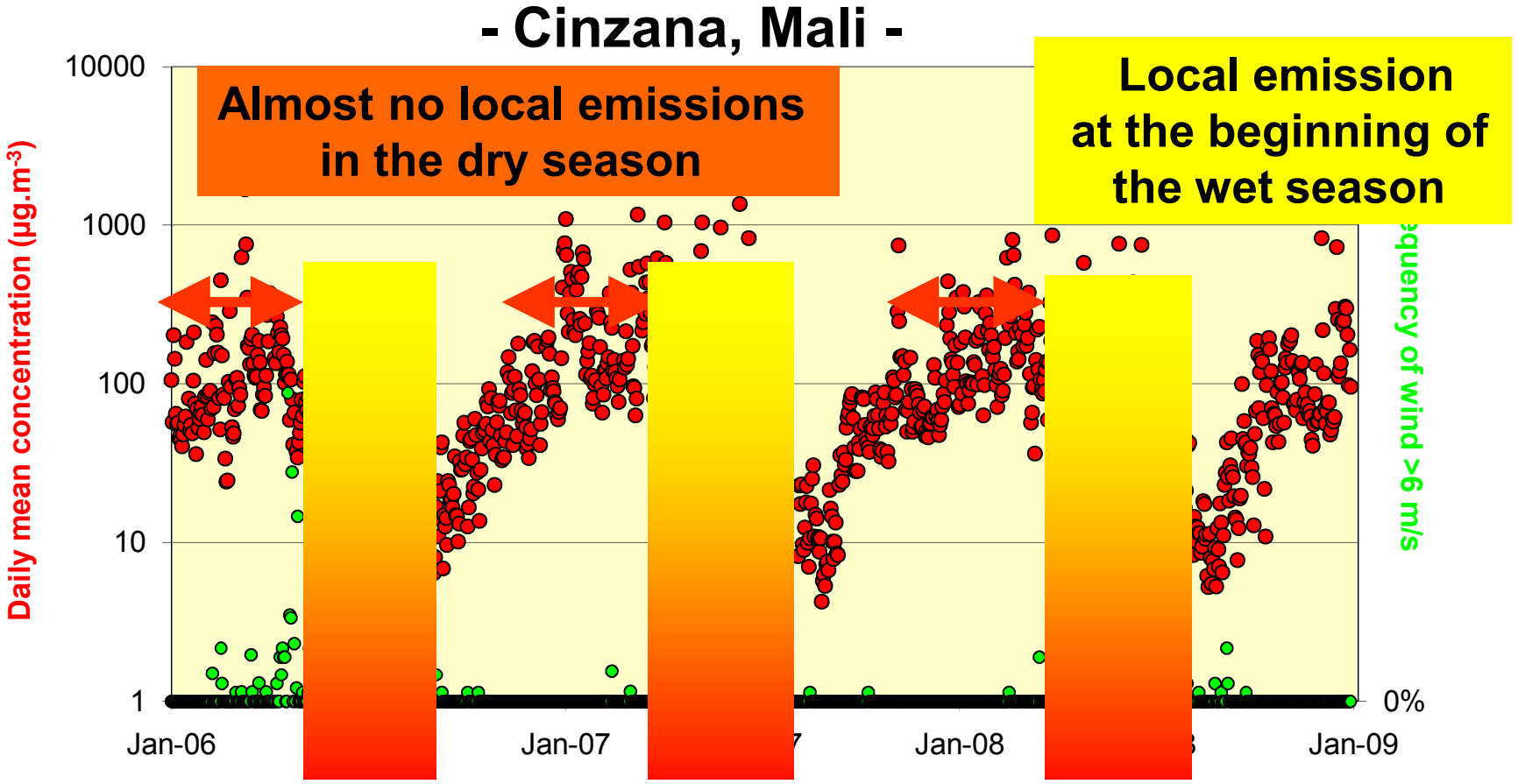

⇨**The annual maximum in concentration is observed during transport of Saharan air masses (low layer); local emissions are observed at the beginning of the rainy season** ***(Marticorena et al., ACP, 2010)***

Annual deposition fluxes measured along the three stations of the SDT

ANNUAL TOTAL DEPOSITION FLUXES

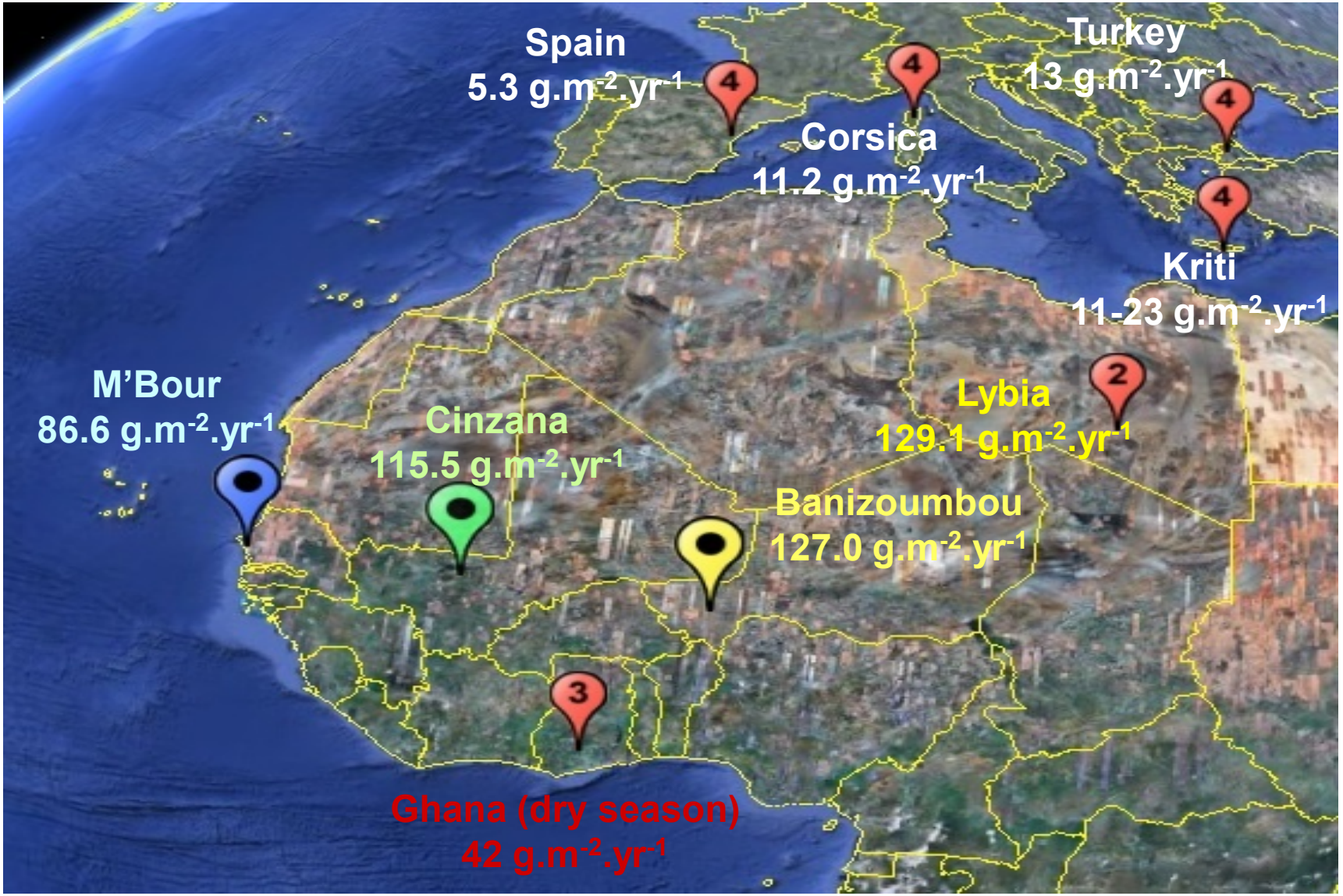

Annual deposition fluxes measured over the North of Africa and in the Mediterranean basin ((2) O'Hara et al. (2006); (3) Breuning-Madsen and Awadzi (2005); (4) Avila et al. (1997), Bergametti et al. (1989), Kubilay et al. (2000) ; Mattson and Nehlen (1996))

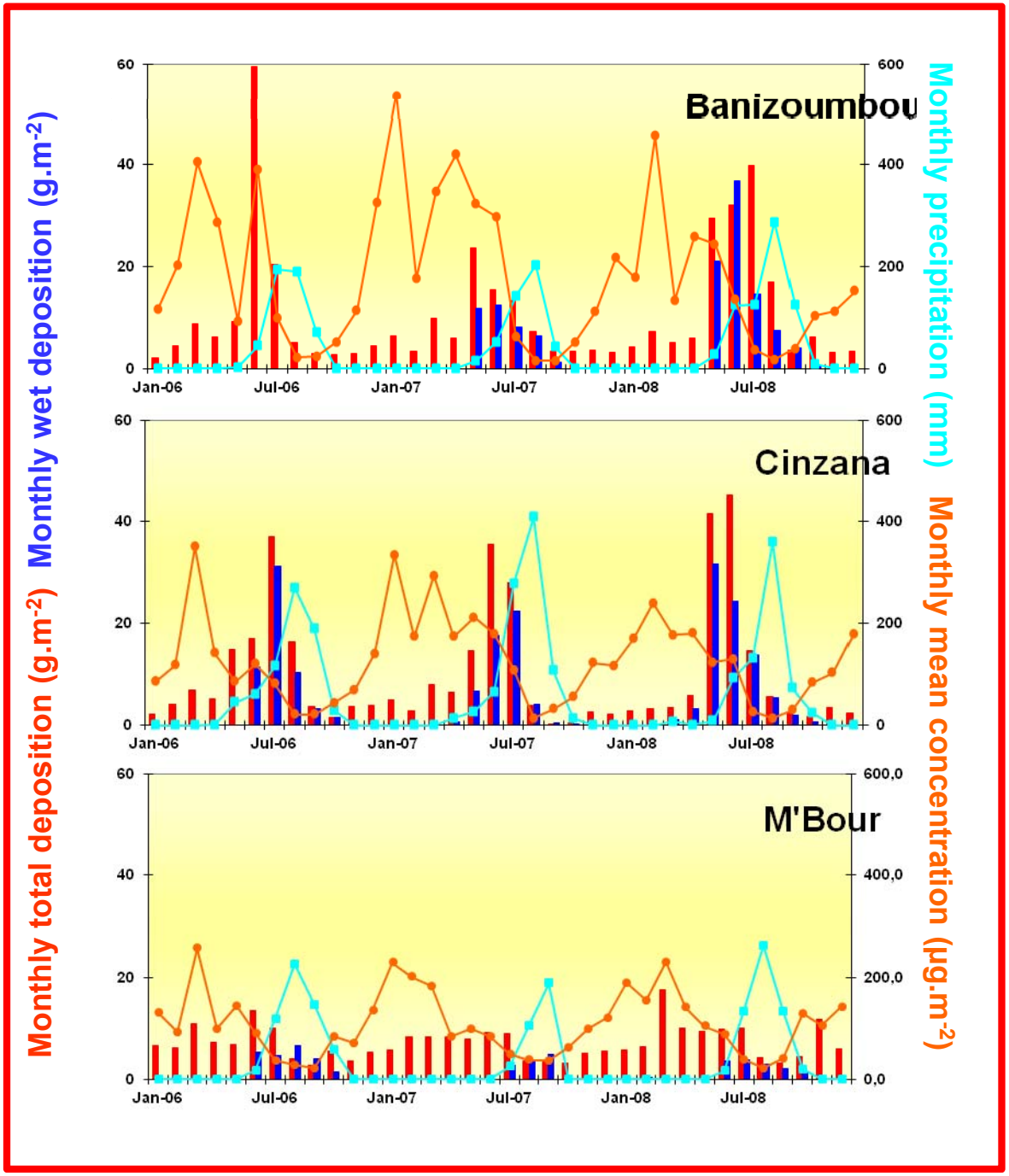

Monthly total and wet deposition fluxes, precipitations and mean atmospheric dust concentrations at the three stations of the STD from 2006 to 2008 (note that wet deposition measurements are not available for the wet season 2006 in Banizoumbou)

Total deposition fluxes exhibit a clear seasonal cycle in Banizoumbou and Cinzana. The highest values are recorded at the beginning of the rainy season, when precipitation occurs while atmospheric dust concentrations are still high.

The seasonal cycle in M'Bour is mainly driven by dry deposition occuring in spring and summer.

Whatever the stations, there is no clear and simple link between dust concentrations and total deposition fluxes in the dry season at the monthly scale.

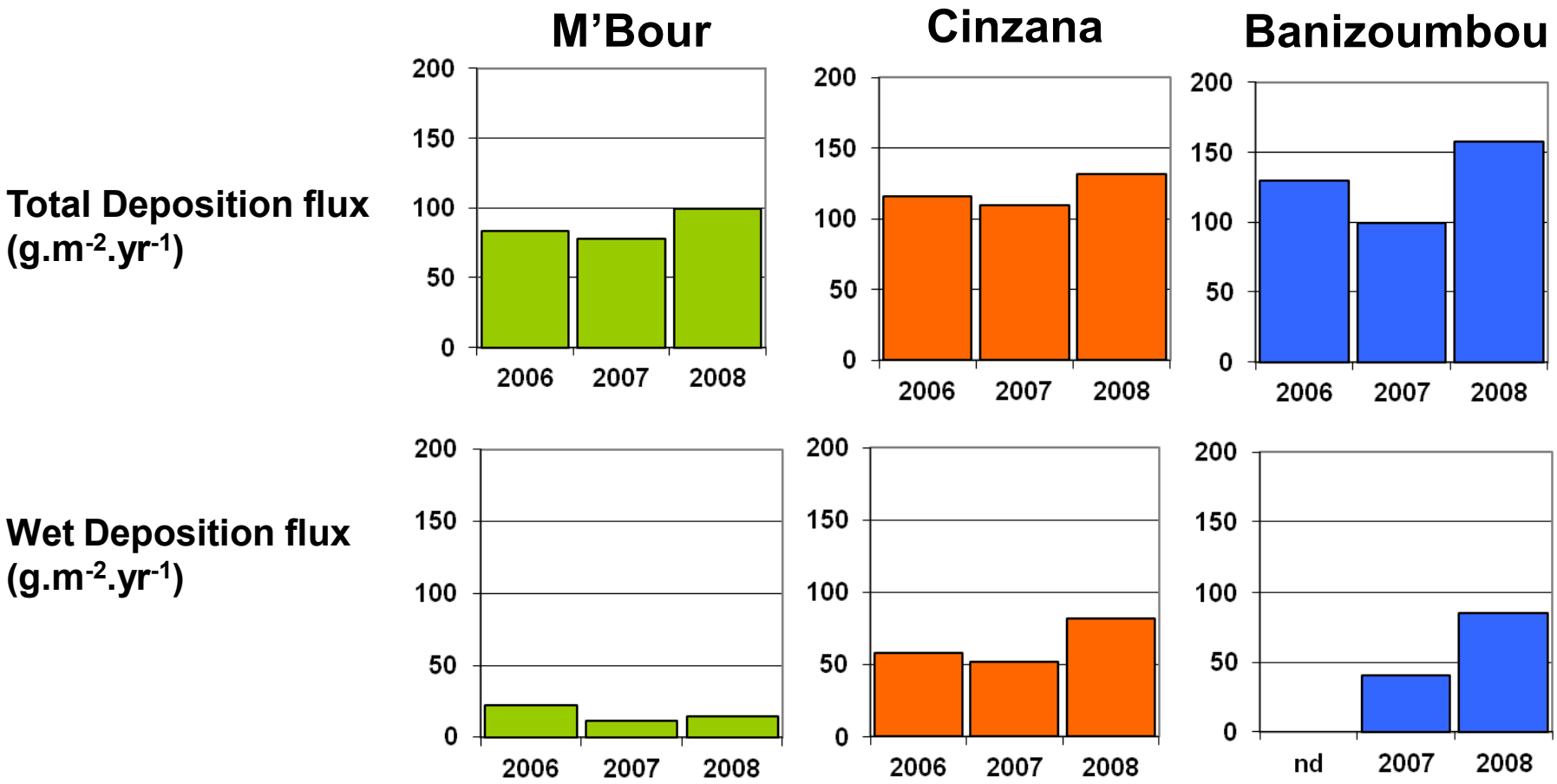

Annual total deposition fluxes ranges from 78 (M'Bour in 2007) to 158 $g.m^{-2}.yr^{-1}$ (Banizoumbou in 2008). The year-to-year variability is low in M'Bour (σ =11%) but a little higher in Banizoumbou and CInzana (σ = 30%). For these two stations, this variability is mainly driven by changes in wet deposition fluxes.

2008 in Banizoumbou as an exemple

Maximum of **concentration** first, then of **deposition** and finally of **precipitation**

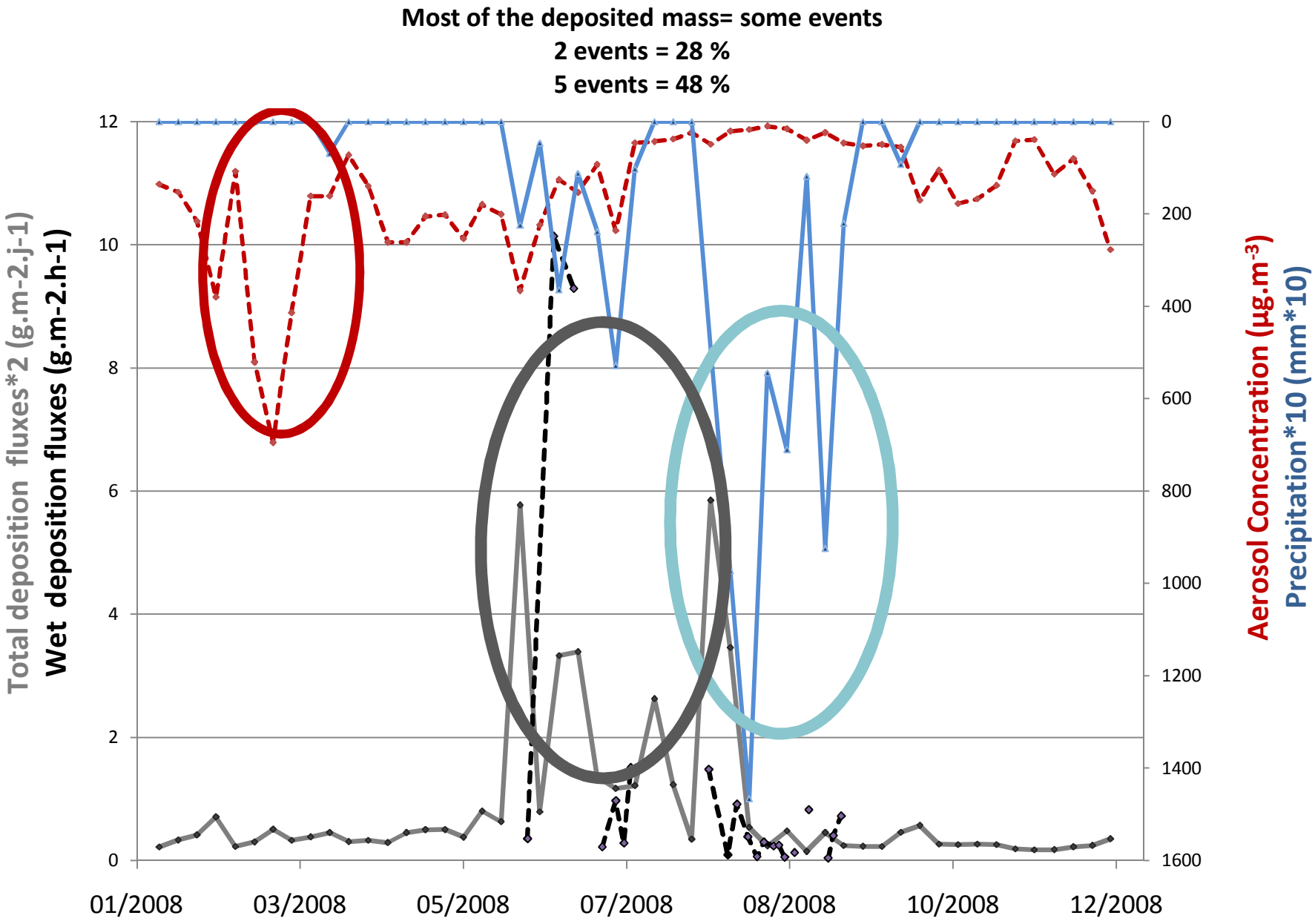

Wet Deposition Fluxes

Wet Flux = Λ [Dust]

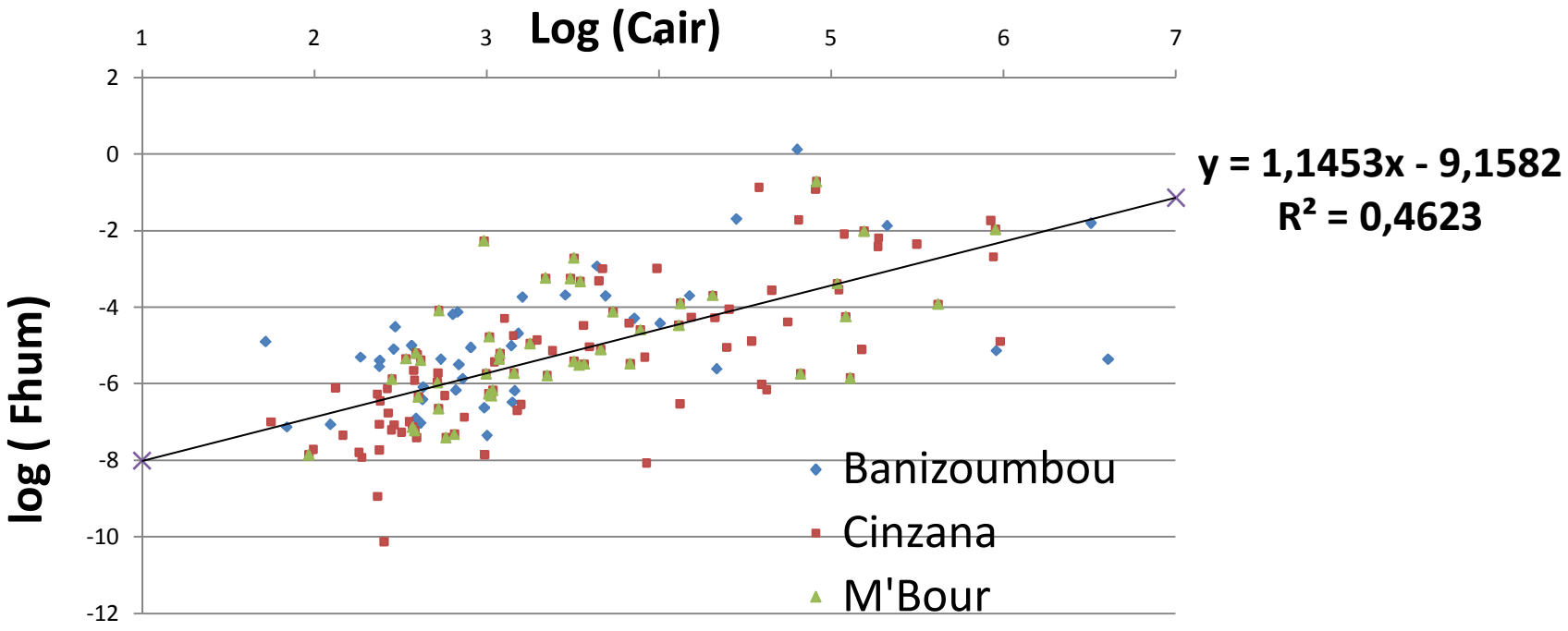

- ***A trend of increasing the wet flux when the dust concentration increases***
- ***However, it remains a large spread of data***

Scavenging efficiency

Λ = (wet deposition flux)/[Dust] = f(precipitation)

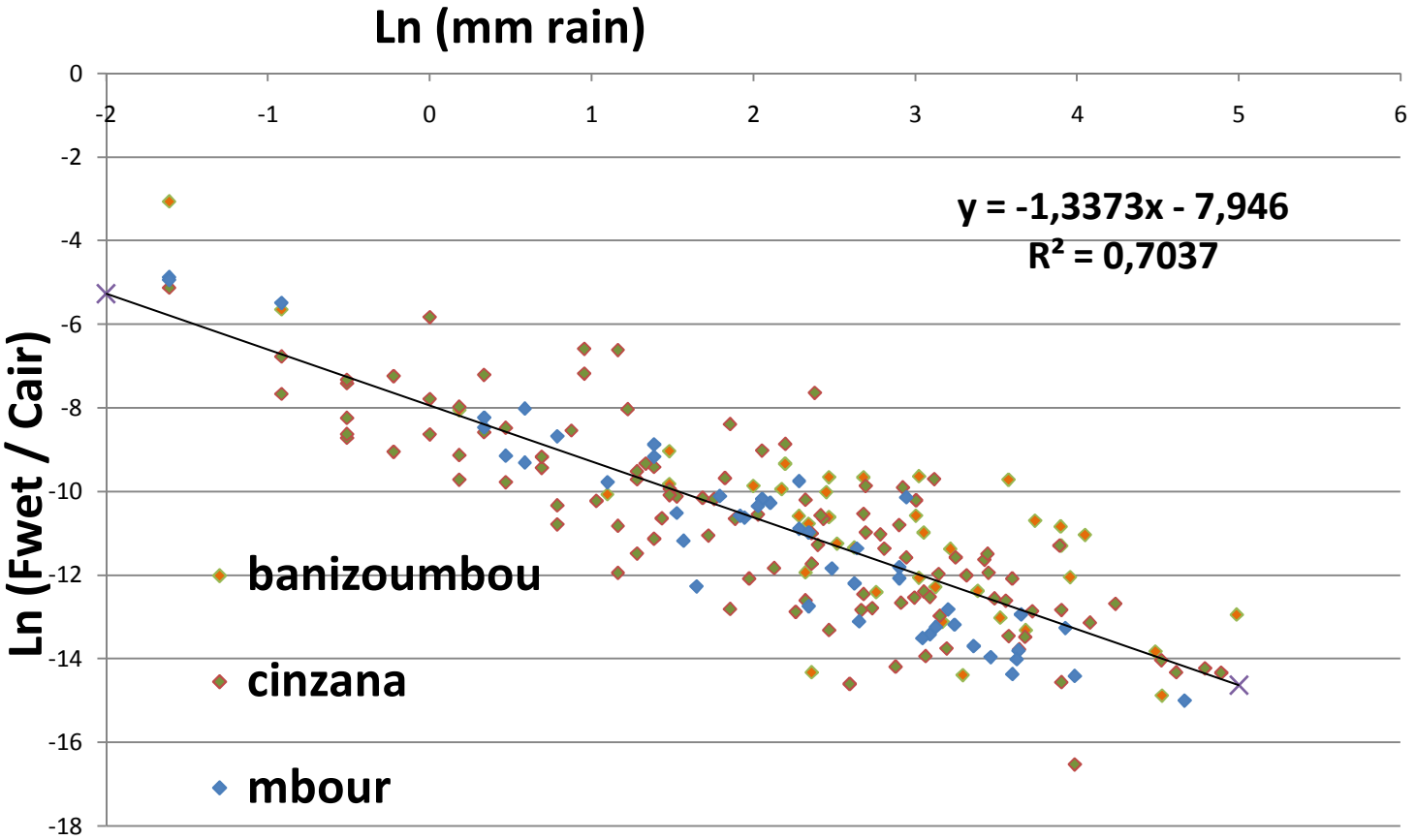

Not constant but decreases with the precipitation amount

Stations of the Mediterranean deposition network

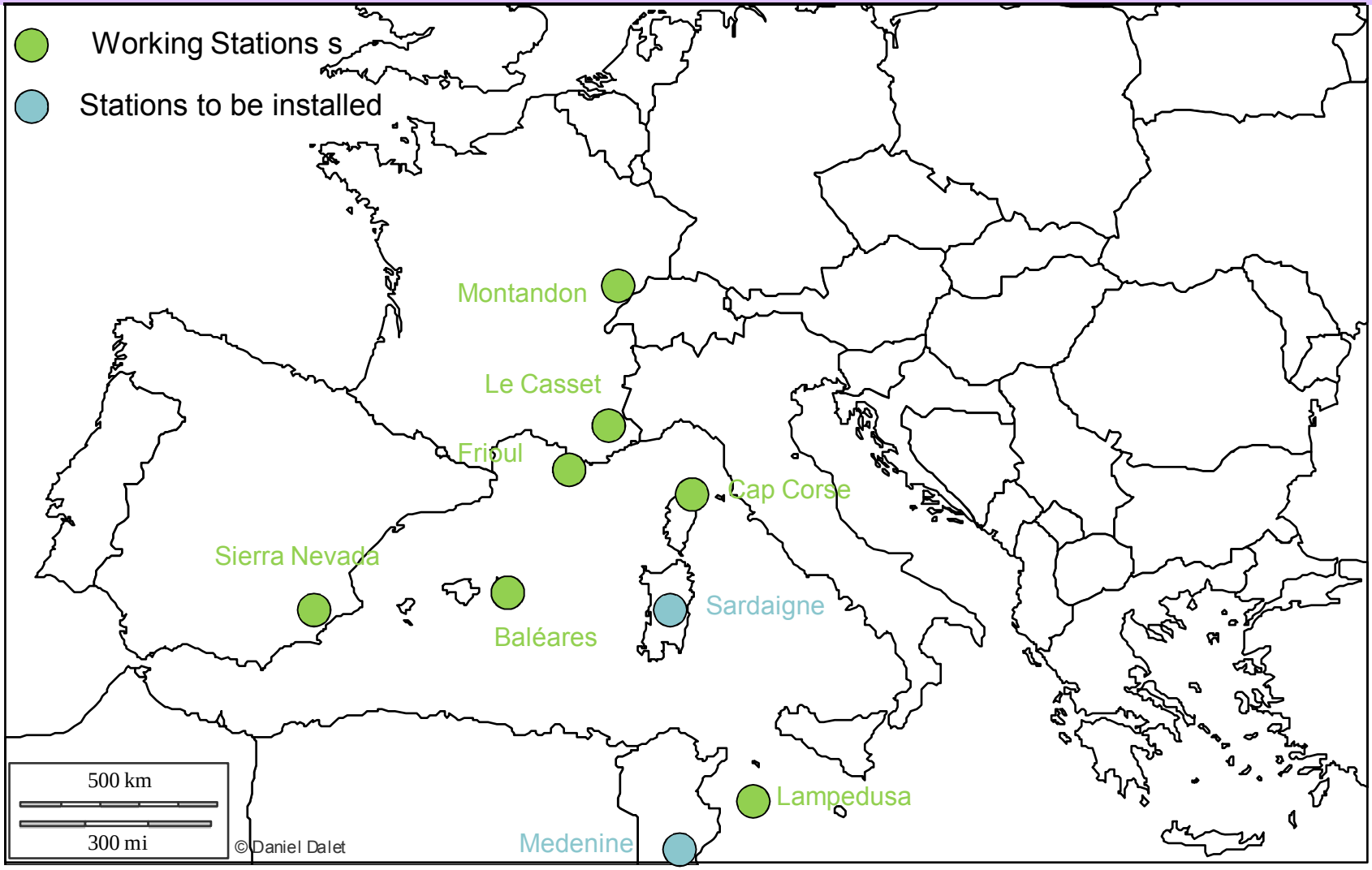

MONTANDON

FRIOUL

CORSICA

Some of the stations

LAMPEDUSA

BALEARES

CONCLUDING REMARKS

Large uncertainties on simulated dust deposition

- *Emission strength*
- *Initial mass size distribution*
- *Removal processes including transport and precipitation*
- *Treatment of the size dependent processes*

Needs:

- *Measurements of the size distribution in source-regions over a large size range*
- *Implementation of international deposition network, with standardized instruments and procedure, and performing measurements close to and far from the source areas*


Thank you for
your attention

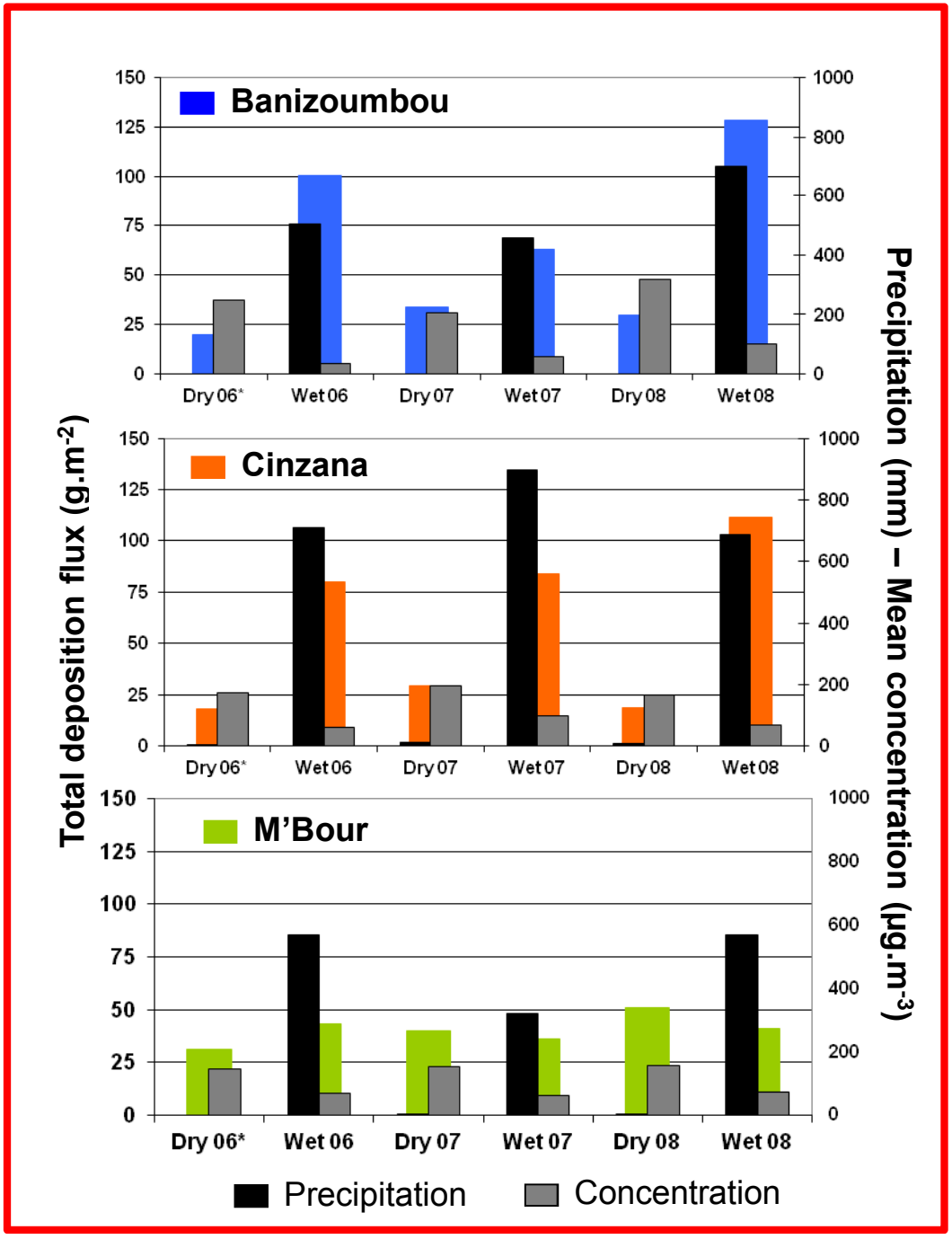

Total deposition fluxes, precipitation and mean atmospheric dust concentrations during the dry (Nov-Apr) and wet seasons (May-Oct) of 2006, 2007 and 2008 at the three stations of the SDT (Dry season of 2006: *Jan-Apr)

Due to the contribution of wet deposition, total deposition fluxes are higher during the wet season than in the dry season, despite lower monthly mean atmospheric dust concentrations.

Conclusions et perspectives

- taux de récupération des données est supérieur à 90%

- flux de dépôt total est d'environ 100 $g.m^{-2}.a^{-1}$
- Gradient de dépôt -> gradient de concentration
- Cohérence avec les données publiées -> distance zone source
- Variabilité de la contribution du flux humide
  (70% au Mali ; 10 % au Sénégal)

- flux de dépôt -> Paramètre clé = concentration
- flux de dépôt humide -> diminution du coefficient de lessivage avec la quantité de pluie
- flux de dépôt sec -> autres paramètres ?

Améliorer le bilan de masse et paramétrer les dépôts

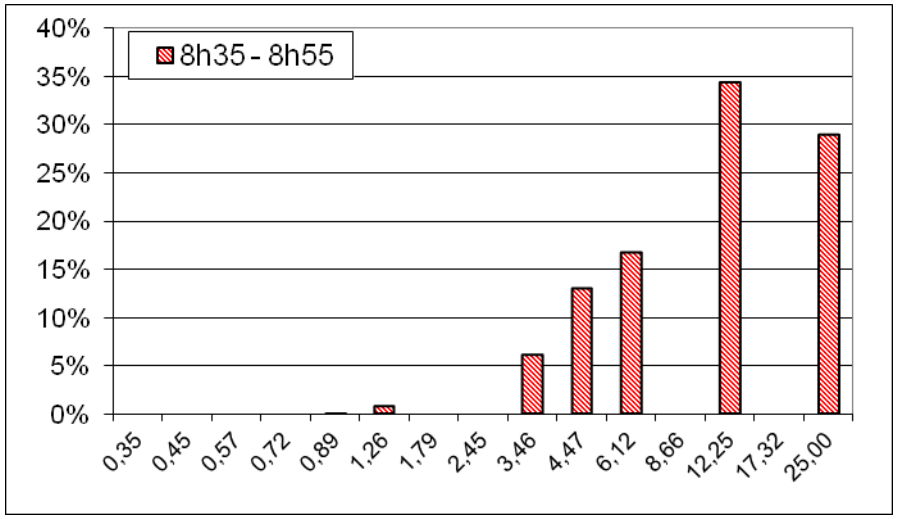

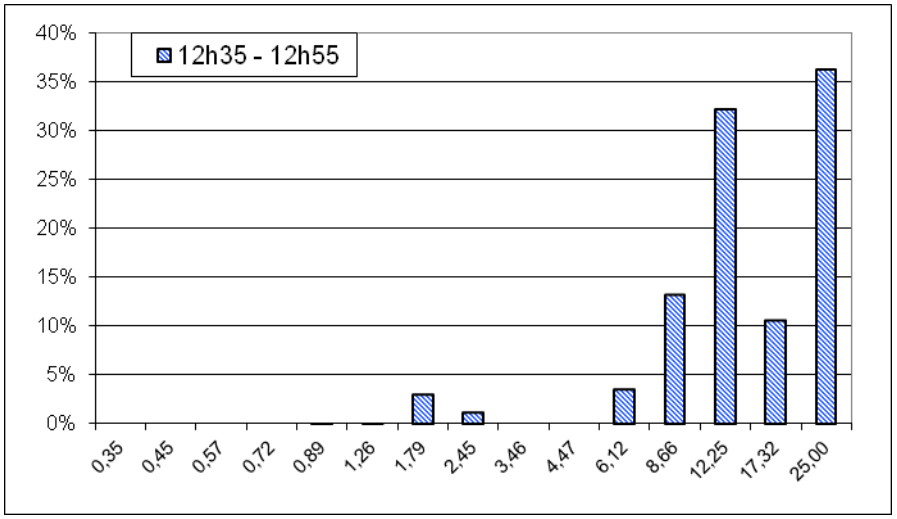

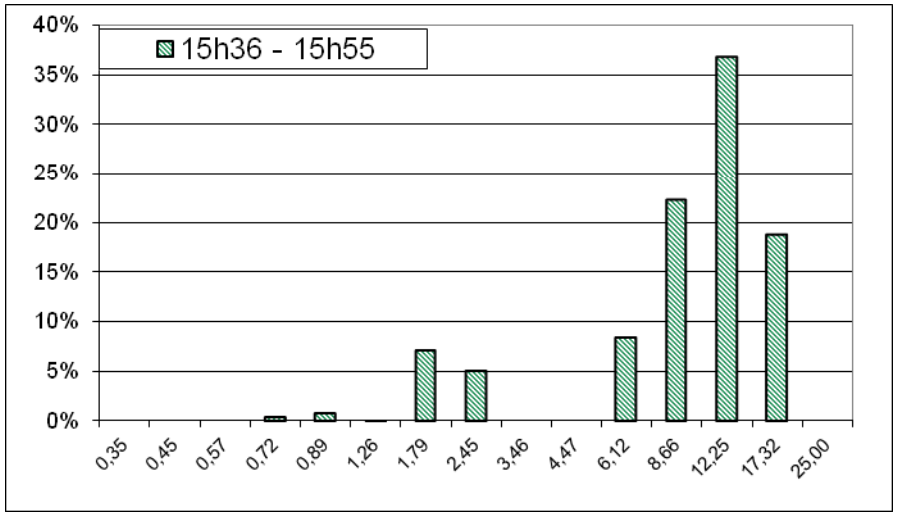

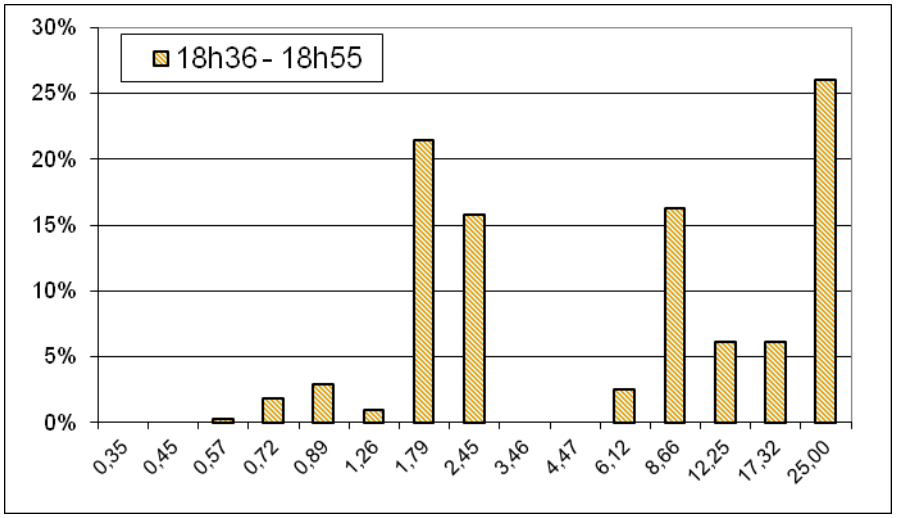

Relative contribution of particle size classes to the deposition flux during 4 time periods.

Les flux de dépôt total mensuel

Cycle saisonnier marqué à Banizoumbou et Cinzana (dépôt humide)

Min à M'Bour = 4 g.m-².mois-1
Max à Banizoumbou = 60 g.m-².mois-1

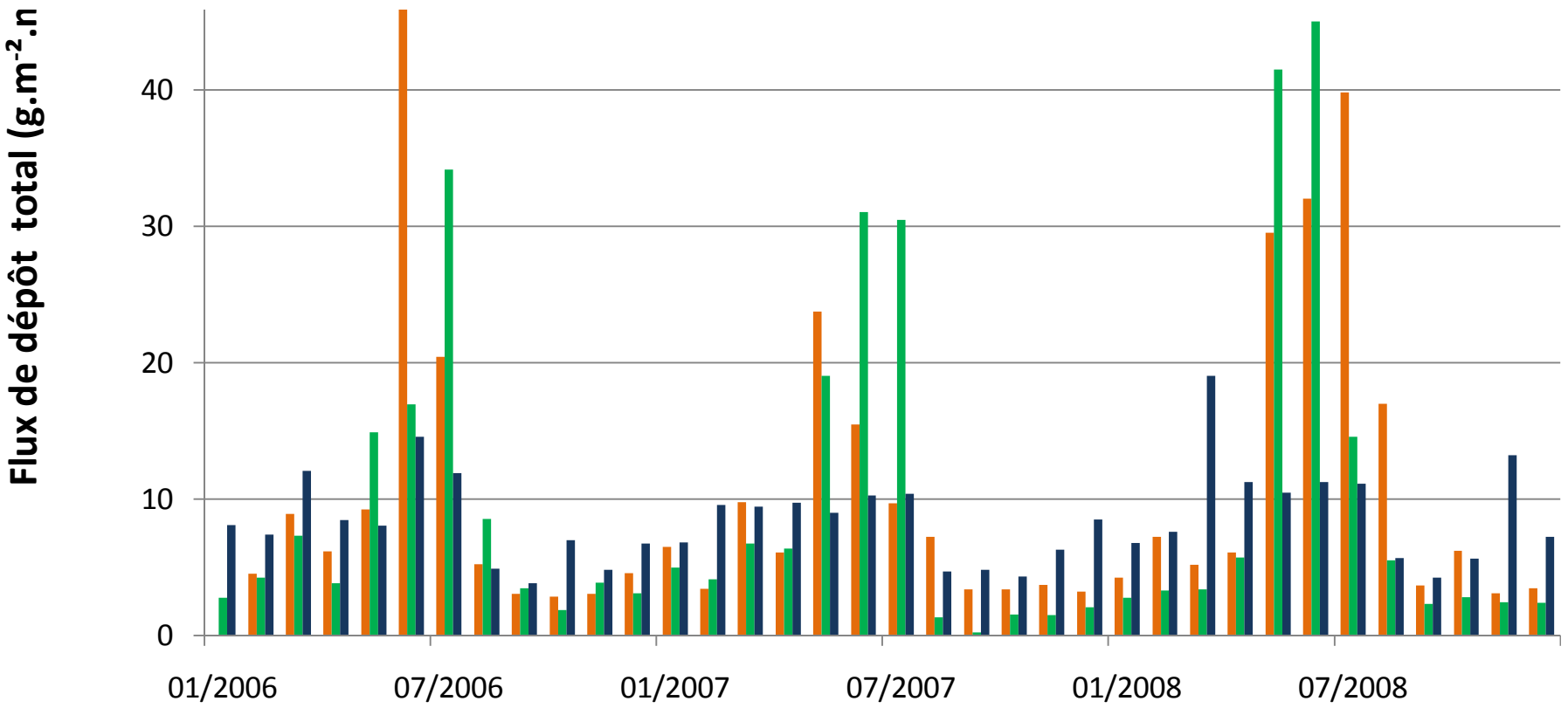

Analyse du flux de dépôts sec

Flux sec = [Aérosols]. Vd

Avec Vd = vitesse de dépôt

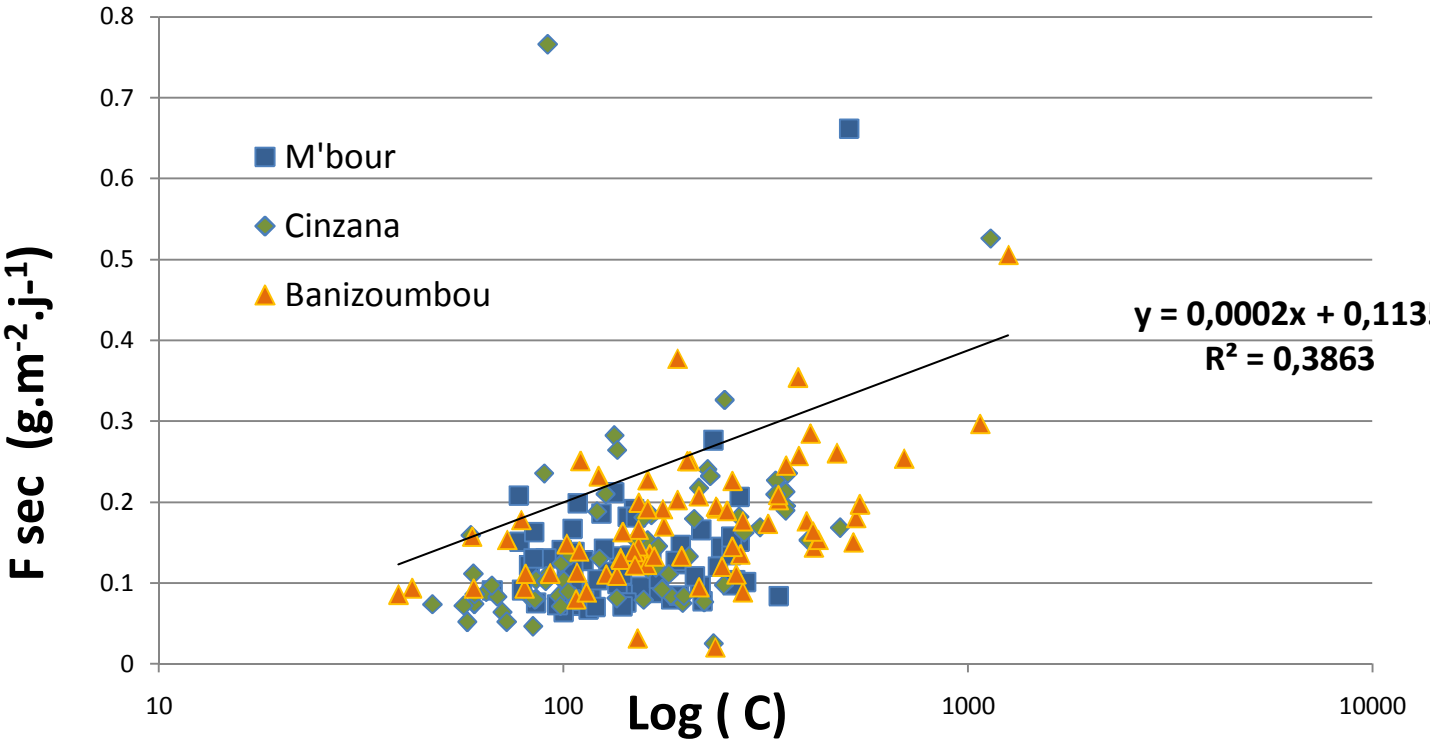

- ***Tendance à l'augmentation du flux de dépôt sec avec les concentrations***
- ***Grande dispersion du flux sec***

Dust emissions processes : SANDBLASTING

Simulated dust size distribution (Alfaro and Gomes, 2001)

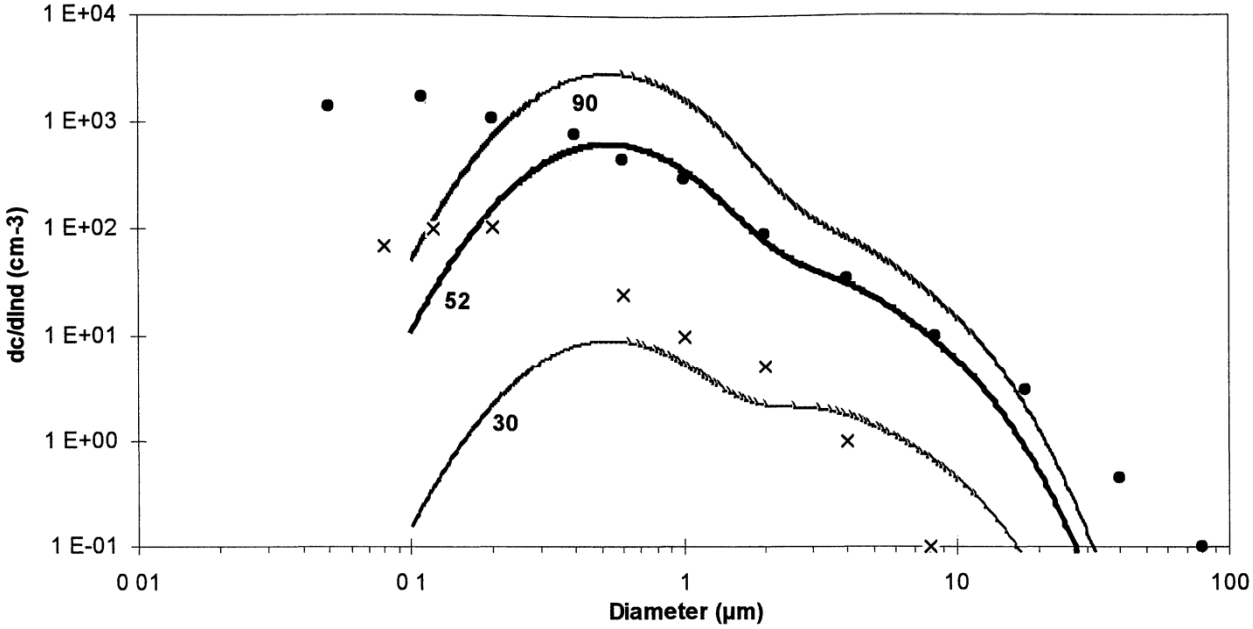

Figure 5. Comparison of the (concentration) size distributions of the aerosols released by a smooth FS soil at three different u^* (30, 52, and 90 cm/s) with field measurements in 'background' (crosses) and 'dust storm' (circles) conditions [after *d'Almeïda*, 1986]

-The proportion of the finest modes increases as wind friction velocity increases because of higher kinetic energy flux

Influence de l'éfficacité du collecteur de dépôt total

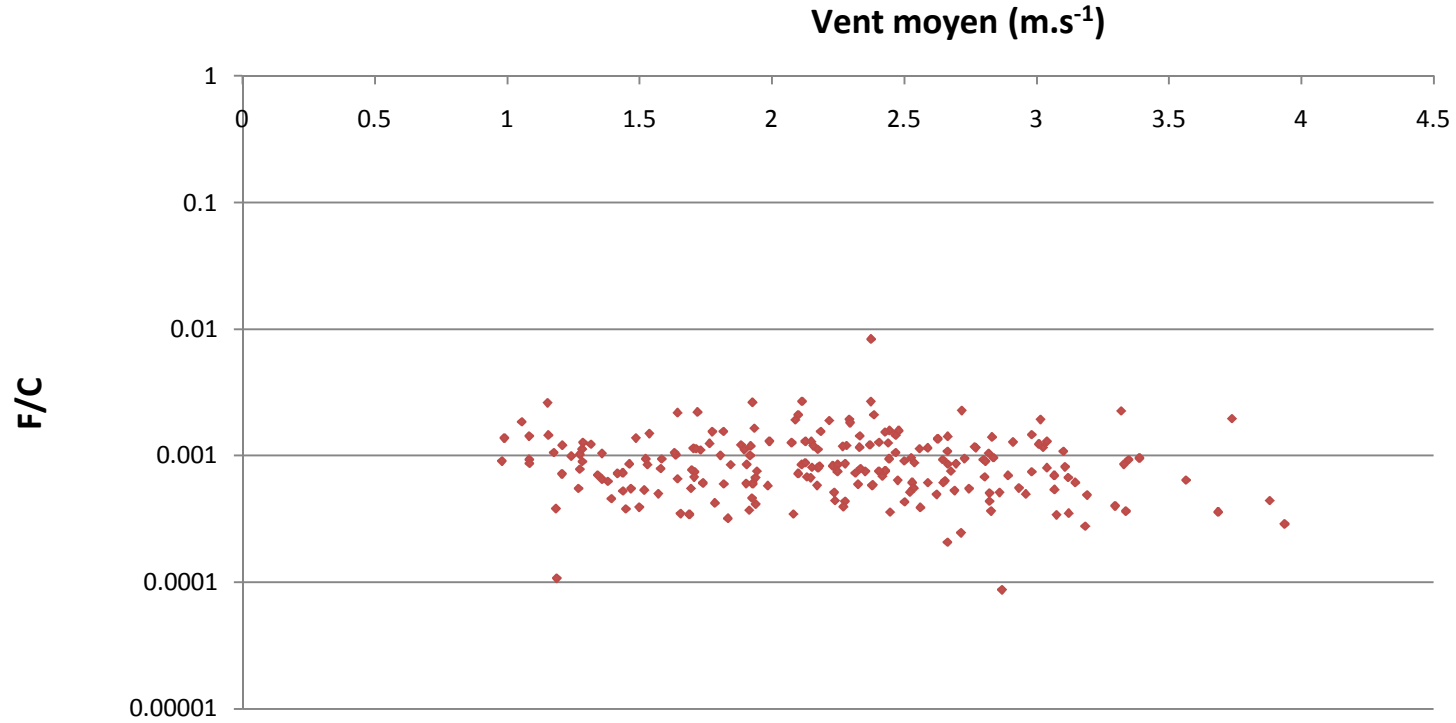

- ***Pas de biais notable en fonction de la vitesse du vent***
- ***D'autres facteurs sont responsables de la dispersion***

Etude événementielle en 2008 à Banizoumbou

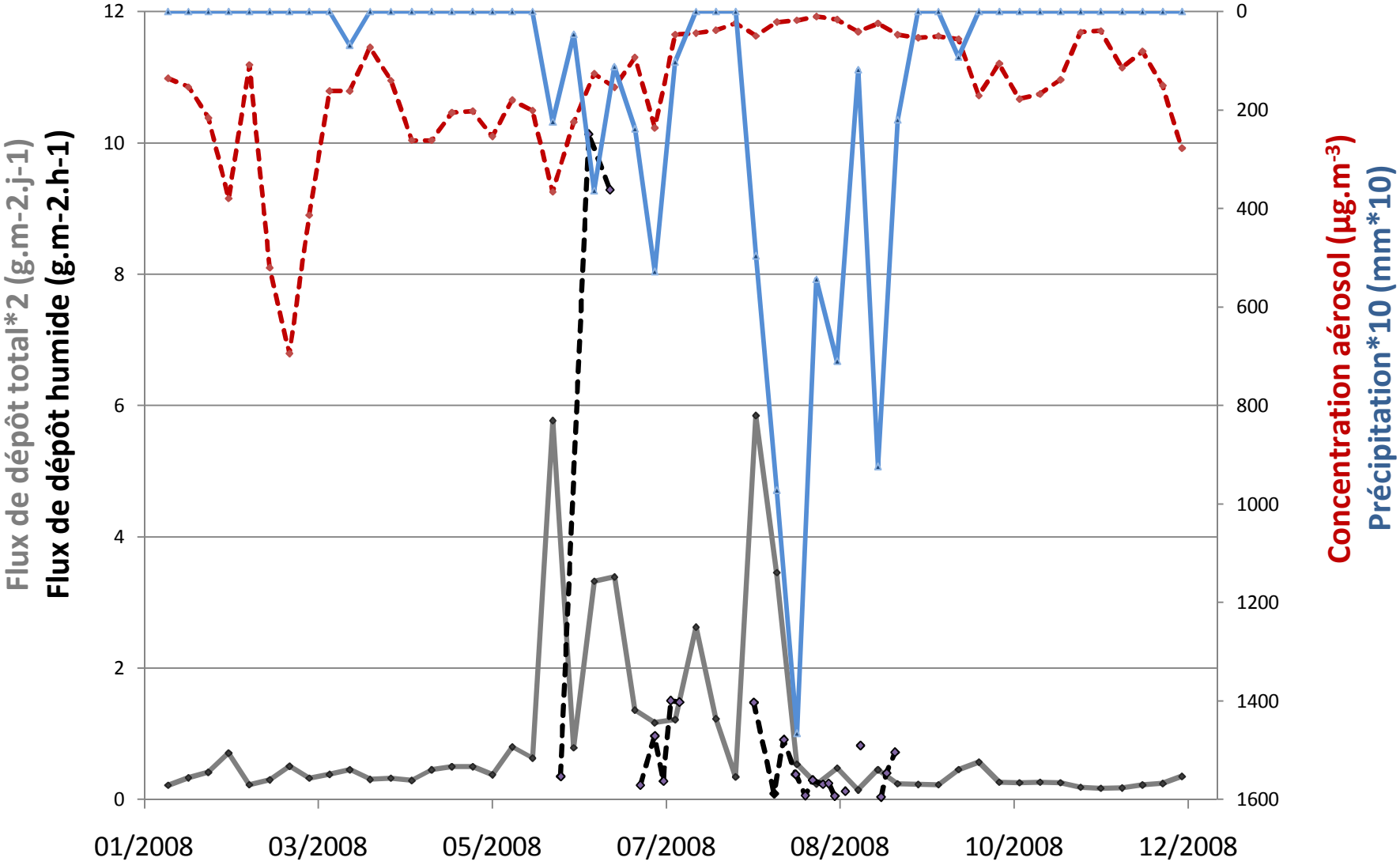

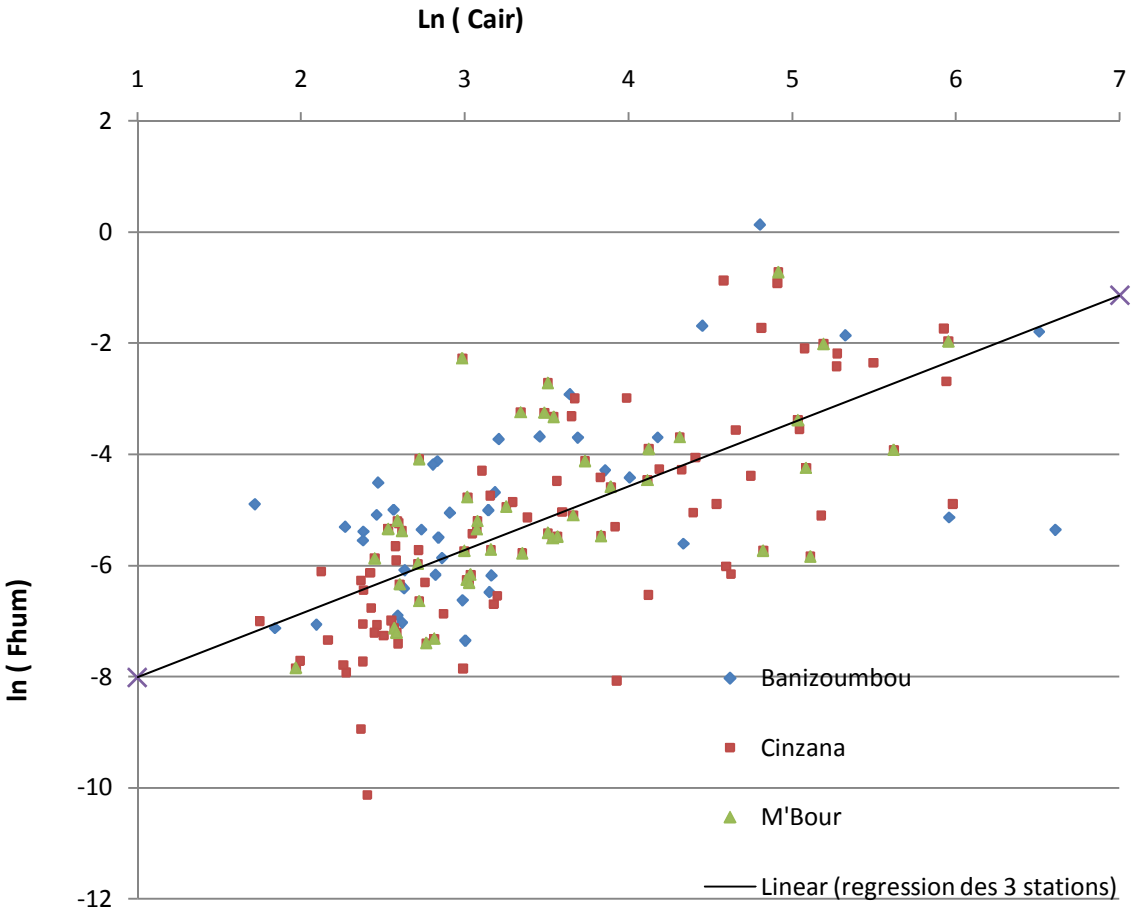
Ln (Cair)
1
2
3
4
5
6
7
2
0
-2
-4
-6
-8
-10
-12
ln (Fhum)
Banizoumbou
Cinzana
M'Bour
Linear (regression des 3 stations)

Emissions dues au passage de systèmes convectifs

Concentration et vent de surface (Cinzana, Mali)

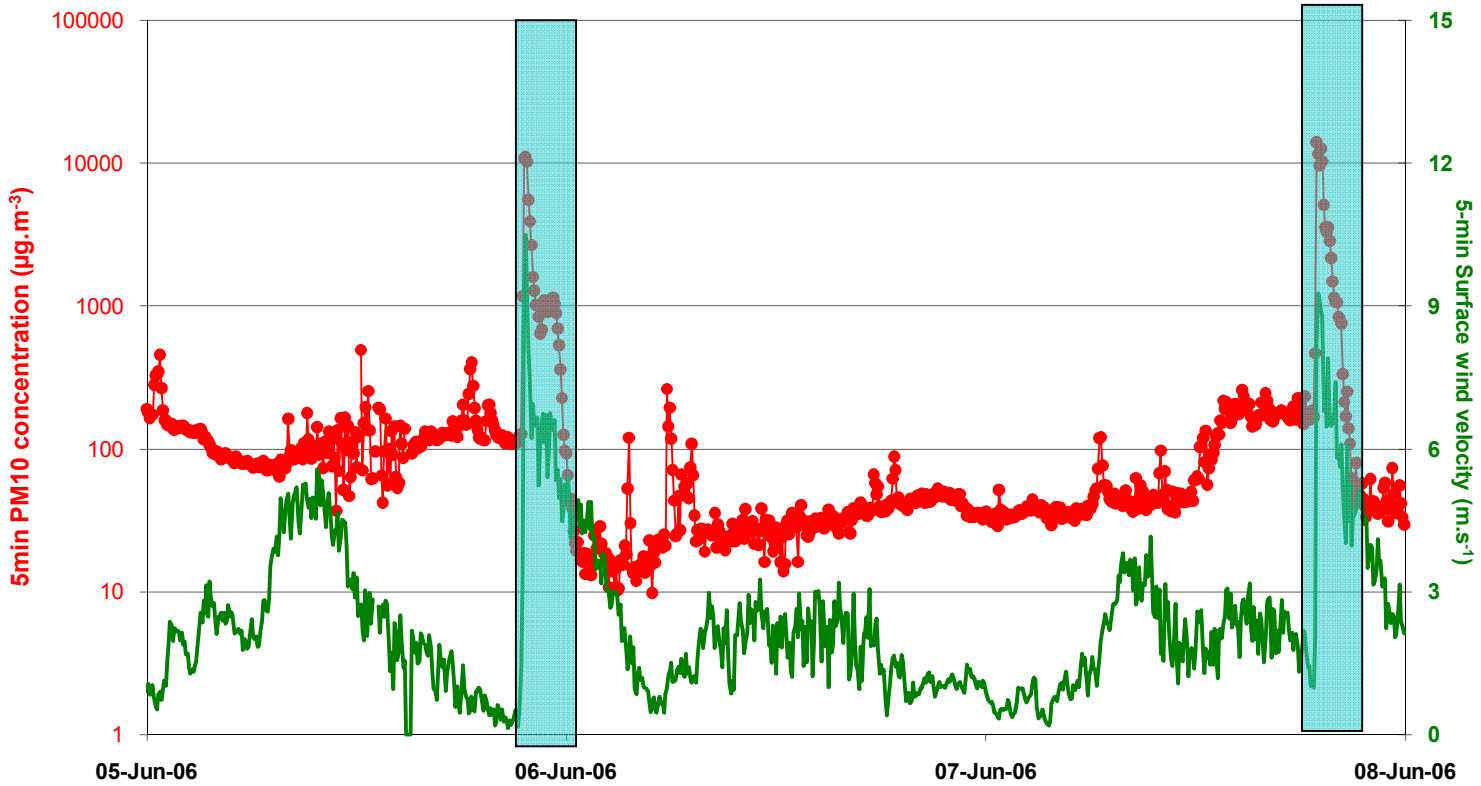

⇨ **Emissions locales produites par le passage des systèmes convectifs = durées très courtes; arrivées soudaines**

Flux émissions vs dépôt

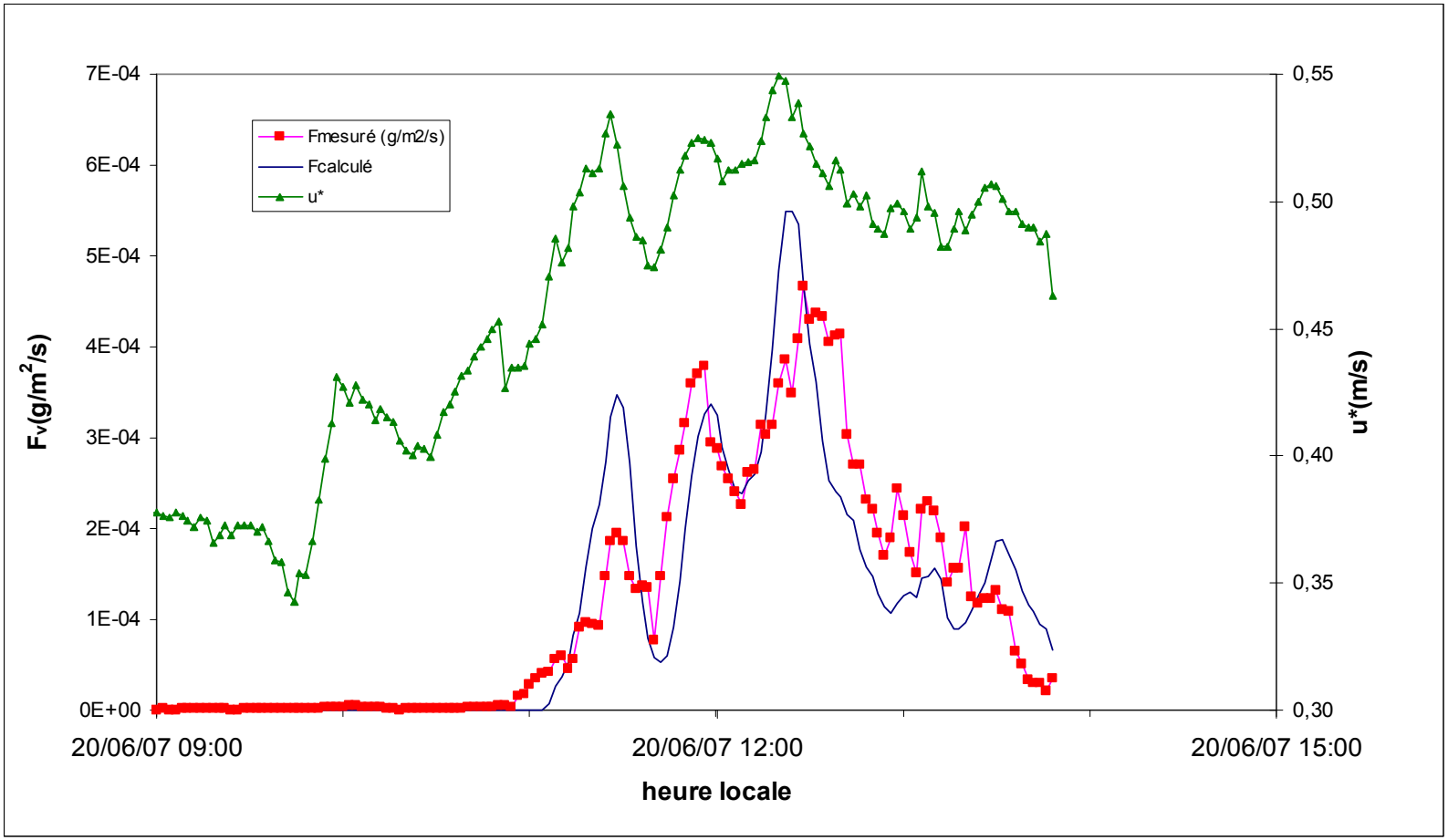

Figure 50: Evolution temporelle de la vitesse de friction (courbe verte) et du flux vertical mesuré avec les microbalances TEOM (courbe rouge) pendant l'évènement d'érosion du 20 juin 2007. Le flux prédit grâce à la paramétrisation mise au point dans ce travail est également représenté (courbe bleue).

Le graph de la thèse de MS montre sur trois heures (=10000s) un flux d'émission de 2.10-4 g.m-²/seconde: ce qui fait environ : 2g.m-².3h ;

sur la même période le flux total mesuré est de 0.8g.m-².jour.

Les dépôts humide et sec sont faibles sur cette période :

Humide= 0.08 g.m-².min de pluie

Sec = 0.4g.m-².jour.

Le flux d'émission est donc supérieur et rapporté à 3h ; il est 20 fois inférieur.

Flux émissions vs dépôt

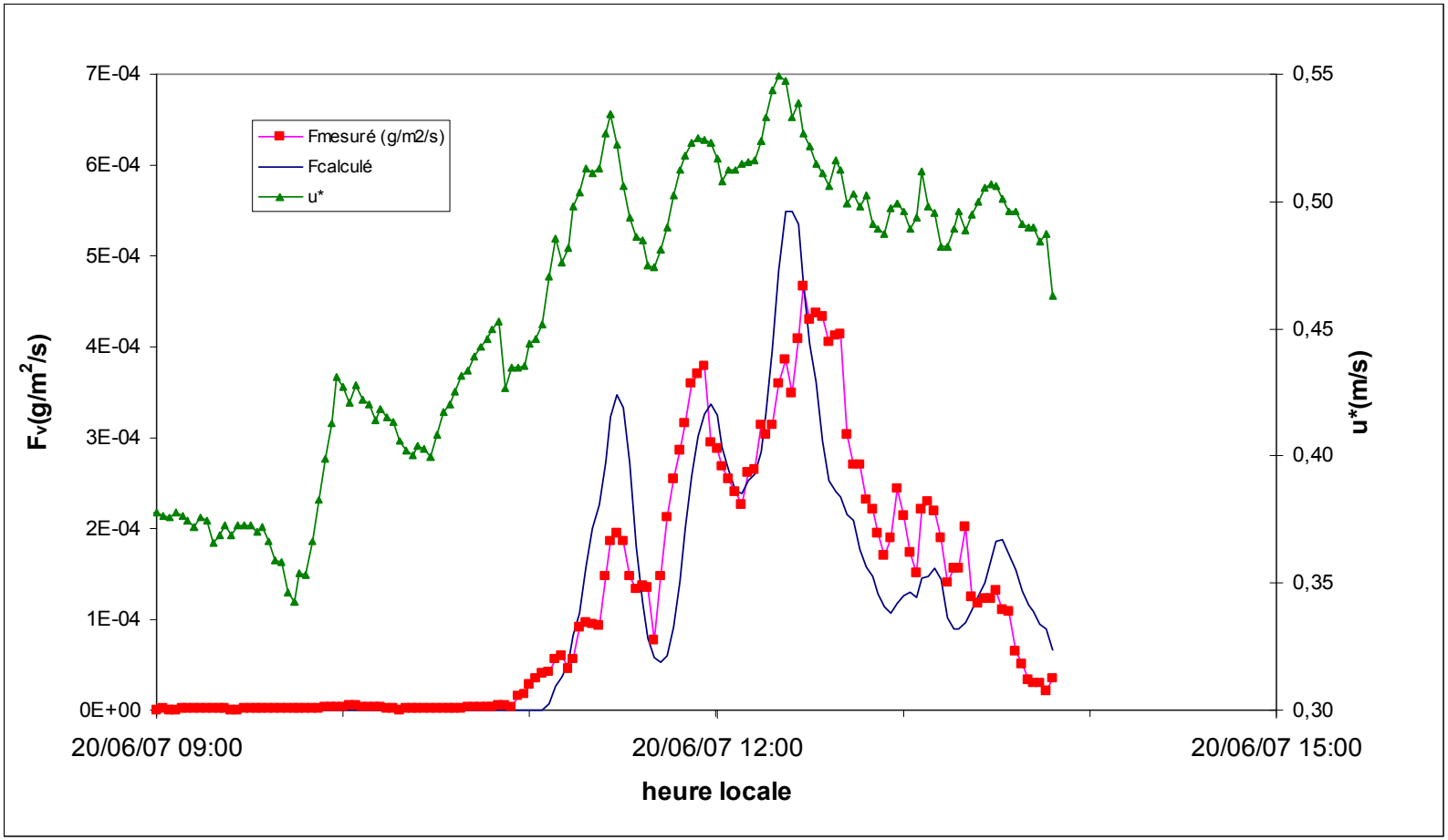

Figure 50: Evolution temporelle de la vitesse de friction (courbe verte) et du flux vertical mesuré avec les microbalances TEOM (courbe rouge) pendant l'évènement d'érosion du 20 juin 2007. Le flux prédit grâce à la paramétrisation mise au point dans ce travail est également représenté (courbe bleue).

Le graph de la thèse de MS montre sur trois heures (=10000s) un flux d'émission de 2.10-4 g.m-²/seconde: ce qui fait environ : 2g.m-².3h ;

sur la même période le flux total mesuré est de 0.8g.m-².jour.

Les dépôts humide et sec sont faibles sur cette période :

Humide= 0.08 g.m-².min de pluie

Sec = 0.4g.m-².jour.

Le flux d'émission est donc supérieur et rapporté à 3h ; il est 20 fois inférieur.

Analyse du flux de dépôts humide

$$\textit{Flux humide} = \Lambda\,[\textit{Aérosols}]$$

Λ = coefficient de lessivage

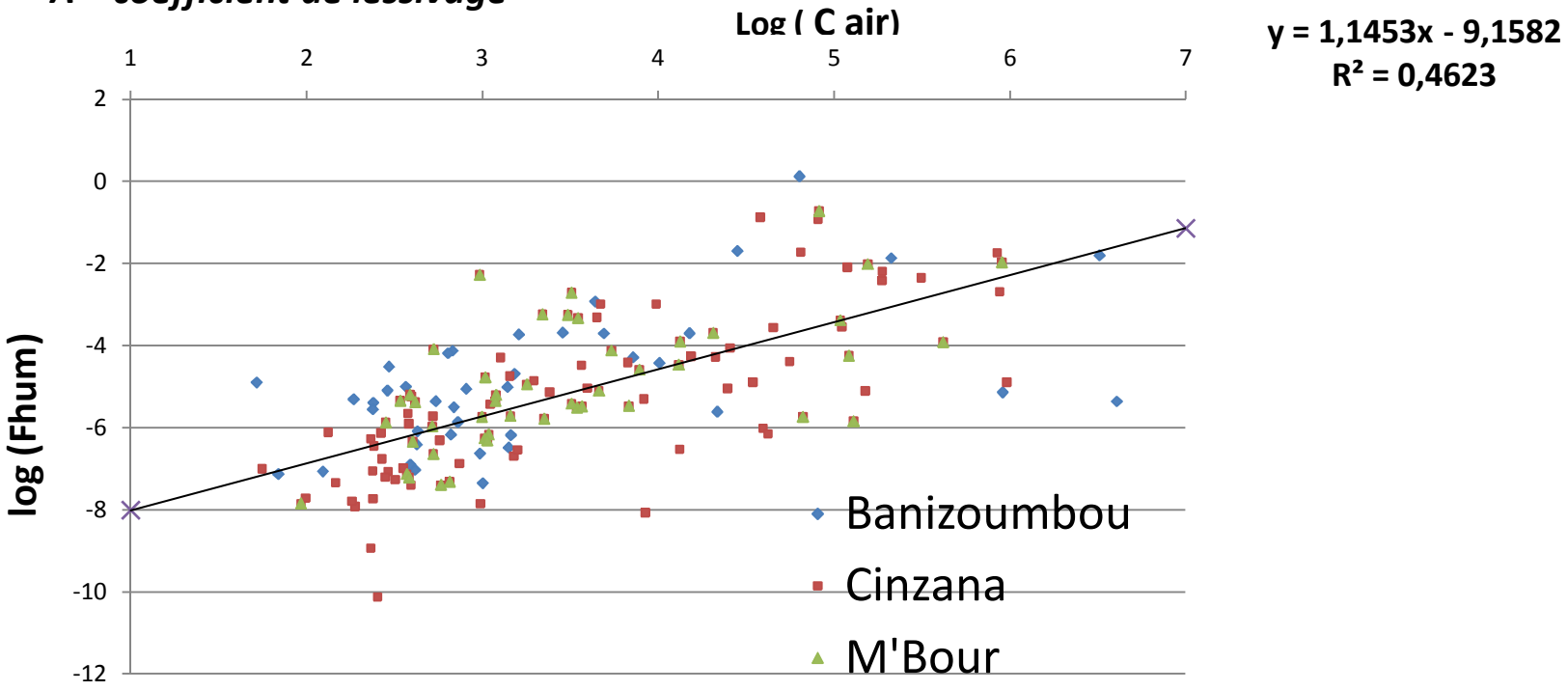

Analyse du flux de dépôts humide

M'Bour	pente	ord.origine
coefficient	-1,6550	-7,5722
écart-type	0,08	0,21
R^2	0,90	
Cinzana	**pente**	**ord.origine**
coefficient	-1,2735	-8,1717
écart-type	0,09	0,21
R^2	0,68	
Banizoumbou	**pente**	**ord.origine**
coefficient	-1,3524	-7,2964
écart-type	0,16	0,48
R^2	0,65	
Les trois stations	**pente**	**ord.origine**
coefficient	-1,3373	-7,9460
écart-type	0,06	0,16
R^2	0,70	

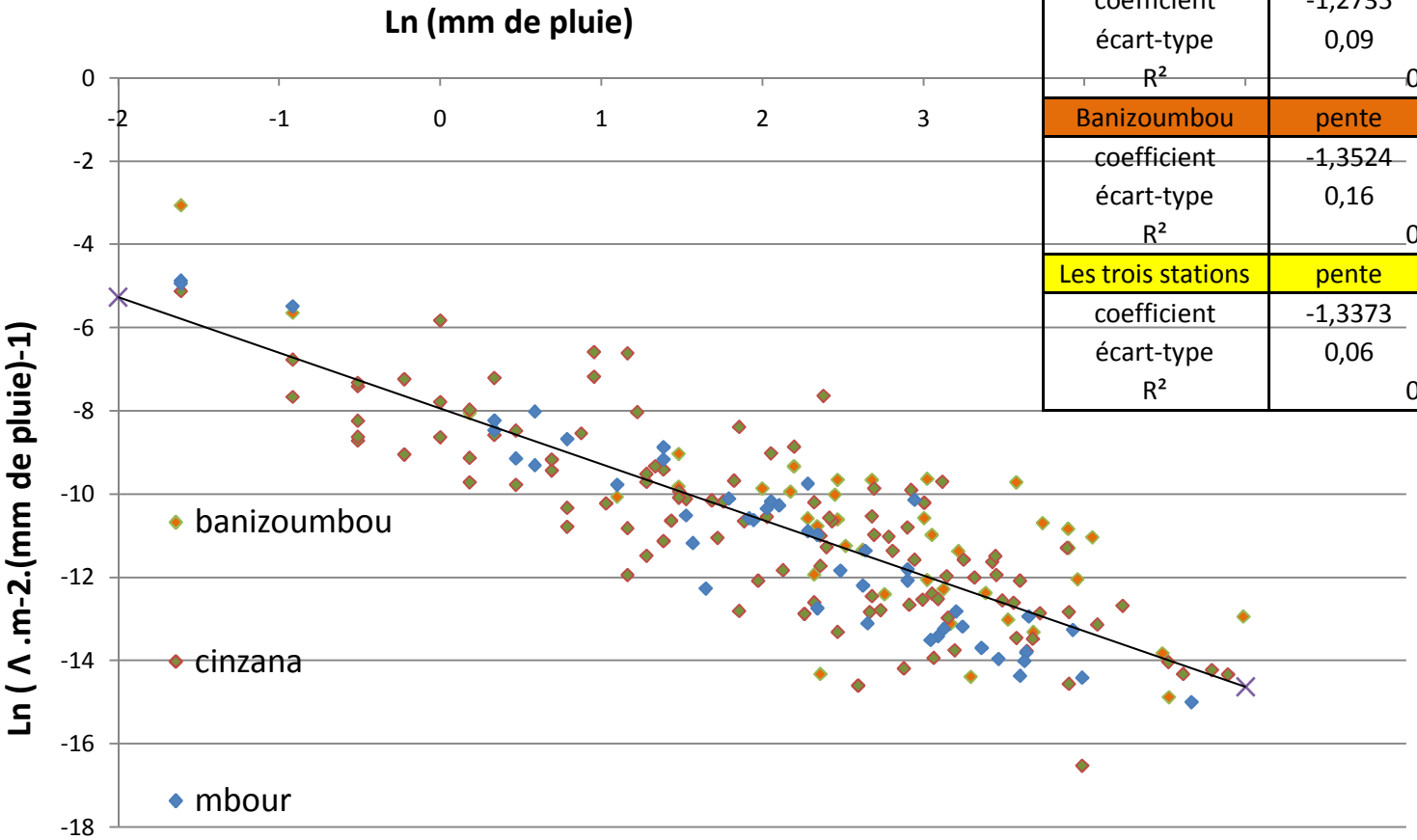

Comparaison des dépôts totaux et des dépôts secs

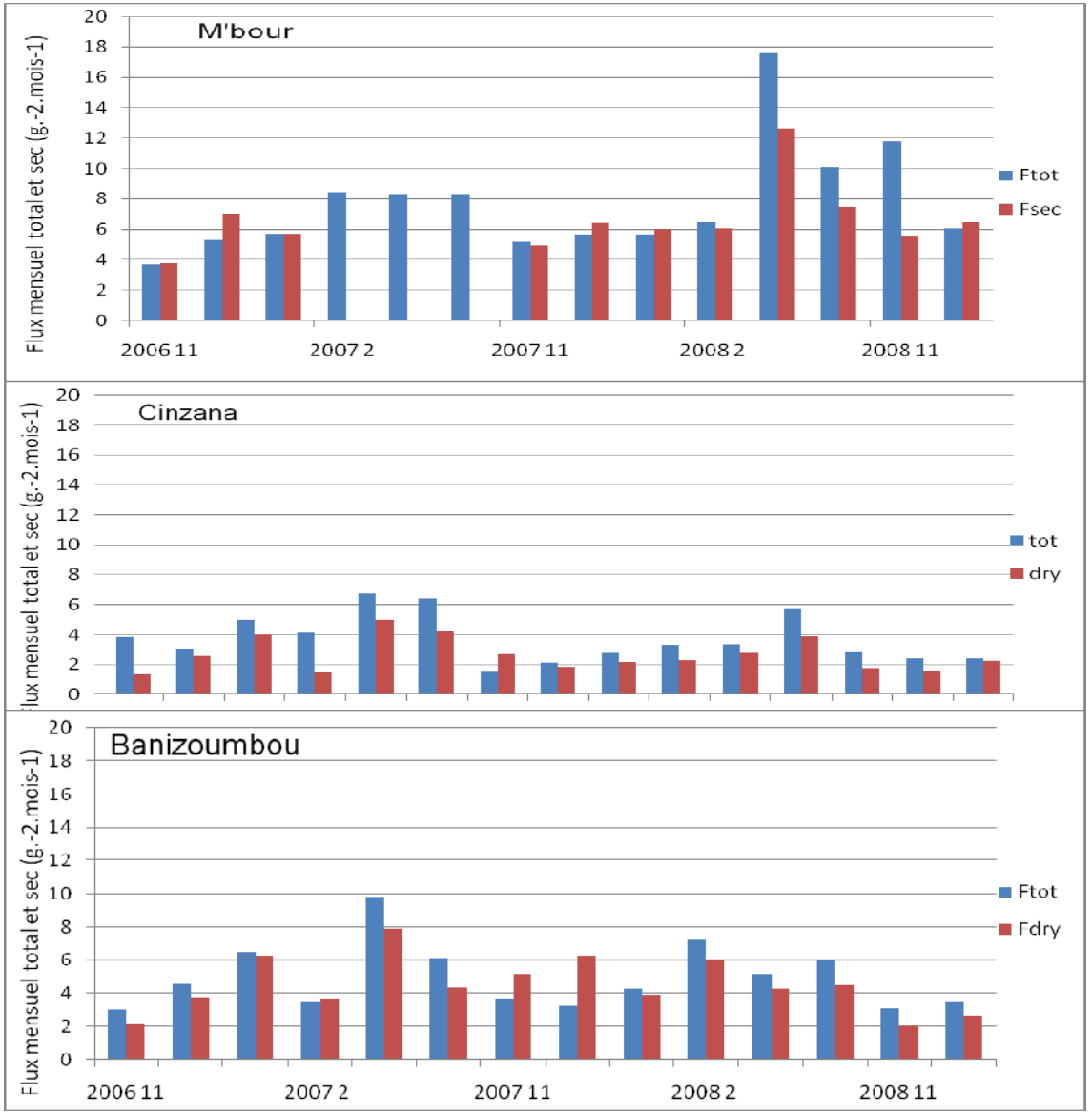

Flux de dépôt humide et de dépôt total à l'événement

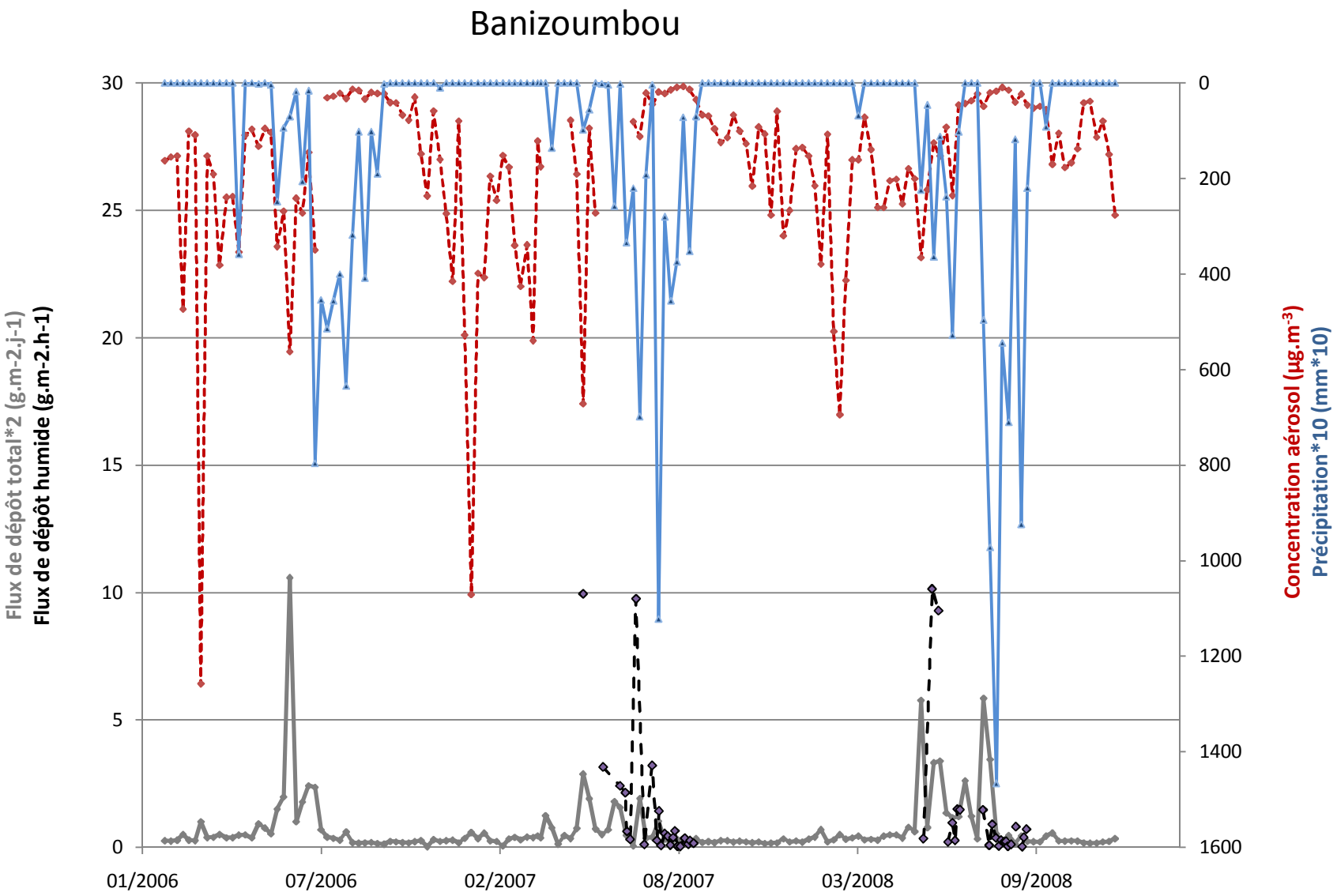

Flux de dépôt humide et de dépôt total à l'événement

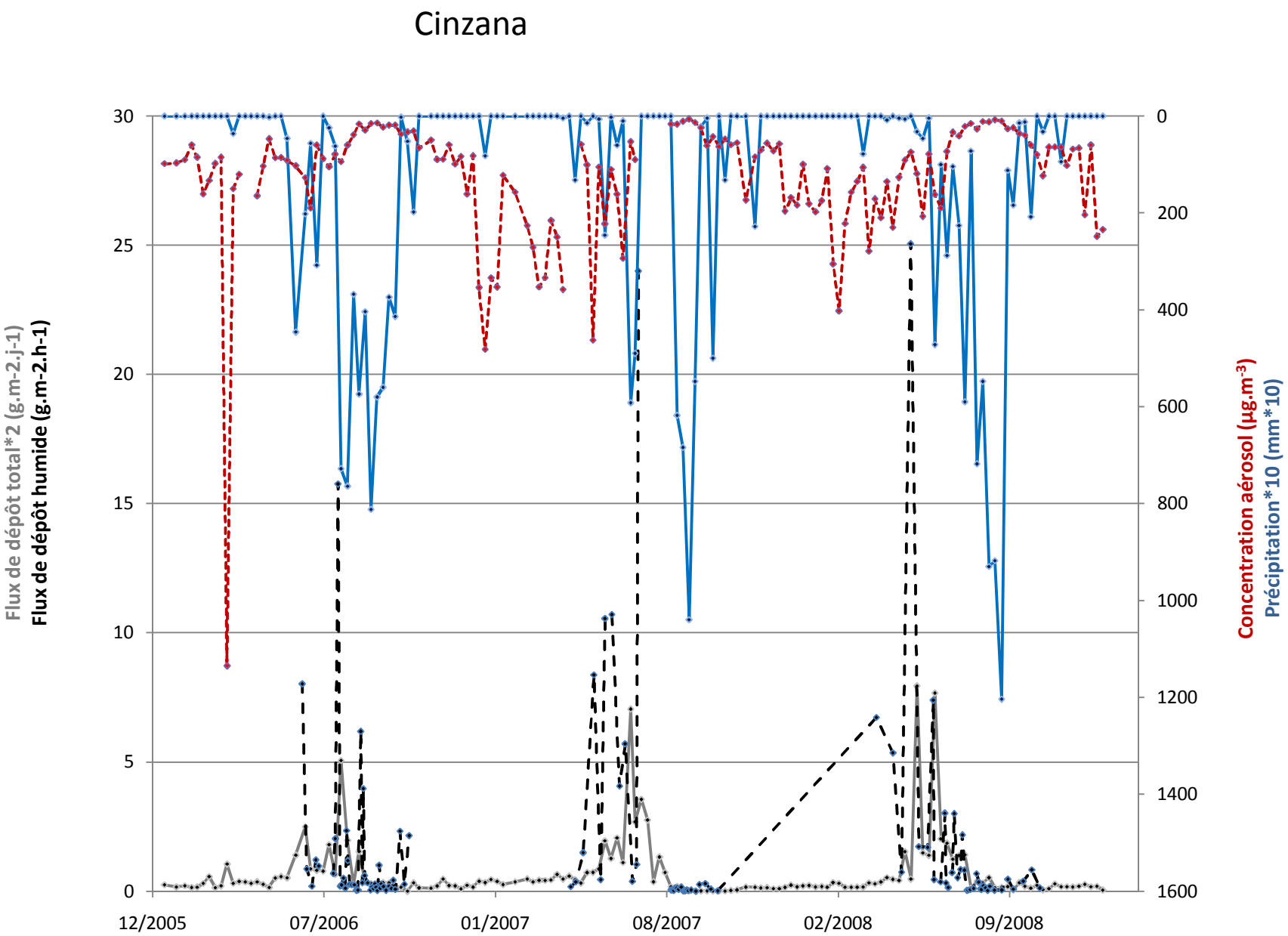

Flux de dépôt humide et de dépôt total à l'événement

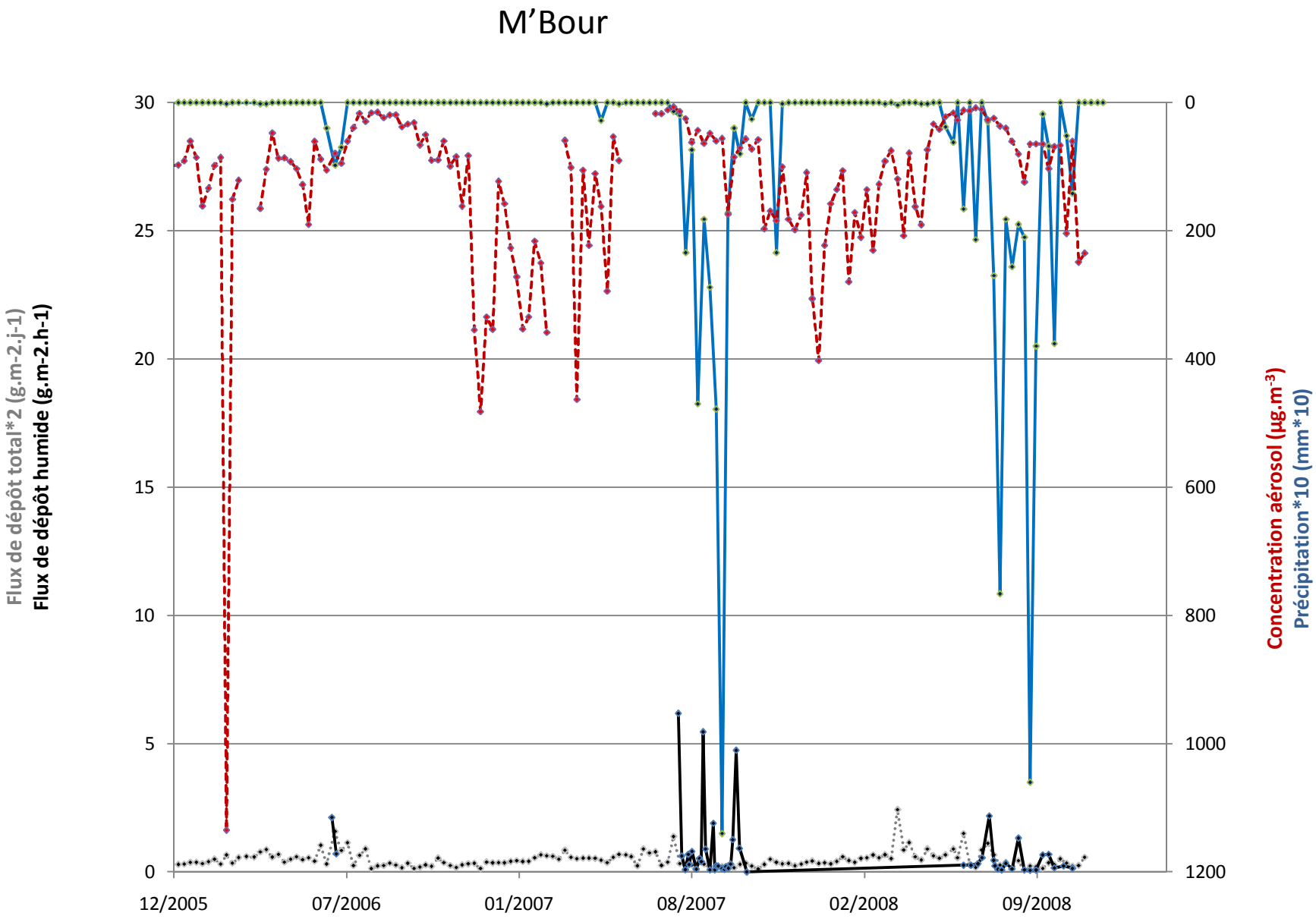

Flux total annuel ($g.m^{-2}.an^{-1}$)					
M'Bour	**2006**	**2007**	**2008**	**moyenne**	**écart-type**
flux total	83,2	77,8	98,8	86,6	10,9
flux sec	65,7	73,7	92,9	77,5	14,0
flux humide	17,5	4,1	5,9	9,2	7,3
% sec	79	94,7	94	89,4	8,9
% humide	21	5,3	6	10,6	8,9
Cinzana	**2006**	**2007**	**2008**	**moyenne**	**écart-type**
flux total	105	109,6	131,7	115,5	14,3
flux sec	47	-0,1	50,9	32,6	28,4
flux humide	58	109,7	80,8	82,8	25,9
% sec	44,8	-0,1	38,6	28,3	24,3
% humide	55,2	100,1	61,4	71,7	24,3
Banizoumbou	**2006**	**2007**	**2008**	**moyenne**	**écart-type**
flux total	127,7	95,7	157,6	127	31,0
flux sec		56,7	72,3	64,5	11,0
flux humide		39	85,4	62,2	32,8
% sec		59,2	45,8	50,8	9,5
% humide		40,8	54,2	49	9,5

Variabilité des concentrations en aérosols minéraux au Sahel

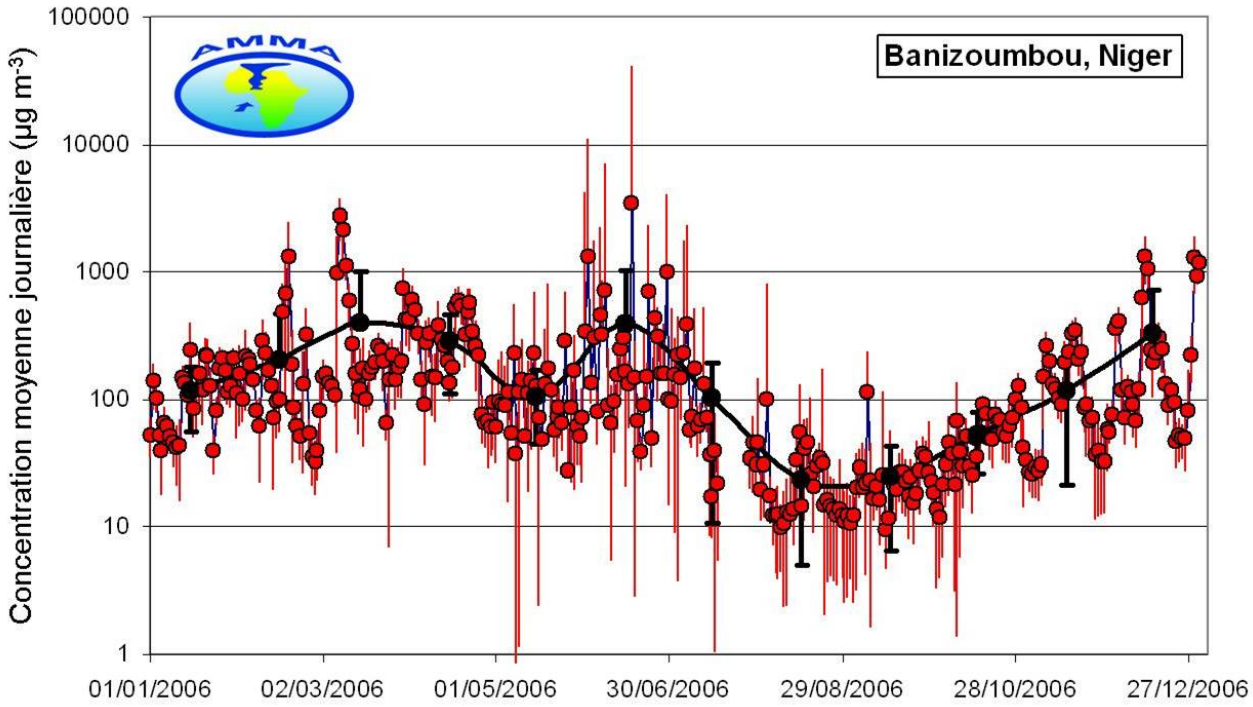

⇨ **Grande variabilité aux échelles annuelle, mensuelle et journalière !**

Outil adapté = modélisation méso-échelle

Seasonal total deposition

Total deposition fluxes ($g.m^{-2}.year^{-1}$)

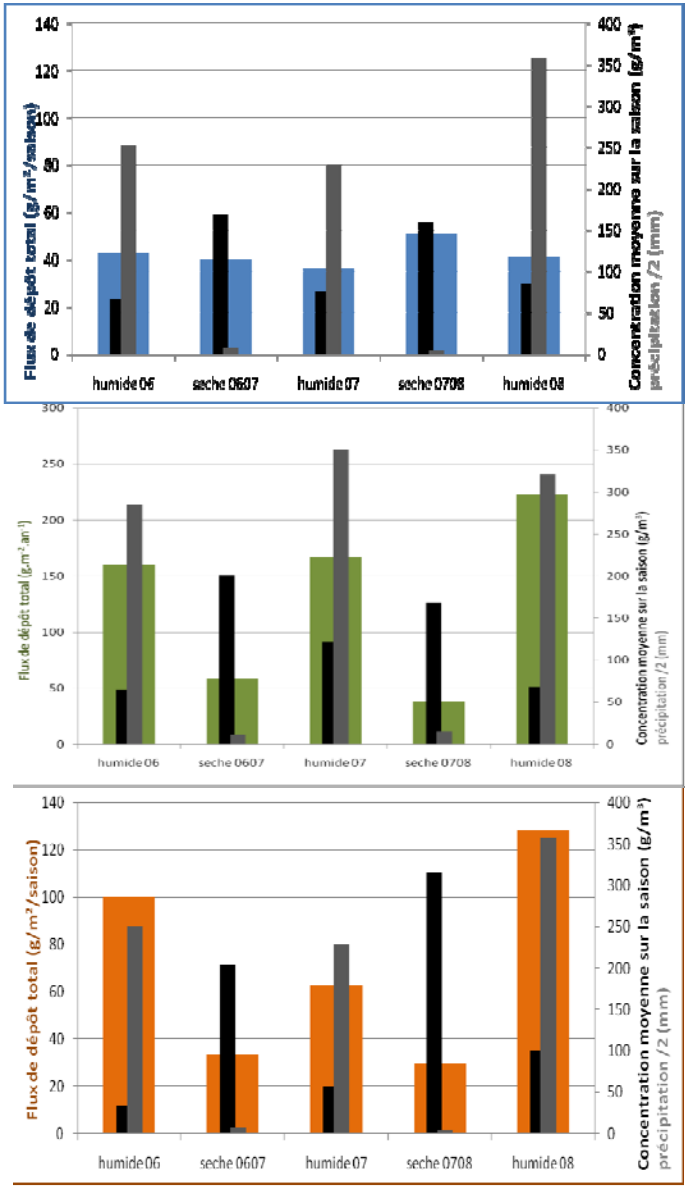

M'Bour

Cinzana

Banizoumbou

Precipitation (mm/2)

Mean dust atmospheric concentration

Wet season = may to october

Dry season=n ovember to may

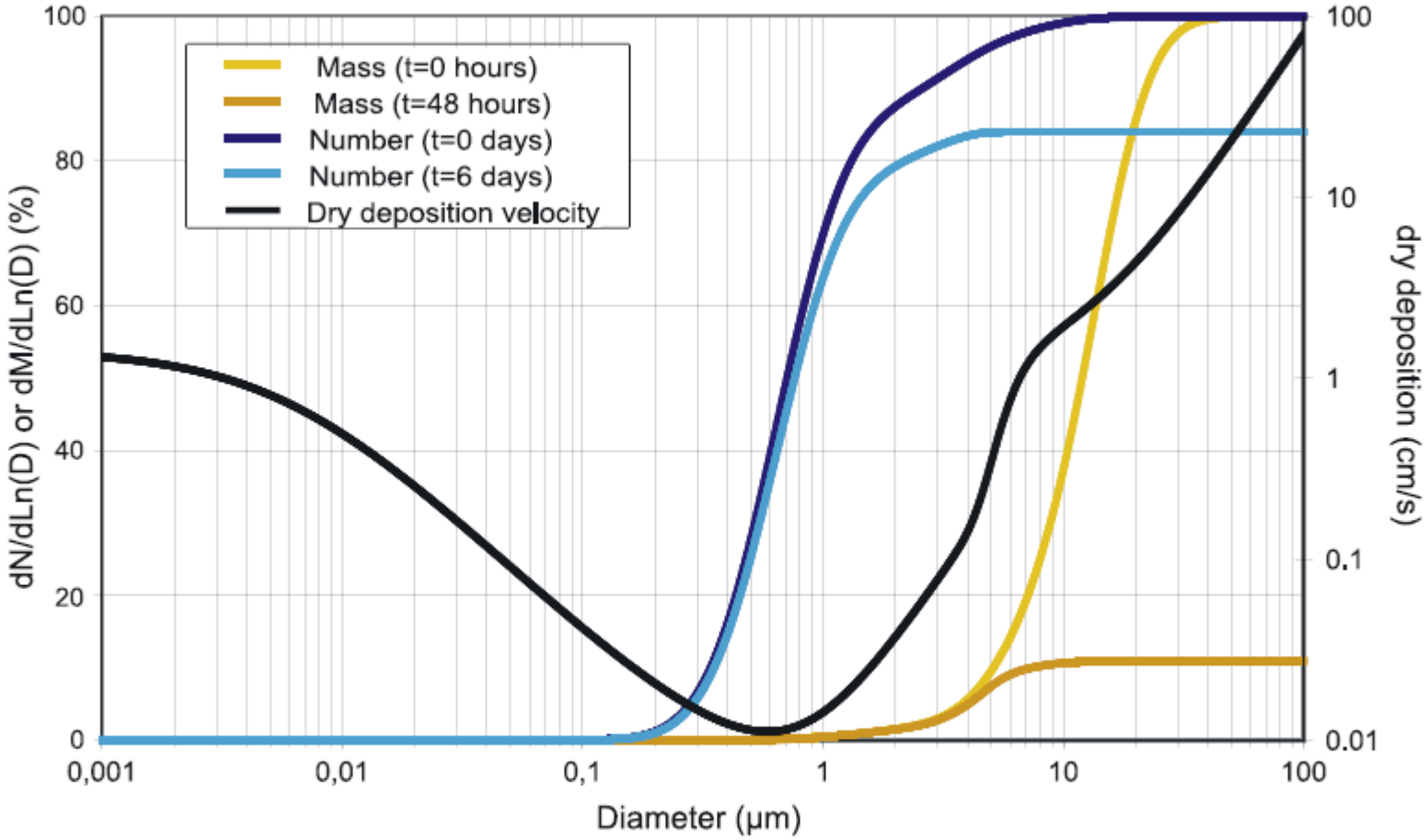

Figure 2. Cumulative mass (yellow) and number (blue) reference particle size distributions at initial time, and respectively after 2 days (light yellow) and 6 days (light blue) of simulation of dry deposition. Black curve is the dry deposition velocity.

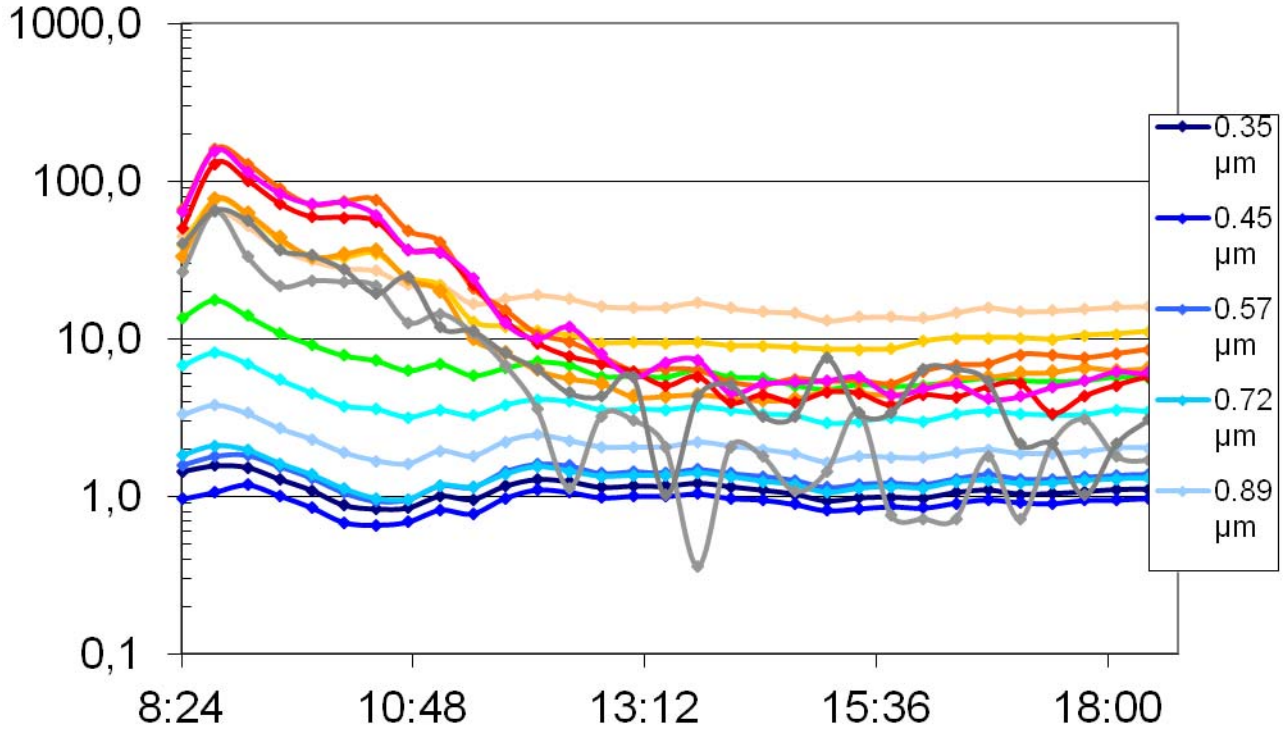

Temporal evolution of mass concentration (10^{-12} µg m^{-3}) as a function of particle size as measured by the lowest GRIMM. Each curve is referred by the median diameter (µm) of the corresponding GRIMM channel.

Le traitement des données

3 ans et 3 stations

METEO

vent (max,moy),précipitation,
HR, T°,P° à 5min

≈300 000 données

Concentration

Concentration moyennée à 5min

≈300 000 données

Dépôts

Collecteur (1 mesure/semaine)
≈450 mesures

Collecteur de dépôt humide
(quand il y a des pluies 30mesures/an)
≈350 mesures

METEO

vent (max,moy),précipitation, HR, T°,P° à 5min sur 3 ans pour les 3 stations

≈300 000 données

Concentration

Concentration moyennée sur 5min sur 3 ans pour les 3 stations

≈300 000 données

dépôts

Frisbee (1 mesure/semaine)
≈ 3ans*52sem*3stations ≈450 mesures

Collecteur de dépôt humide
(quand il y a des pluies 40mesures/an)
≈ 350mesures

1

Découpage des :

fichiers METEO Concentration **et** fichiers de

2

Calcul : vent, précipitation (somme,durée,moy,max, σ)

Calcul : concentration (moy,max,σ)

2

Récupération des données et assemblage dans Excel

3

Le calcul des flux de dépôts

$$: Flux\ collecté = \frac{Masse\ collectée}{(surface\ collecteur) * (tps\ prélévement)}$$

$$Ftot = \frac{Mtot}{(Scoll.Dech.)}$$

$$Fhum. = \frac{Mhum.}{(ScollDpluies)}$$

Dech = durée entre les relevés de l'échantillon

Dpluies = Durée des pluies repérées sur la météo

$$Fsec = \frac{(Mtot. - Mhum.)}{(Scoll.Dech.)}$$

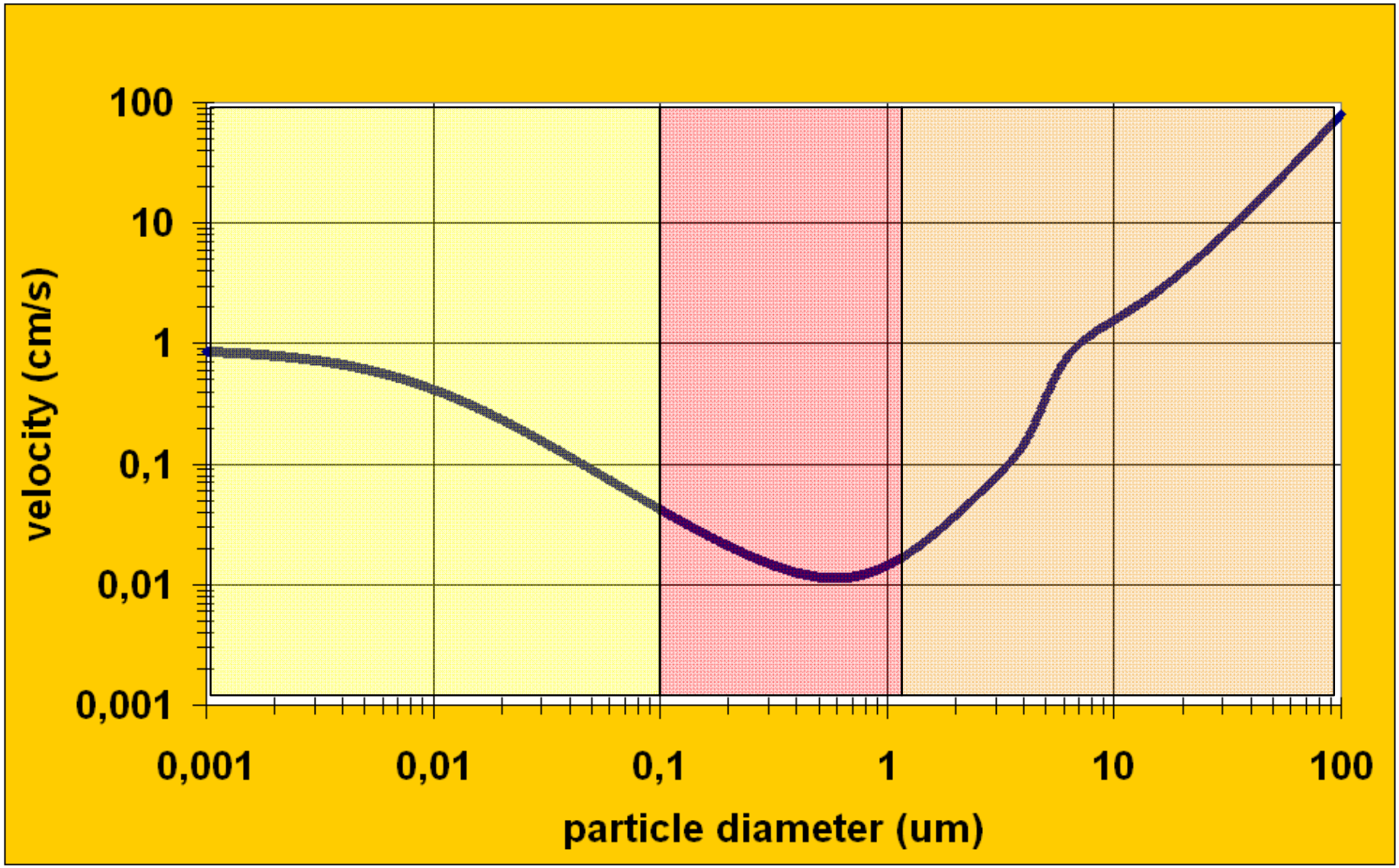

DRY DEPOSITION VELOCITY OF DUST PARTICLES vs PARTICLE DIAMETER

lisa | Laboratoire Inter-Universitaire des Systèmes Atmosphériques

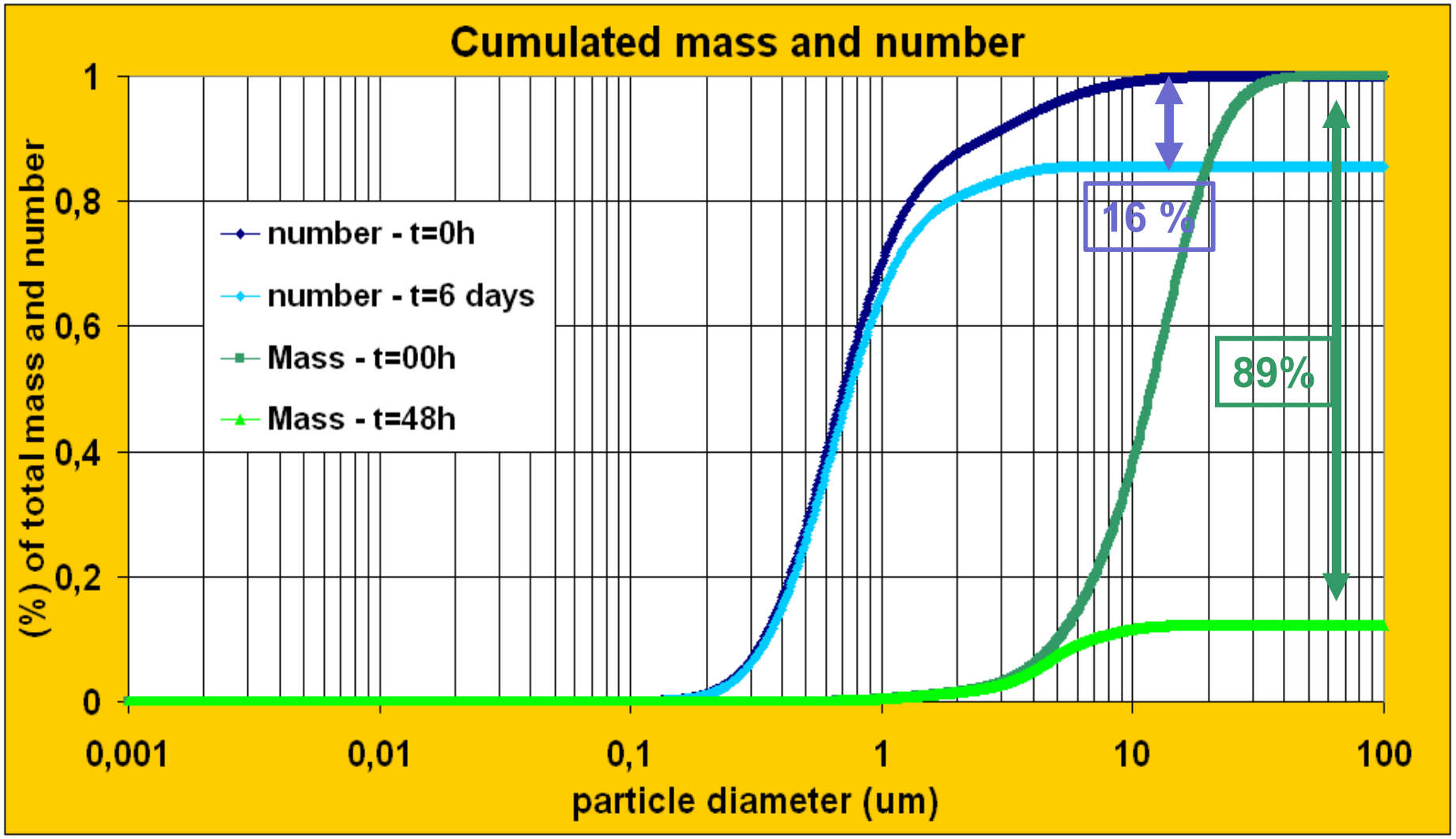

IMPACT OF DRY DEPOSITION ON DUST NUMBER AND MASS SIZE DISTRIBUTIONS AFTER 6 DAYS OF TRANSPORT

lisa | Laboratoire Inter-Universitaire des Systèmes Atmosphériques